

U-006-105.10

555

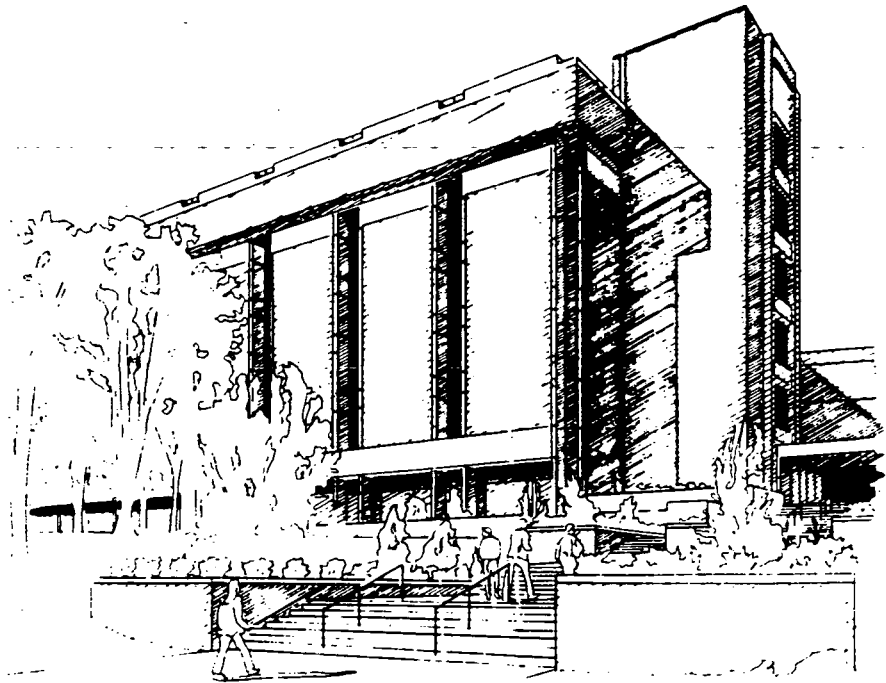
**A PROBABILISTIC RISK ASSESSMENT FOR THE
K-65 SILOS AT THE FMPC**

10-1-90

**UC/DOE-FMPC
FMPC/SUB-02A UC-702**

250-194

REPORT



UNIVERSITY OF CINCINNATI
COLLEGE OF ENGINEERING

Final

Revision 1

**A Probabilistic Risk Assessment
For The K-65 Storage Silos At The FMPC**



September 28, 1990

555

**A Probabilistic Risk Assessment
For The K-65 Storage Silos At The FMPC**

Final

Revision 1

University of Cincinnati

**Mr. Randy Janke
Mr. Robert Janke
Mr. Talaat Ijaz**

Principal Investigator - Dr. Roy Eckart

September 28, 1990

A2

Table Of Contents For Final Report

1.0 Introduction	1-1
1.1 Overview Of Probabilistic Risk Assessment (PRA)	1-8
1.2 K-65 Structure Evaluation	1-14
1.3 Failure Potential	1-15
1.4 Release Potential	1-15
1.5 Exposure Assessment	1-16
1.6 Risk Characterization	1-17
2.0 K-65 Silo Failure Evaluation	2-1
2.1 Silo Structure	2-2
2.2 Potential Failure Modes	2-7
<i>Acute Failures</i>	2-8
<i>Chronic Failures</i>	2-8
2.3 Failure Initiators	2-9
<i>Severe Weather</i>	2-9
<i>Seismic Activity</i>	2-29
<i>Long Term Weathering And Wear</i>	2-33
2.4 Radionuclide Inventory	2-60
2.5 Failure Sequences And Release Potential	2-63
3.0 Exposure And Dose Assessment	3-1
3.1 Environmental Transport Considerations	3-1
<i>Environmental Transport Models</i>	3-1
3.2 Probability Of Release And Transport	3-6
3.3 Characterizing The Exposure Setting	3-18
3.4 Identification Of Exposure Pathways	3-19
3.5 Pathway Analysis And Dose Assessment	3-24
<i>External Radiation Pathway</i>	3-25
<i>Inhalation Of Resuspended Dust</i>	3-26
<i>Inhalation Of Gaseous Plume</i>	3-29
<i>Summary Of Exposure Assessment</i>	3-34

4.0 Risk Characterization	4-1
<i>Risk Coefficient Method</i>	4-5
<i>Carcinogenic Slope Factor Method</i>	4-8
<i>Summary Of Risk Characterization Results</i>	4-24
5.0 Discussion of Uncertainty	5-1
Uncertainty In Silo Structural Integrity	5-1
Uncertainty In Tornado Related Probabilities	5-2
Uncertainty In Exposure And Dose Assessment	5-3
Uncertainty In The Risk Estimates	5-3
6.0 Discussion Of Results	6-1
7.0 References	7-1
Appendix A	A-1

1.0 INTRODUCTION

This section discusses the overview of the K-65 Probabilistic Risk Assessment (PRA) including the background and the nature of the problem. The task of performing a risk assessment on structures containing radioactive materials includes both the probability of failure of the structures and the consequences of the failure. In this way both the probability of failure and the probability of human exposure are considered in the risk estimates. The objective of this study is to evaluate the risk associated with the K-65 silos in terms of the potential for human exposure from environmental radioactive contamination. The basis of this study is centered around the existing or current conditions of the silos. The assessment considered a five year time framework for the analysis. This point is critical in terms of both the determination of the failure probability and modeling the environmental transport of contaminants as a result of a release of the radioactive residue material. There are essentially three tasks in evaluating the risk from the silos: assessment of the failure potential, estimation and prediction of the environmental transport potential, and the potential for exposure and dose assessment.

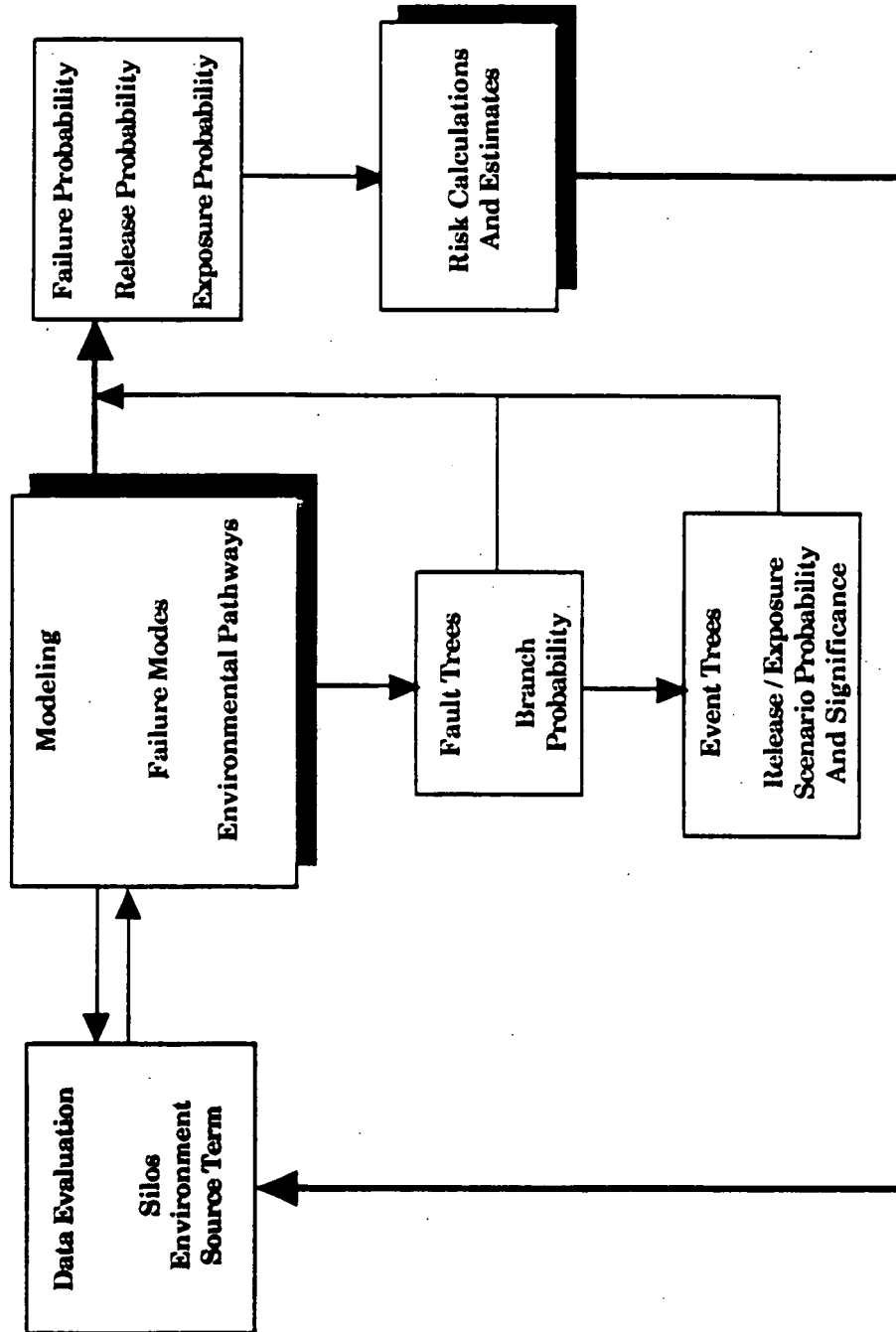
The risk assessment project consists of three coupled problems linked in parallel. The problems are: the silo structure analysis, 2) the release mechanism and transport of contaminants, and 3) the assessment of exposure and dose. Figure 1.1 illustrates this approach and delineates the tasks associated with each path. Evaluation of the potential failure modes required extensive background research on both the silo structures and contents. Block diagrams were constructed to illustrate the interdependence of the various components with a specific failure mode. A failure potential was evaluated after which a release term was determined; then a pathway analysis was performed.

Background Information

The background information required in order to evaluate the risk imposed by the silos covers a variety of areas. These areas are presented in the following manner: 1) history of the silos, 2) data collected, and 3) assumptions and conditions applied.

The history of the silos is necessary in order to evaluate two important aspects of the study: 1) the nature of the waste and the 2) the design and construction of the silo. Specific information was obtained and evaluated describing the early stages of design, construction, application, and later modifications to the structures. Additionally details covering the waste mass, including the method of waste treatment and composition, were obtained and assessed.

Figure 1.1 K-65 Risk Assessment Project Organizational Flow Chart



The structures considered in this assessment are silos 1 and 2. These structures were built between 1951 and 1952 in order to provide an interim storage capacity for the residues of the pitchblende processing. These residues were assigned the identification name of K-65 in reference to the radium bearing raffinate present in the processed pitchblende.

The structures are essentially cylindrical concrete storage vaults. The original silos included a drainage system in the floor, walls with access vents for dumping the raffinate, and a dome cover with a number of penetrations or access ways. The overall system for the storage of the residues also include a sump tank for holding the residual moisture collected from the drying slurry. The silos were originally free standing structures approximately 80 feet in diameter and almost 36 feet high at the center. Figure 1.2 and 1.3 depict the silo structures (1 -4) including the addition of the earthen berm around silos 1 and 2.

Detailed engineering drawings and various reports were evaluated for additional details of the original design and construction. Information concerning the modifications to the silos such as the earthen mound, surrounding the walls of the silo, and the additional support structures added to the dome center are also taken into account in the modeling and analysis. The time span between initial construction, use, and subsequent modifications is also required in order to evaluate the overall failure potential of the structures.

The contents of the silos are predominantly composed of residues obtained from the processing of uranium ore. The primary radionuclide present is radium-226; however, other radionuclides in the decay chain as well as small concentrations of uranium and thorium are expected to be significant in the final inventory calculation. The exact quantity of radium-226 present has not been provided; however, a credible range has been determined based on existing reports and other related papers or memos. The range is expected to be between 2,300 to 4,600 grams of radium (WMCO,1989). This correlates to an activity of 2,970 to 4,600 Curies (Ci). Since the half life of radium-226 is 1600 years the activity is not expected to have changed significantly over the thirty plus years that the waste has been residing in the silos. The composition and form of the material in the silos considered in the evaluation of the release potential and the ultimate transport in the environment.

Another aspect of the source term evaluated was the radon-222 content. The half life of radon-222 is 3.8 days and can easily be taken to be in secular equilibrium with the radium-226 parent. The production rate of radon is simply the decay rate of radium-226 multiplied by its activity. The content of radium-226 therefore has the potential of producing approximately 2,970 to 4,600 Ci of radon gas within the silos. The actual quantity of radon-222 available is the determined by the production rate minus the loss rate. There are essentially two loss mechanisms: 1) the natural decay of the radon gas (3.8 day halflife and 5.5 day mean life) and

Figure 1.2: Picture Of The K-65 Silos And Silos 3 And 4



Figure 1.3: Picture Of The K-65 Silos Alone With Berm Evident



the escape of the gas from the silos. The nature of radon, being an inert gas, results in the continual release of the radionuclide from cracks, pores, or openings in the concrete structure. The better the silos are sealed the less radon that will be able to escape prior to decay. This imposes a number of additional considerations on the risk assessment project particularly in terms of the release modes. The silos may only suffer cracking or partial damage and the potential source term can still be significant. All of the radionuclides must be considered and evaluated in terms of source strength, transport potential, and eventually their contribution to the dose of the public and the work force on site.

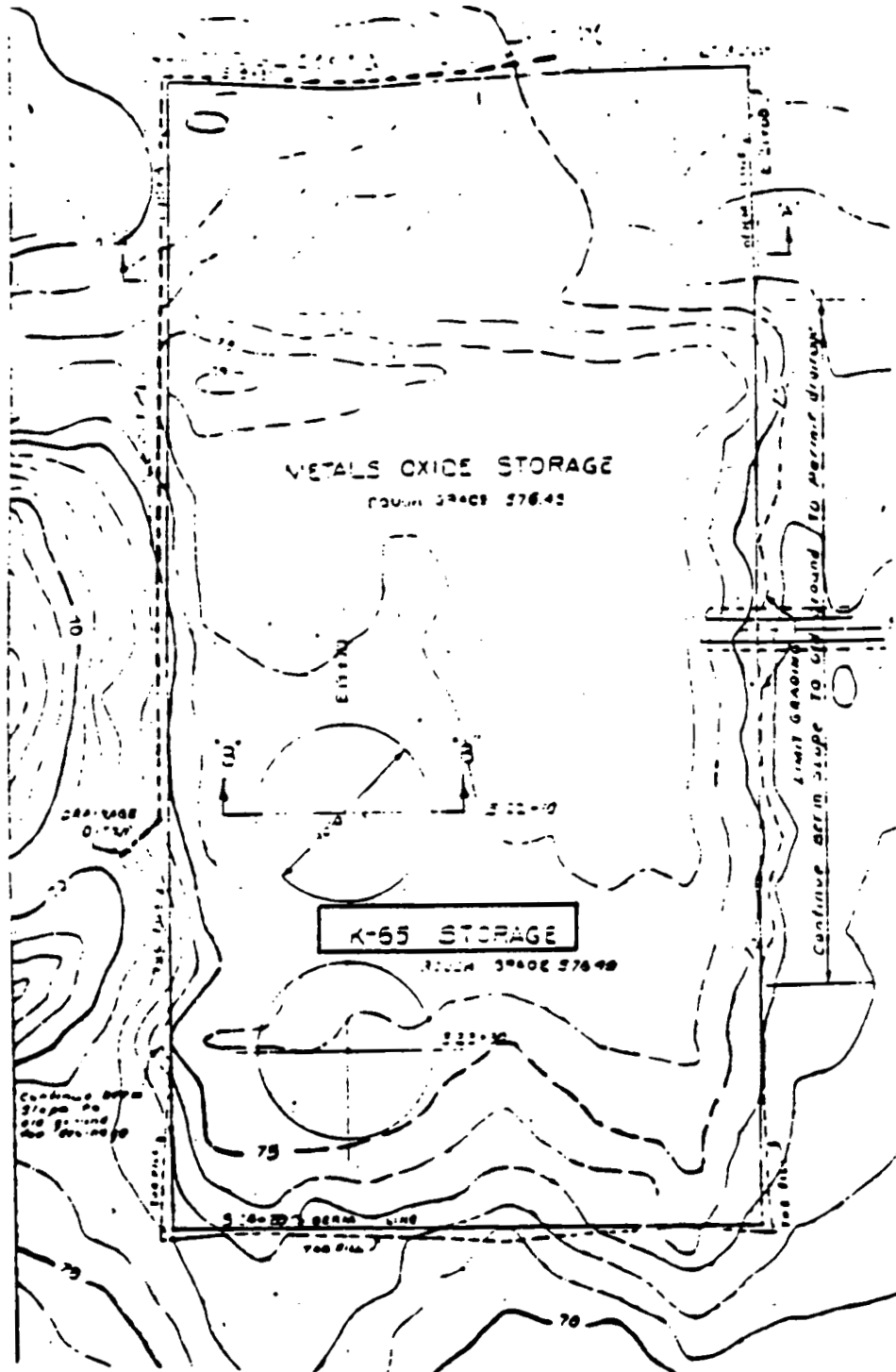
The data reviewed for this project was extensive. Data was also evaluated concerning the physical nature of the environment in the vicinity of the silos, the meteorological and seismological characteristics of the region, and the location, size, and nature of the population centers in the vicinity of the site. Figure 1.4 illustrates the vicinity near the K-65 silos. The quantity of data required is of course dependent on the confidence of the results needed as well as the activity of the source term and the potential for transport.

Information concerning both seismic activity and severe weather in the region was collected and evaluated to determine the probability of silo failure and the potential mechanisms for environmental transport. The frequency and the severity of severe weather will provide a basis for both failure probability and the atmospheric transport potential of the silo contents. The frequency and severity of seismic events, however, will only yield part of the solution. Once the failure of the silo is postulated, based on seismic activity, then the atmospheric and other environmental conditions at the time of the failure must be considered in order to predict the release and distribution of radionuclides.

Data requirement for the structural condition of the silos was an integral part of this analysis and had a direct bearing upon the potential failures present. The structural analysis conducted by Camargo Associates, Limited (Cincinnati) has been studied in depth and was used to form the basis of the failure probability of the structure. The purpose of this analysis was to determine the structural stability of the silos, and to identify any potential structural problem that would require remedial action. The conclusions of this study have a direct bearing upon this present analysis; the non-destructive testing results were used to identify and quantify the possible failure mechanisms.

A number of key assumptions were made in order to evaluate the failure probability and the transport probability. Some assumptions were dependent on the detailed data or information available. Others were determined by the nature of the study. The goal of this study was to estimate the risk associated with the silos over a five year time frame. This time span dictated the bounds of the transport potential, the probability of silo failure, and the activity of the source term. The specific assumptions

Figure 1.4: Diagram Showing The Topography In The Vicinity Of The K-65 Silos



used in this project are discussed as required in the evaluation of the basic event probabilities and in the modeling of the transport processes as well as with the pathway and dose analysis sections.

1.1 Overview Of Probabilistic Risk Assessment (PRA)

This section is included to provide information on the nature of risk assessments concerning the failure of some structure or composite of systems and structures. The methodology described here was first employed in the evaluation of the potential for a severe accident at a nuclear power reactor. It is important to note that this study is an adaptation of nuclear industry approved methodologies. Where necessary, Nuclear Regulatory Commission PRA procedures have been implemented for this analysis, however, due to the difference in scenarios, some concepts have been modified for adaptation to this study.

The assessment of risk with respect to the K-65 silos is intended to achieve the following objectives: 1) identify initiating events and event sequences that might contribute significantly to risk, 2) provide realistic quantitative measures of the likelihood of the risk contributors, 3) provide a realistic evaluation of the potential consequences associated with a hypothetical failure of the silo structures, and 4) provide a reasonable risk-based framework for making decisions regarding the continued storage, removal, or other alternatives with respect to the radioactive inventory. The risk associated with the K-65 silos is considered linear, and can be represented as in Equation 1.1.

$$\text{Risk} = \text{probability} \times \text{consequences or } R = p \times C \quad (1.1)$$

where:

R - Risk
p - Probability
C - Consequences

Clearly the probability in this equation relates directly to the potential failure of the silo in some given time frame. In this case the term potential failure relates directly to structural failure of the silos and does not relate to the continuous release of radon gas. The equation is the same in the continuous release case with the probability of release or "failure" equal to one. The consequences are then represented in two parts: 1) the failure of the silos and 2) the dose (therefore the health impact) received as a result of the release of radioactive contaminants to the environment. The modeling used in this study also provides an estimate on the probability of a given dose (to the population or a maximally exposed individual) from a given source term. In this way the PRA methodology is being expanded to include the environmental transport as well as the failure modes of the structure. In this way the probabilistic and deterministic nature of the environmental transport modeling can be investigated. The results of this facet of the risk assessment will provide detailed information on the potential for transport in the near and far field as well as in the near and

long term. The individual details of the methodology will be covered in a latter section. The intent here is to provide some of the basic concepts associated with this type of study.

The basic components of a PRA analysis are: 1) familiarity with the system, structure, or plant, 2) initiator selection, 3) building the event trees, and 4) developing the fault trees. The familiarity component of the project is obviously reflected in the background research and the initiator selection process which must take into account situations (events) which have the potential for inducing failure of the silos. The remaining considerations relate to the modeling of the failure modes, the environmental transport, and the exposure scenarios. These considerations are taken into account in the building of comprehensive event and fault trees.

The event trees are used to describe all possible outcomes from a given initiator. The trees take into account the structure and the possible ways in which a failure can lead to a release of radioactive material. A typical event tree is illustrated in Figure 1.5 where the failure or success of the individual events can lead to the release of radioactive material. Each path illustrated in the tree is a potential scenario and is labeled a sequence. A typical sequence or path is illustrated in Figure 1.6. The probability of each event in the sequence is multiplied and the result is the total probability of that sequence.

The use of the event trees provides for the possibility of ranking the various events in order of highest to lowest probability. This ranking is the first step in quantifying the overall risk associated with the silos. An event tree will be developed for each failure mode and each release mode. The individual branches in the event tree are considered a top event in a fault tree. The relationship between the event tree and the fault tree is illustrated in Figure 1.7. This figure clearly shows that each specific failure branch of the event tree must have a corresponding fault tree. The fault tree provides the probability of failure for that event. The probability of success is simply one minus the probability of failure. Ultimately in the risk assessment the central concern is on the failure probability since if the system is successful then there is no risk. The discussion that follows describes the fault tree methodology and the concepts of the "OR" and "AND" gates used in the design of the trees. This method follows from the constructs of "Boolean algebra" or logic analysis.

Fault tree analysis is a technique by which many events that interact to produce other events can be related using simple logical relationships (AND, OR). These relationships permit a method for building a mathematical model that statistically represents the system under consideration. The evaluation of the probability of the system response (silo dome, wall, and floor) is then determined by the individual basic events. The basic events are determined from the detailed analysis of the results of the non-destructive examination. To construct a fault tree which best represents the system it is necessary to take into account all possible events

**Figure 1.5: Loss Of Integrity From Natural Forces
(Tornado) Event Tree For K-65 Storage Silos**

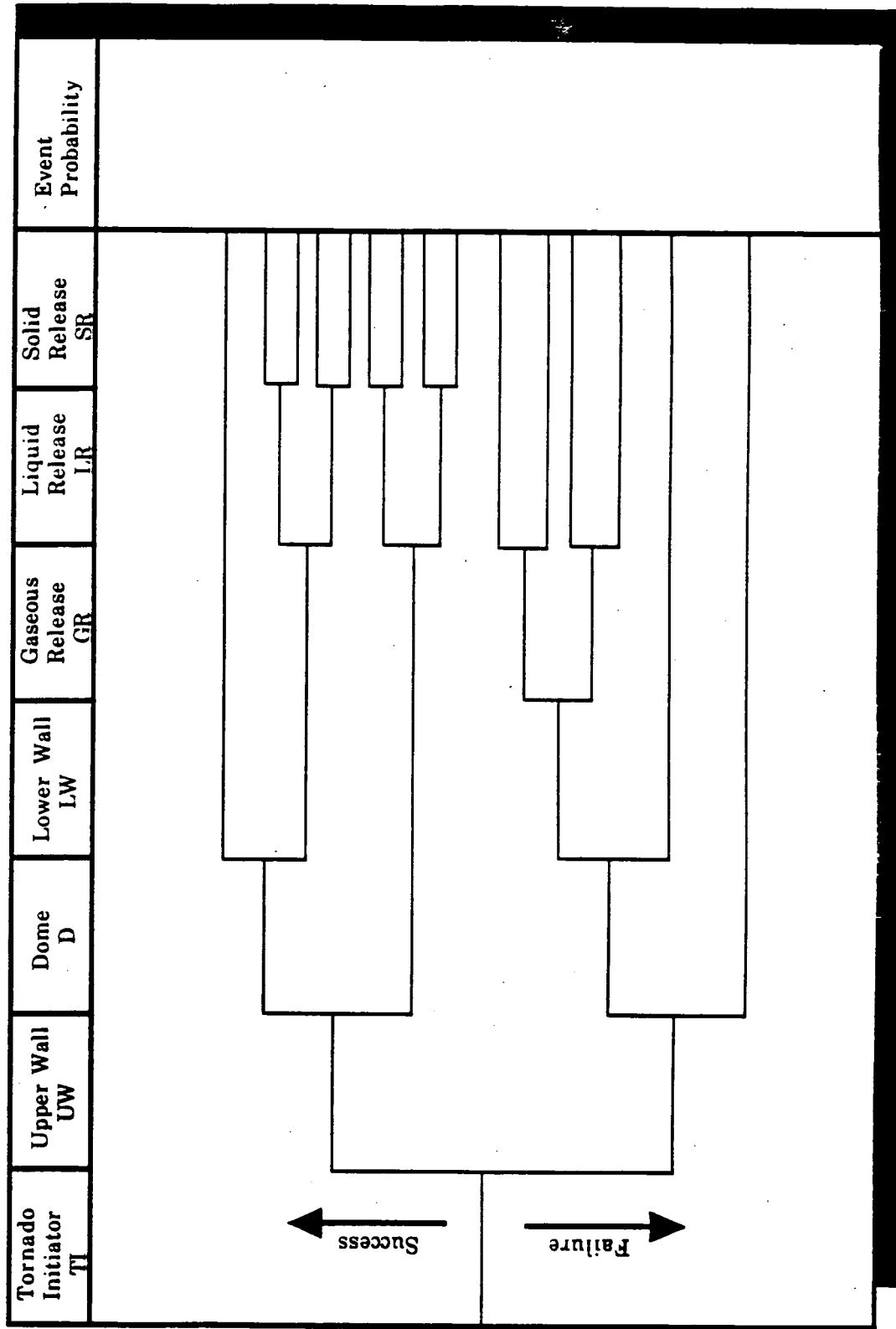
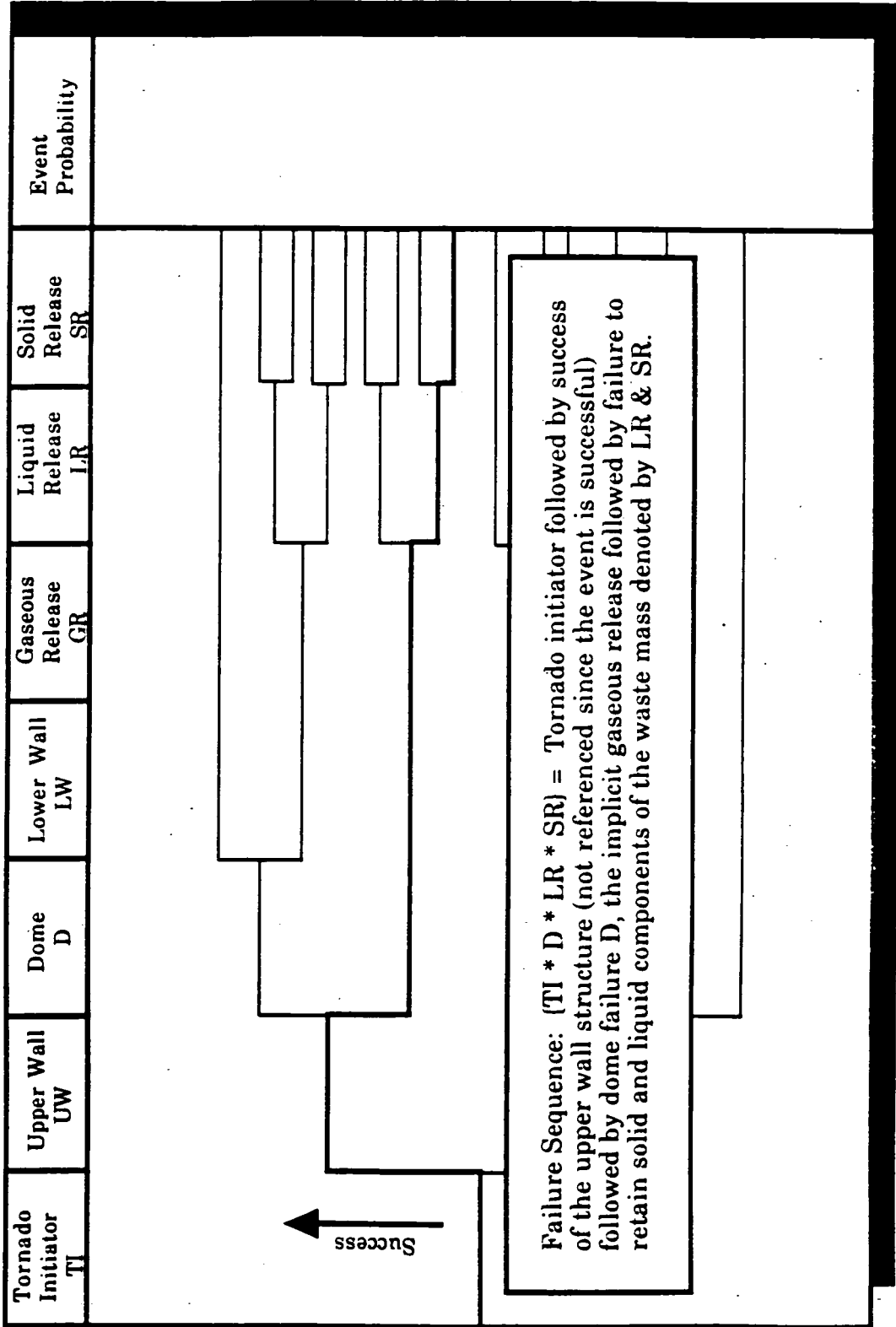


**Figure 1.6: Loss Of Integrity From Natural Forces (Tornado) Event Tree
For K-65 Storage Silos Illustrating A Typical Sequence**



which may cause a potential failure of that system. In order to accomplish this task detailed knowledge of the system as well as its function is required. Once the system function is fully defined, block diagrams relating one component or subsystem to the others can be constructed. The block diagrams are evaluated against the actual system and modifications are made if needed. The constant refinement of the block diagrams forms the basis of the fault tree construction. Once the final block diagrams are made the interaction of the components and subsystems are modeled using logical constructs following Boolean Algebraic techniques.

The relationships can be modeled using these methods and then represented using the logical gates such as "AND" and "OR" as well as others. These two gates are the basic operators used in Boolean Algebra. The "AND" gate implies that all of the events are required to occur to reach the next level of results. The "OR" gate means that any of the events can occur and the next level of results is reached.

In fault tree construction, the system failure event that is to be studied is called the *top event*. Successive subordinate (subsystem) failure events which may contribute to the occurrence of the top event are then identified and linked to the top event by a series of logical functions ("AND" and "OR" gates). The subordinate events are subsequently broken down to their logical contributors, and in this manner, a fault tree is constructed.

When a contributing event can no longer be further divided, the corresponding branch is terminated with a *basic event*. Basic events are statistically independent unless they are common cause failures. Such failures are those that arise from a common initiating event. Such is the case for the *external events* (seismic activity and severe weather) used in this analysis.

1.2 K-65 Structural Evaluation

The structural evaluation of the silos was made by Camargo Associates and Bechtel National Incorporated. The structural evaluation was made using finite element modeling. The finite element model was used to simulate a variety of loads on the silo dome and walls. Both live and dead loads were evaluated and the results were provided in terms of stresses and strains on the structure as well as critical loads to the dome center and outer regions (Camargo,1986; Bechtel,1990).

These two studies were the principal sources of detailed information concerning the silo structures for the UC risk assessment. The data, results, and conclusions obtained in these reports was considered in the analysis and the inconsistencies and discrepancies in the data and results were accounted for in as a practical fashion as possible.

The limitations associated with the Camargo and Bechtel reports had significant influence on this study in the areas of structural response to a variety of forces and on the current state of the structure. The primary affect is in the estimation of degradation rates associated with the reinforcing steel and concrete quality. The determination of the effect a tornado will have on the silo structure is also affected by the uncertainties in the two studies. Details of the response of the silos to tornados and to earthquakes is covered in the next section.

1.3 Failure Potential

The modes of failure considered in the risk assessment cover two main areas: 1) natural forces and 2) concrete degradation. These two areas were selected initially due to the severity of the consequences in the event of failure. Since the risk is the probability multiplied by the consequences, the risk will be greater provided that one or the other or both of the following are available; 1) the probability of failure is high or 2) the consequences of failure are high. The failure modes or initiators considered are: 1) failure, of the silo, due to concrete and supports suffering extensive fatigue from weathering and wear, 2) failure due to a seismic event, and 3) failure due to severe weather. The first failure mode corresponds to the case where the consequences are low to moderate and the probability is considered great. The second failure mode is taken to be moderate to low probability and moderate to low consequences. The third failure mode is considered to be a moderate to high probability with the consequences expected to be quite severe.

These three failure modes are therefore expected to bound the risk associated with the K-65 silos from low to high. The analysis illustrates the relationship between the failure modes considered, the resulting consequences, and the overall risk. Failure sequences containing the event trees for each failure mode will be described in detail in section 2 of this report. The total number of possible sequences is directly related to the number of events in the tree. In the case of the degradation of the concrete failure mode, the event tree has a total of four events plus the initiator. The total possible sequences is then simply 16 or 2^n where n represents the number of events not including the initiator. The total possible paths are then considered the failure sequences for the system in question.

The probability of each sequence was evaluated and ranked according to significance. These failure sequences are then linked with the release and transport sequences in order to evaluate the total probability of exposure given some initiating event. The overall relationship of these event trees are described in section 2.

1.4 Release Potential

The release potential of the residue material was evaluated after determination of the possible failure modes. The release potential was much more difficult to address due to uncertainties in the waste mass form and composition. The amount of water and silicates can alter significantly affect the mobility of the radioactive contaminant component.

Detailed analysis of the forces associated with the initiating events and external events resulted in a variety of scenarios depicting the release of waste material. The types of release mechanisms involved consist of removal of the waste material by means of wind action, rain or flooding, violent seismic events, and by human interaction. The human interaction

potential was eliminated due to security measures taken at the site. The results of intense seismic action can affect the silo structure but do not produce accelerations necessary to remove waste residues.

The effects of wind and rain however must be evaluated in detail to examine the possibility that waste material will be released following a hypothetical failure of the structure. The three principal initiating events considered in this study (seismic, severe weather, and weathering & wear) were evaluated and found to correspond to two primary groups of release potentials. The first group consisted of normal or calm weather conditions (including light rain) and the second was determined by turbulent weather conditions and violent periods of precipitation.

1.5 Exposure Assessment

As described above, event trees relating probabilities to the transport routes were developed. This facet of the project required a new approach to environmental transport modeling using the PRA methodologies. This method has the advantage of enabling the analyst to quickly determine the significant transport routes from the total array of mechanisms. This determination is made using event and fault trees to represent the physical situation. The event trees have a number of other factors quantified in addition to the sequence probability. These other factors will include the time frame under consideration, the concentration of the contaminant, and the spatial dependence of the transport process. Applying the PRA approach to the transport processes results in a function instead of merely a probability. This function was manipulated in a manner consistent with accepted practices resulting in a more detailed and informative solution set.

Typically in PRAs associated with nuclear power facilities the consequences of a release are modeled only over the time frame of the accident. The principal transport route recognized as applicable in nuclear power plant PRAs is the atmospheric pathway. This study was commissioned to evaluate the risk from the silos over a five year time frame. The extent of transport of radioactive contaminants in the environment over a time span of five years can be significant. The region in the vicinity of the silo structures located on the FMPC site is a small creek which is frequently at saturated conditions (flowing water) during parts of the year, which can add significantly to the water transport routes (both in surface and ground water). Additionally the ground in this region is of variable slope. This results in an increase in the potential for transport by the erosion and runoff processes. The surface vegetation growth in this area is primarily composed of grasses. This open field situation tends to increase the transport of surface contamination via the atmospheric resuspension process. The details concerning the transport of radioactive material in the environment are more complex and less understood than the considerations in a typical PRA.

Pathway Analysis And Dose Assessment

The pathway analysis is inherently linked to the transport processes. The additional considerations and calculations involve specifically those routes through which radionuclides can result in the dose of humans. The transport processes of most interest are those which lead to radionuclides entering the food chain, being available for inhalation, or are present on surfaces and contained in materials, buildings, and other places which can lead to external doses. The foodchain is primarily affected when radionuclides are present in vegetation, water, and livestock. The inhalation route is determined by airborne contaminants either as a result of the initial release or from the resuspension of contaminated dust. The residues of the various transport mechanisms result in the contamination of buildings, the ground surface, plants, roadways, and even people from the deposition processes, erosion, and surface water sources drying out.

Each of the possible pathways leading to the exposure (potential or actual) must be evaluated in order to evaluate the consequences (in this case the dose) and eventually the risk. Detailed pathway analysis techniques and models have been established and were evaluated using the same PRA techniques as described for the transport processes. The solutions of the pathway models resulted in a quantity that is represented using a column matrix or column vector. This approach permits the additional information to be taken into account in the risk estimates and still assumes the models are linearly related. The complexity associated with using nonlinear models for either the pathways or the transport processes is beyond the scope of this project. Assuming these processes are linear naturally induces a measure of uncertainty. The uncertainty analysis will consider this fact in the calculations of the confidence levels associated with the final risk estimates.

1.6 Risk Characterization

After completion of the transport and pathway probabilities, the final step in the risk assessment is performed. This step involves the quantification of the consequences. The consequences are based on the dose received by a member of the public or a member of the workforce on site. The dose alone can be evaluated with respect to any and all applicable standards or in terms of the expected non-stochastic effects (short term or immediate). Another method for evaluating the consequences is in terms of the stochastic effects (long term cancer incidence) associated with exposure to low doses of radiation. These effects are much more difficult to quantify due to the nature of the effect of radiation on the human body and due to the inherent uncertainties involved with the dose analysis. The currently accepted risk estimates associated with exposure to radiation are represented as a risk of developing a fatal cancer in an individuals lifetime as a result of receiving a unit quantity of dose (from all sources). This unit is typically taken as the rem or sievert. A seivert is a unit of absorbed dose equivalent and is equal to 100 rems.

The risk estimate used for this study was 2×10^{-4} per rem (ICRP,1988). Which implies that an individual who receives one rem of dose from all sources of radiation has a 2 in 10,000 chance of developing a fatal cancer in his or her lifetime. The BEIR V results have also been reviewed and considered in the characterization of the risk associated with the exposure to radioactive material in the environment. BEIR V results were not used directly in this study due primarily to the continuing debate concerning the appropriate use and applicability of those results. It is estimated that the risk may increase by a factor of 3 to 5 when using the BEIR V results. The difficulty associated with this type of risk estimate is that there is no consideration of the time frame of the exposure or the long term response of a population to the latent effects of the initial exposure ie the individual in question may have genetic predisposition to or a tolerance for developing a cancer.

The approach taken in this study was to use the previously accepted (prior to BEIR V) risk estimates as the basis of comparison for the final risk resulting from the hypothetical failure of the silos and from the continuous release of radon gas. These comparisons will be presented in a number of different formats to provide the greatest measure of confidence and perspective given the nature of the situation being assessed. As an example consider the risk of developing a fatal cancer after suffering a dose of one rem, this can be compared to the expected or natural cancer incidence. The natural or background cancer rate is on the order of 2.1 in 10 and this indicates that two individuals out of every ten in the general public will develop a fatal cancer whether exposed to radiation or not (AAA,198?).

The purpose of this study is to evaluate and assess the risk from the present condition of the silos. The time frame for this evaluation was taken to be 5 years and the risks from continuous and hypothetical releases of radioactive materials were considered. The risk coefficients described above were used across the various stages of the exposure assessment and therefore can be considered consistent. EPA slope factors were also considered to provide an additional measure of the risks as well as the variability and uncertainties. For these reasons the doses and risk estimates made serve as a basis for comparison between the trivial and significant contributors to the overall health impact.

2.0 K-65 SILO FAILURE EVALUATION

This section discusses the silo structures in detail with primary emphasis on the failure potential in both mode and probability. This section of the report deals with the specific data used in this analysis and the general form and condition of the silos. The silo failure evaluation section is also intended to provide the models used and the assumptions employed in the evaluation of the failure potential of the K-65 silos. The background information, concerning the silos and use, is provided here for completeness and continuity. Most of this information can be found in other reports describing the silos. Some of these additional reports were used as reference material in the preparation of this report and are cited in the reference section.

This section is divided into six parts. The first and second parts concern the silo structure with the first discussing the historical, present, and future conditions and the second dealing with the potential failure modes. Part three considers the failure initiators and part four provides the specific failure sequences analyzed. The radionuclide inventory or source term is presented in the fifth section. Section six presents the overall probability of failure and release including the release mechanisms and magnitudes. The majority of the available data is discussed and analyzed in this section. Some information dealing with the surrounding area and population distributions will be presented in the next section where the exposure assessment is considered.

To determine the structural condition of the silos and the probability of failure much of the analysis was dependent on the work of Camargo Associates Limited and Bechtel National Incorporated, whose reports addressed the structural integrity of the silos through both destructive and non-destructive testing techniques (Camargo, 1986) and (Bechtel, 1990). Additional data and information was supplied by WMCO and the U.S. National Oceanic and Atmospheric Administration (NOAA).

The non-destructive testing results, conducted for Camargo, provides the data that is used for the evaluation of the probability of dome failure due to natural conditions. It is important to note that significant discrepancies were found in these results. Test locations for the non-destructive testing procedures do not correspond to initial design specifications. The validity of this analysis is determined in part by the availability, quality, and accuracy of the information supplied to the University of Cincinnati.

2.1 Silo Structure

The K-65 silos are essentially large concrete waste containers. The design and use of these structures was for temporary storage of radium bearing residues remaining from uranium ore processing. The waste containment structures, silos 1 and 2, are located at the west side of the FMPC site. These silos were constructed in 1952 and have been used since then as storage facilities for the radium bearing residues from pitchblende processing. The silos are cylindrical in construction with an internal diameter of 80 feet. The corresponding cylindrical height of these silos is approximately 27 feet. A concrete dome rises to just over 9 feet above the top wall line; the thickness of the dome is 4 inches at the center and tapers to 8 inches at the wall/dome intersection.

Remedial Actions

By 1963 the exterior surface of the silos had suffered major deterioration. Large areas of the concrete walls have degraded which has lead to the exposure of the post-tensioning wires. Subsequently, patches of the wires have become severely corroded and eventually broke. Repairs to the damaged surface began in 1964, at which time a waterproof sealant was applied to the external walls. In addition, an earthen embankment was built to the top of the walls. This embankment was intended to provide an external force to counteract the internal pressure applied to the wall from the waste mass. In addition, the embankment was expected to significantly reduce radon emission. The recommendations of subsequent structural investigations, have resulted in the construction of a temporary steel and wood dome, with a 20 foot radius, to be placed on top of the existing domes. In addition, a neoprene membrane was applied over the outside of the dome to minimize radon emanation and to prevent water seepage into the silo dome cracks. Table 2.1 delineates the chronology of the construction and use, the various modifications, and major studies made on the silo structures.

Table 2.1 illustrates the various changes that have occurred to the silo from the beginning of the construction to the present. The physical processes acting on the silo have not remained constant over the life of the structure due in part to these modifications and adjustments. The addition of gunite to the exterior walls in 1963 and the earthen berm in 1964 Would have considerably reduced the wear and tear on the silos. Since no significant testing or analysis was performed during this time frame, in order to quantitatively evaluate the structural integrity, the results of the Camargo and Bechtel studies are assumed to apply to the overall life of the silos. The total age of the silos is essentially 38 years, however, since the silos were filled to capacity by 1958, the berm was added by 1964, and the Camargo study was completed by 1986 another estimate of the age of the structures for evaluating the probability of dome failure was taken to be 28 years. Both of these estimates of the life of the structure are considered in the evaluation of the potential for failure due to natural processes.

Table 2.1 K-65 Chronology Of Events

<u>Date</u>	<u>Milestone or Event</u>
1951	Construction begins
1952	Construction complete
1958	Silos filled to capacity
1963	Repairs made to the silos
1964	Earthen berm added
1979	Vents sealed
1983	Embankments enlarged
1985	Camargo non-destructive tests
1986	Protective covers added to center 20 ft.
1986	Waterproof membranes added to dome top
1987	Foam coating applied to domes
1989	DOE inspections
1989	Bechtel performs further analysis

Current Conditions

A complete structural analysis of the K-65 silos was conducted, under contract of the Westinghouse Material Company of Ohio, by Camargo Associates, Limited (Cincinnati). The purpose of the analysis was to determine the structural stability of the silos, and to identify any potential structural problem that would require remedial action. The conclusions of this study have a direct bearing upon this present analysis; the non-destructive testing results will be used to quantify the possible mechanisms of failure.

The major conclusions of the Camargo analysis are:

1. Major portions of the domes are capable of supporting their weight plus a live load of 20 psf. The center portion of each dome is critical for any loads. There is a general thinning of the concrete domes with sharp undulations of the interior surface. Associated with the thinned dome sections are large cracks; the interior surface exhibits various stages of deterioration. The silo dome thickness and general quality deteriorates progressively moving from the dome/wall intersect to the dome top.
2. The walls are believed to be stable as the material and berm are counteracting. The silo wall thickness, concrete quality and remaining percentage of horizontal preload wires have deteriorated progressively moving from wall top to bottom.

3. The base slab (floor) was not fully investigated due to the embankment. The condition of the base slab is thought to be similar to that of the walls.

4. The walls and the base slab are considered acceptable from a structural standpoint; Camargo quotes a maximum life expectancy of between 5 to 10 years. The domes were considered to be structurally defective and were assessed to have no life expectancy in 1985.

Field Investigations

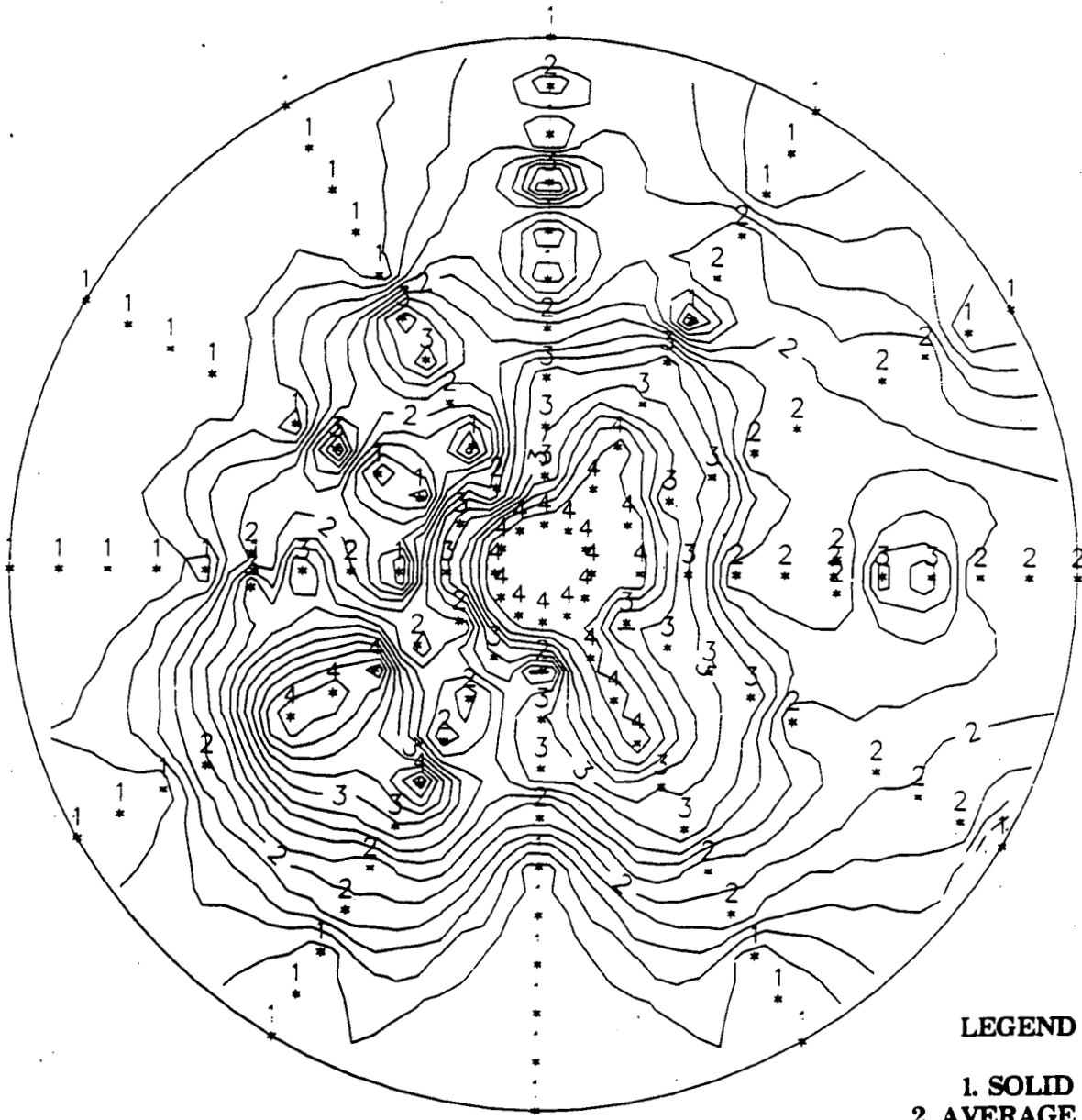
Pulse-echo techniques were used to determine concrete quality. These investigations were conducted by Muenow and Associates, Inc. on behalf of Camargo. This analysis is expected to provide quantitative results for:

1. Compressive stress of concrete
2. Thickness of dome and walls
3. Percentage of reinforcement remaining in dome and walls.

From this data, regions of substantial weakness can be identified. Percentage loss in compressive strength, thickness and, reinforcement will aid in substantiating failure probabilities. Initial conclusions from the analysis show that there is considerable spalling of the interior surface of the dome. There is no pattern to the thinning, however, there are significantly large areas of spalled concrete. Figure 2.1 is a topographical map of the dome surface of Silo 1; values of concrete quality are shown relative to their position. As will be explained later, quality 1 is rated as being good and increases to quality 4 which is questionable. The quality is shown to deteriorate towards the center of the dome where there are larger areas of quality 4.

Considerable wall cracking and loss of post-tension wires is present in both silos. Maximum reduction in wall thickness is approximately 2 inches, however, the vast majority varies between 0.05 to 1.0 inches. Figure 2.2 shows the variation of wall thickness with wall height. A maximum of 25% of the horizontal reinforcement steel has been lost in specific areas.

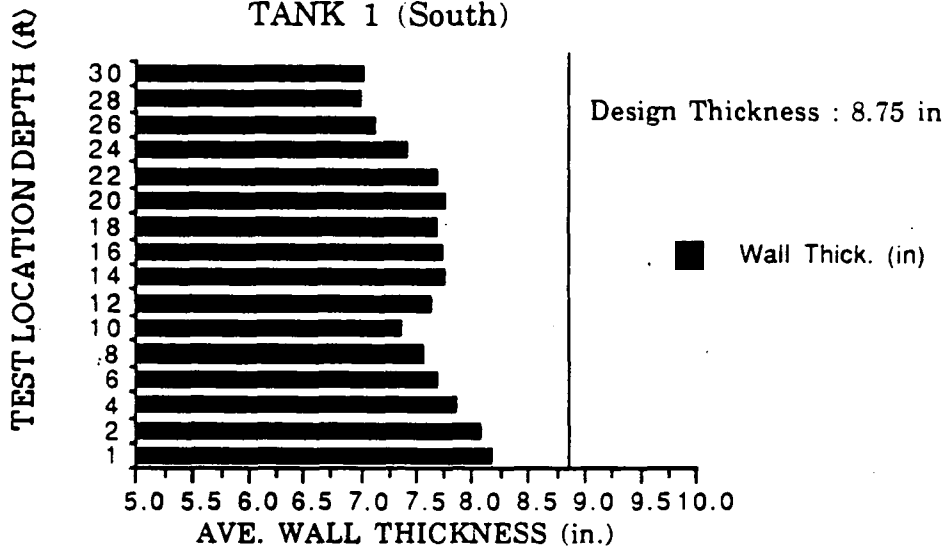
Figure 2.1:
Topographical Map of Concrete Quality:
Dome: Silo 1



LEGEND
1. SOLID
2. AVERAGE
3. MODERATE
4. QUESTIONABLE

Figure 2.2 : Reduction in Wall Thickness

TANK 1 (South)



2.2 Potential Failure Modes

There is a wide range of possible ways in which the silo structures can fail. The results of a particular failure are also widely varied. For the purposes of this PRA analysis the entire range of failures were grouped into two specific categories: 1) those relating to the possibility of an acute release of the radioactive waste material and 2) those failures leading to long term or chronic releases of radioactive material and radon gas. By grouping the potential failure modes into these categories the analysis was performed with the ultimate consequences, and therefore risk, in mind.

Each failure mode is represented using an event tree to describe the specific events that lead to the acute or chronic release sequences. The event tree is a powerful tool for evaluating those sequences that represent the greatest consequence and therefore the highest risk. These event trees represent the possible sequences associated with the lowest, intermediate, and highest magnitude tornado events. The specific nature of the sequence initiators is discussed in the next section.

Failure Modes Considered

The modes of failure considered for this analysis cover two primary initiators; 1) severe weather conditions (tornado) and 2) natural degradation of the concrete structure due to long term weathering and wear. A third failure initiator considered was seismic activity. The response of the silo structures to seismic events was evaluated using the results of the finite element model by Camargo and Associates and the results of a similar study by Bechtel. Analysis of these results found that the structural response of the silos to a seismic event would not lead to failure. The two primary failure initiators considered represent the greatest consequences (with respect to the release of the waste material) in the event of failure. Relevant silo failure possibilities were developed and qualified in the status report, (February, 1990). Of the three substructures considered, (Wall, Floor slab, Dome), the silo domes present the highest probability of immediate failure and the highest risk related consequence.

The wall and floor failure consequences, when compared to that for the dome, do not contribute significantly to risk. The potential for failure of the wall to impact on the dome was considered to be significant and was therefore modeled and analyzed. The wall was divided into two components for evaluation. The division was made with respect to the area balanced by the waste mass and burm, the lower wall, and the region with only the burm acting on the wall, the upper wall structure. Information regarding the temporary dome structure is not available on which to evaluate a basic event contributor.

Acute Failures

The acute failures are regarded as those failures which result in structural damage coupled with a short term high magnitude release mechanism. The short term release mechanism is based on the assumption that WMCO will take immediate corrective or remedial action in the event of an acute failure. The high magnitude relates to the quantity of radon-222 released or the total amount of residue material removed.

Acute failures include structural failures that can result in large quantities of radon gas, residue material, and leaching or washout of residue material. The evaluation of this class of damage and release modes forms the basis of the dose and exposure assessment. Models which best represent the physical situation and take into account the uncertainties in the composition and form of the residue material are needed. The models used were based on the ability for high winds to remove the waste material.

Chronic Failures

The chronic failure modes consider the current situation where radon gas, through the process of diffusion, is constantly being released. Subtle changes in the silo structure may result in the increased release rate of the radon gas and therefore must be considered and analyzed.

Damage classes corresponding to minor cracks in the wall and dome are grouped in the chronic release mode due to the time frame under which the radon-222 is released. Minor cracking may take days or even months to develop to the point where increased emissions of radon would be noticed. This time frame results in a release, transport, and exposure associated with chronic failures. The bridge between the chronic and acute cases was also determined by the availability for residue material to be released coincident with the radon gas. The chronic modes are assumed to release only the radon gas.

The analysis of the release and transport of the chronic emission of radon gas was made using actual monitoring data and numerical dispersion models. The details of this analysis is presented in the Exposure And Dose Assessment Section.

2.3 Failure Initiators

This section of the report considers specifically the failure initiators. The potential for failure of the silos to contain the radium bearing waste and the radon gas as originally intended can be addressed by assessing the causes or events which initiate the failure of the structure. The potential for failure is increased by a number of different factors. These include events both internal and external to the structures themselves. The internal events are simply those corresponding to the structural integrity of the container to continue to support the static loads resulting from the mass of the waste material.

The external events are considerably more difficult to quantify. These include the action of the natural environment on the structure, such as freezing, thawing, and erosion. Additional natural external events are not as evident or probable, these being seismic activities and severe weather. Seismic activity sufficient to cause structural damage is considered to be extremely remote (Camargo, 1986). The action of the wind, either from strong uniform gusts or from tornado type cyclonic turbulence is considerably more probable and devastating. This section of the risk assessment deals with the natural internal failure initiators and the natural external failure initiators namely tornados or severe weather.

Severe Weather

This section addresses the external events of severe weather in the form of tornado type cyclonic wind action. The data evaluation, analytical methods, and the estimated probability of occurrence and associated impact of this external event, on the silos, is presented here. Considerable data was obtained from NOAA detailing the occurrence of severe weather phenomena throughout the United States. For purposes of this study only severe weather occurring in Ohio, Indiana, and Kentucky was initially considered. The data evaluated covered a time frame from January 1916 to April 1989. Some gaps in the quality and usefulness of the data existed and therefore the probabilities used in the assessment were based on the data which was the most complete and applicable.

Tornados are ranked first in number of deaths and second to tropical storms in total dollar damage in the United States, when considering atmospheric-related catastrophes (excluding air pollution). Since 1963 the average annual dollar damage resulting from tornados is approximately 200 million (Dames, 1975). The cost damage potential of a single tornado as in the Xenia, Ohio tornado of April 3, 1974 can nearly reach the 200 million dollar figure. A series of funnel clouds were reported as recently as June of 1990. The storm system from which these tornados were spawned covered nearly five counties in Ohio and Indiana. The damage resulting from these tornados was estimated at or above the 20 million dollar figure further indicating the damage potential and frequency of occurrence. One tornado was also reported to have touched down within a mile of the FMPC

site. This most recent tornado occurrence was added to this report for two reasons: 1) to illustrate the frequency, destructive power, and the proximity to the FMPC site and 2) to serve as a reminder that tornados are random occurrences of nature and that this single event will not significantly influence the probability calculations or the estimates of risk that result.

A tornado striking one or both of the silos has a real potential for significant damage as well as possible environmental consequences. This risk assessment is centered around the probability and consequences of just such an occurrence. To insure that a certain risk level is attained or exceeded for the K-65 silos, a statistical description of the recurrence of a given intensity of tornadic forces is desired. Since "direct" measurements of tornadic occurrence and the associated forces are generally not possible, it is important to critically examine the existing data and related meteorological information in order to understand the phenomena.

Statistical analyses are limited by the quality and quantity of the data. The statistical approach used in this study incorporates the best data and methods available at the time of the analysis. Only tornado incidents where the location, time, date, path length and width, strength, and damage estimates were used in the study. The data collected covered the three state region of Ohio, Indiana, and Kentucky for the years from 1978 through April 1989. Tornado reports based on sightings by members of the public and generally not substantiated by radar or official observations were not included in the probability analysis due to uncertainties created as a result of unknown bias. These types of biases in the state of Indiana's and Kentucky's tornado reports resulted in the use of only the data from Ohio.

The intensity of a given tornado was found to be directly related to the path width and the track length (Pearson, 1971). The potential for destruction is directly proportional to the intensity. The length of time that the tornado is in contact with the ground also has significant contribution to the damage potential. The data used for this study included 117 tornados in Ohio over approximately a 9 and 1/4 year period from January 1980 through April 1989. The tornados were ranked according to wind speeds, intensity level, area covered, and damage. The Fujita intensity scale was used to classify the tornados and is provided in Table 2.2. The classification of the tornados for this study were taken from NOAA reports. This information was compiled by National Weather Service stations throughout Ohio, Indiana, and Kentucky.

Due to the requirements of this risk assessment, to evaluate the risk from the K-65 silos, three related analyses are needed. The first is obviously the probability of occurrence of a tornado, the second relates to the characterization of the tornado, and the third is the evaluation of the damage resulting from the atmospheric turbulence. The methodology and results of the occurrence probability will be presented first followed by the methodology used in estimating the damage or destructive potential which will include a discussion on the characterization of the tornado event.

Table 2.2: FPP Tornado Scale

(Fujita and Pearson - May 1978)

Scale	Maximum Windspeed (miles per hour)	Path Length (miles)	Path Width (miles)
F0	40 - 72	0.4 - 0.9	0.0034 - 0.0097
F1	73 - 112	1.0 - 3.1	0.0102 - 0.0312
F2	113 - 157	3.2 - 9.9	0.0318 - 0.0994
F3	158 - 206	10 - 31	0.10 - 0.30
F4	207 - 260	32 - 99	0.40 - 0.90
F5	261 - 318	100 - 315	1.0 - 3.1

Probability Of Occurrence

The ranking of the tornados resulted in the tabulation of the frequency of occurrence, of each tornado class, as well as the probability per unit area and per year for a tornado of a given intensity. These results are illustrated in Table 2.3. Further analysis of the data provided a relationship between a given wind speed and the wind loading. The forces resulting from a tornado are complex and extremely difficult to model. Most of the available data has come from tests performed in wind tunnels. The direct applicability of these results is not clearly known at this time. General empirical equations have been developed from these tests and are readily used in the nuclear power industry to evaluate the response of a given structure to tornados. The NRC Regulatory Guide 1.76 delineates the maximum wind speeds and pressures drops required to be analyzed for applicability to structural response.

Approach

It is realistic to consider tornados as random phenomena in nature as are hurricanes, earthquakes and floods. Natural phenomena may be described as either deterministic or probabilistic. The probabilistic approach is by no means vague or unreliable. Probability, like other theories, should be viewed as a conceptual structure and its conclusions rely on logic.

The overall approach applied to the quantification of the frequency of a tornado and the effect of the phenomena on a specific structure was broken into two types of analyses. The first used straight forward statistical analysis of the total number of tornados, the area affected, and the time frame covered. The second involved two separate probability distributions in order to evaluate both the probability and the consequences of a single tornado event at the FMPC site.

The first approach assumes that the distribution of tornado events in time is random and that the distribution fits a Normal distribution. This allows for the estimation of the mean and variance for the occurrence of tornado events per time, in a given area, and for a given intensity class. The second analysis evaluates further the relationship between the occurrence of a tornado and the effect the event will have on a given structure.

This is accomplished by utilizing two coupled distributions. The first distribution governs the discrete probability of a tornado event in time and the second distribution approximates the continuous distribution of the resulting wind velocities. The discrete distribution used is the Poisson and the continuous approximation utilizes the Gaussian distribution. This approach results in the estimation of a risk level associated with the occurrence and effect of a single tornado event in the assessment period.

**Table 2.3: Summary Results Of
Tornado Data From 1980 To 1989**

Intensity	Area Covered (sq. mi.)	Number of Occurrences	Probability Per Year-Per Square Mile
F0	0.74	18	1.91E - 06
F1	14.23	68	3.65E - 05
F2	11.02	23	2.83E - 05
F3	7.59	5	1.95E - 05
F4	4.77	2	1.22E - 05
F5	10.25	1	2.63E - 05
Total	Total	Total	Total
	48.62	117	1.25E - 04
Total Area Of Interest (sq. mi.)			
41,004			

555

The risk level is defined as the probability of at least one occurrence during the life expectancy of the system considered. The risk analysis consists of collecting data on tornados with their assigned intensity classifications. A point process, Poisson, was used in modeling the tornado occurrences, thus providing the relationship between the risk level and the ratio of the return period to the life expectancy (5 years as defined in the contract). The combination of results from a best-fit density function and a best-fit point process yields the return period and thus tornado intensity (wind velocity) for the specific loads identified as critical for the K-65 silos.

Density Function

Although a discrete intensity scale is used for tornado classification, the wind speed will be the parameter ultimately used for the damage potential on the silos. Therefore, a continuous rather than a discrete density function will be used for the risk analysis. The mean wind speeds will be used to describe each intensity class. The normal or Gaussian distribution was selected to represent the tornado distribution. The X^2 test is used to compare the expected results with the data. The mean and standard deviation are estimated using the maximum likelihood method given by Equations 2.2 and 2.3.

$$\widehat{m} = \bar{x} = \frac{\sum_{i=1}^n x_i}{n} \quad (2.2)$$

$$\widehat{\sigma}^2 = \frac{\sum_{i=1}^n (x_i - \widehat{m})^2}{n - 1} \quad (2.3)$$

where:

\widehat{m} = Mean value.

$\widehat{\sigma}$ = Standard deviation.

n = Number of elements in the sample.

x_i = Wind speed (mph).

The point process is based on the Poisson process which assumes the rate of occurrence is constant and independent of time. Using the Poisson process allows for the relationship between the risk level and the ratio of the return period to life expectancy to be site independent.

In the Poisson process the density function for t, the time between occurrences is given by Equation 2.4 (Dames, 1976).

$$f_T(t) = \mu e^{-\mu t} \tag{2.4}$$

and the distribution function of t is given by Equation 2.5 (Dames, 1976).

$$F_T(t) = 1 - e^{-\mu t} \tag{2.5}$$

and the probability function for 'N' occurrences as a function of the rate of occurrence μ is given by Equation 2.6.

$$P(N = n/\mu, t) = \frac{e^{-\mu t}}{n!} (\mu t)^n, \quad n = 0, 1, 2, \dots \tag{2.6}$$

where:

- μ = Rate of occurrence.
- T = Life expectancy.
- t = Time of interest.
- $f_T(t)$ = Probability density function.
- $F_T(t)$ = Probability distribution function.
- n = Number of elements in the sample.
- $P(N, t)$ = Probability of 'N' occurrences.

If the rate is assumed uniform inside the area, then the rate in a smaller area can be obtained by reducing the rate by an areal ratio. For example if 'a' and 'A' denote the reduced and original areas, respectively, then the rate inside the smaller area 'a' will be given by Equation 2.7.

$$\mu' = \mu \left(\frac{a}{A} \right) \tag{2.7}$$

The probability mass function inside the 'a' (in this analysis 'a' represents the area of influence for the silo structures) is then given by Equation 2.8.

$$P(N' = n/\mu', t) = \frac{e^{-\mu' t}}{n!} (\mu' t)^n, \quad n = 0, 1, 2, \dots \tag{2.8}$$

The method of maximum likelihood is easily applied to the density function where the only parameter, μ , is given by Equation 2.9.

$$\hat{\mu} = \frac{n}{\sum_{i=1} t_i} \quad (2.9)$$

Tables 2.4 and 2.5 delineate the data and results of applying the statistical analysis to the tornado data, while the risk factor, for the Poisson process, can be represented by Equation 2.10.

$$r = 1 - e^{-L_x(x) \hat{\mu} \times T} \quad (2.10)$$

The reliability function, $L_x(x)$, for wind speed x , is defined as the probability of the wind speed being at least x and is obtained by numerical integration. The risk factor is estimated assuming that there is a single tornado event in the life of the facility.

Incorporating this assumption removes the conditional probability of tornado occurrence from the calculations. In this way the damage potential of the wind and pressure forces are presented in terms of a risk estimate. The nature of risk estimates dictates that the basic constituents of the probability and consequence calculations be clearly stated and defined. When considering two different risk numbers a comparison can only be made when the basic components are similar.

The calculations presented here form the basis of the final risk estimates associated with the tornado as an initiator. The next step is to evaluate and compare the consequences of a single tornado event. The consequences associated with each phase of the study, such as the estimation of the damage to the silo structure, the release of radon and other radionuclides, and finally the environmental transport leading to human exposure form the basis for overall risk comparisons. Finally the consequences of concern for the overall study are the increases in cancer fatalities (or incidence in the EPA methodology) associated with the exposure to radioactive materials. In order to achieve a basis for comparison the risk estimates provided in Column A of Table 2.5 are presented. The risk factor for the single tornado event in the life of the plant at first glance appear to overestimate the risk of silo failure as a result of a tornado. The intent is to illustrate the significant probabilities and risks associated with the relatively low wind speeds. The numbers provide a comparison that would be less obvious when the probability of the tornado occurring is factored in.

Table 2.4: Results Of The Statistical Analysis

intensity	number of occurrences	expected value	mean wind velocity (mph)
F0	18	16.85	60.0
F1	68	71.32	95.0
F2	23	21.43	135.0
F3	5	4.79	185.0
F4	2	1.37	230.0
F5	1	0.78	290.0
μ		σ	χ^2
	105.0	37.3	0.71

Table 2.5: Probabilities And Risk Factors

intensity	probability $L(x) = 1 - F(x)$	wind velocity (x, mph)	Column A risk factor* r (x)	Column B Risk Based on Probability of Tornado in Five Years
F1	2.5 E - 1	112	3.7 E - 1	2.3 E - 4
F2	1.75 E - 2	135	4.13 E - 2	2.6 E - 5
F3	3.34 E - 3	185	5.78 E - 4	3.6 E - 7
F4	2.78 E - 6	230	6.13 E - 6	3.8 E - 9
F5	2.43 E - 7	290	7.35 E - 8	4.6 E - 11

$$\hat{\mu} = \frac{n}{\sum t_j}$$

$$r(x) = 1 - \exp(-L(x) \hat{\mu} T x)$$

* Based On A Single Event Occurring In The 5 Year Life Time

The obvious comparison here is that the damage potential (risk factor) is significant for average wind speeds on the order of 112 miles per hour. The probability of this wind speed occurring is quite large at 25%. The forces associated with this wind speed are 288 (psf) tension and approximately 50 (psf) compression. These forces are considered (based on the structural analysis) to be sufficient to fail the silo dome. Although these forces are not the maximum values the damage to the silo is expected to be such that a significant quantity of the radionuclide inventory could be released. The risk (consequence of the tornado on the silo) associated with the failure of the K-65 silos over the next five years is best represented by the risk factors in column A of Table 2.5. The risk estimates provided in column B of Table 2.5 are presented to approximate the total probability (tornado frequency and damage potential) and are therefore form a basis of risk comparison with the chronic or continuous release of radon. The values in column B include the damage potential, for each intensity class, and the probability of a tornado event in the five year assessment period.

The probabilities and risk factors presented in Table 2.5 were used to evaluate the maximum damage potential and therefore the maximum quantity of radioactive material that could be released to the environment. The probabilities of silo dome failure, due to natural degradation, and of a tornado occurring, per year and per square mile, were used in the final risk estimates relating the total cancer fatalities or cancer incidence as a result of human exposure to the radioactive material that hypothetically could be released. These values are delineated in Table 2.6. The central difference between the probabilities listed in Table 2.6. and those in Table 2.5 is that the net effect or consequence considered is different. The values in Table 2.6 refer to the frequency of occurrence, of a tornado, and not to the specific damage potential. The values in Table 2.6 were used in the overall risk estimates in order to form a comparative basis of the consequences. The inclusion of the specific damage potential would appear to underestimate the risk from the silo contents on the public.

Characterization And Degree Of Effect

The characterization of the specific tornados of which data was available is essentially dependent on the intensity factor and the recorded wind speeds. The ideal characterization would provide pressure and velocity distributions as a function of position, corresponding to the radius of the tornado. This type of information is rarely available for actual tornados. The next best method, therefore, is to assume some realistic distributions based on the intensity factor, the area covered and the resulting damage.

The forces on a structure resulting from a tornado are of two types: 1) compressive forces and 2) tensile forces. These forces result from the high tangential and translational wind speeds and the effects of large and rapid pressure drops.

Table 2.6: Probabilities Associated With Natural Degradation Of The K-65 Silos And Tornado Occurrence

Probability Of Failure Due To Natural Degradation

Silo 1	Silo 2	
0.0362	0.0389	per year
0.18124	0.19459	over 5 years

Probability Of A Tornado Per Square Mile

per year	over 5 years
1.248 E - 4	6.24 E - 4

The atmospheric pressure gradient at radius 'r' from the tornado axis is given by the cyclostrophic wind equation, Equation 2.11, (Long, 1958), and (Rotz, 1974).

$$dP_a(r) / dr = \rho V_t^2(r) / r \quad (2.11)$$

where:

- ρ = Mass density of air.
- $V_t(r)$ = Tangential wind velocity component.
- $P_a(r)$ = Pressure as a function of position.
- r = Radius of the tornado measured by the wind velocity.

If the tangential velocity profile is assumed to be a Rankine vortex the velocity can be represented as a function of position as provided by Equation 2.12.

$$V_t(r) = \begin{cases} (r / R_m) V_m & (0 \leq r \leq R_m) \\ (R_m / r) V_m & (R_m \leq r < \infty) \end{cases} \quad (2.12)$$

The pressure distribution as a function of position is then represented by Equation 2.13.

$$P_a(r) = \begin{cases} \frac{1}{2} (-\rho V_m^2) (2 - V_{tr}^2 t^2 / R_m^2) & (0 \leq r \leq R_m) \\ \frac{1}{2} (-\rho V_m^2) (R_m^2 / V_{tr}^2 t^2) & (R_m \leq r < \infty) \end{cases} \quad (2.13)$$

where:

- V_m = Maximum tangential velocity.
- V_{tr} = Translational velocity of the storm front.
- R_m = Radius for the maximum tangential velocity.

The maximum forces associated with the above described pressure and velocity profiles can be obtained using the following empirical correlations, Equation 2.14 for compression, and Equation 2.15 for tension.

$$P_c = 0.5 C_p C_s \rho V_{\max}^2 \quad (2.14)$$

$$P_t(0) = \rho V_{\theta m}^2 \quad (2.15)$$

where:

- P_c = Compression force (psf).
- P_t = Tensile forces (psf).
- C_p = Coefficient of lift and drag forces.
- C_s = Coefficient for the shape of the structure.
- V_{\max} , and $V_{\theta m}$ = Maximum wind speeds for the rotational and translational components.

These equations are used for the roof portion of the silo structure for both the compressive and tensile forces. The compressive forces are primarily due to the lift and drag forces of the horizontal wind components. The tensile forces are primarily due to the pressure drop associated with the storm and specifically the local depression in the vortex of the tornado itself. These correlations relate the forces of the turbulence associated with the tornado. These forces are then compared to the critical loadings of the silos to determine the damage potential. The critical loads on the silo dome are approximately 284 psf for the outer portions of the dome and approximately 104 psf for the center portion (determined in the Camargo study). Table 2.7 delineates the forces expected from the various classes of tornados as related to the mean wind speeds. Several diagrams have been added to further clarify the results of the force calculations on the silos. The first diagram, Figure 2.3. illustrates regions of influence. The farther away the region of high tangential wind speeds and high pressure drops (funnel cloud) is from the silo structure the less damage that will be sustained. The area or radius of influence also changes with the tornado intensity. The next diagram, Figure 2.4. illustrates the damage type. The results of these calculations when compared to the critical loading on the dome show that a tornado of at least an F1 intensity or higher has the potential for failing the silo dome structure.

In the event that the dome fails, as a result of the forces from the wind and estimated pressure drop, the next major consideration is the extent of damage to the structure. In this analysis the extent of damage was postulated to range from simple cracking in the event of low wind speeds and a moderate pressure drop to the extreme case where the dome is completely removed, as a result of the maximum wind and pressure forces. The forces exerted in this extreme case would be well in excess of

**Table 2.7: Force Distributions As A Function
Of Tornado Intensity**

Intensity	Maximum Velocity (mph)	Pressure Drop ΔP (psi)	Compressive Force (psf)	Tensile Force (psf)
F1	112	2.0	49.2	288.0
F2	157	2.25	96.8	324.0
F3	206	2.5	167.0	360.0
F4	260	2.75	265.0	396.0
F5	318	3.0	397.0	432.0

Figure 2.3: Modeling Severe Storms For Determining The Initiator Probability

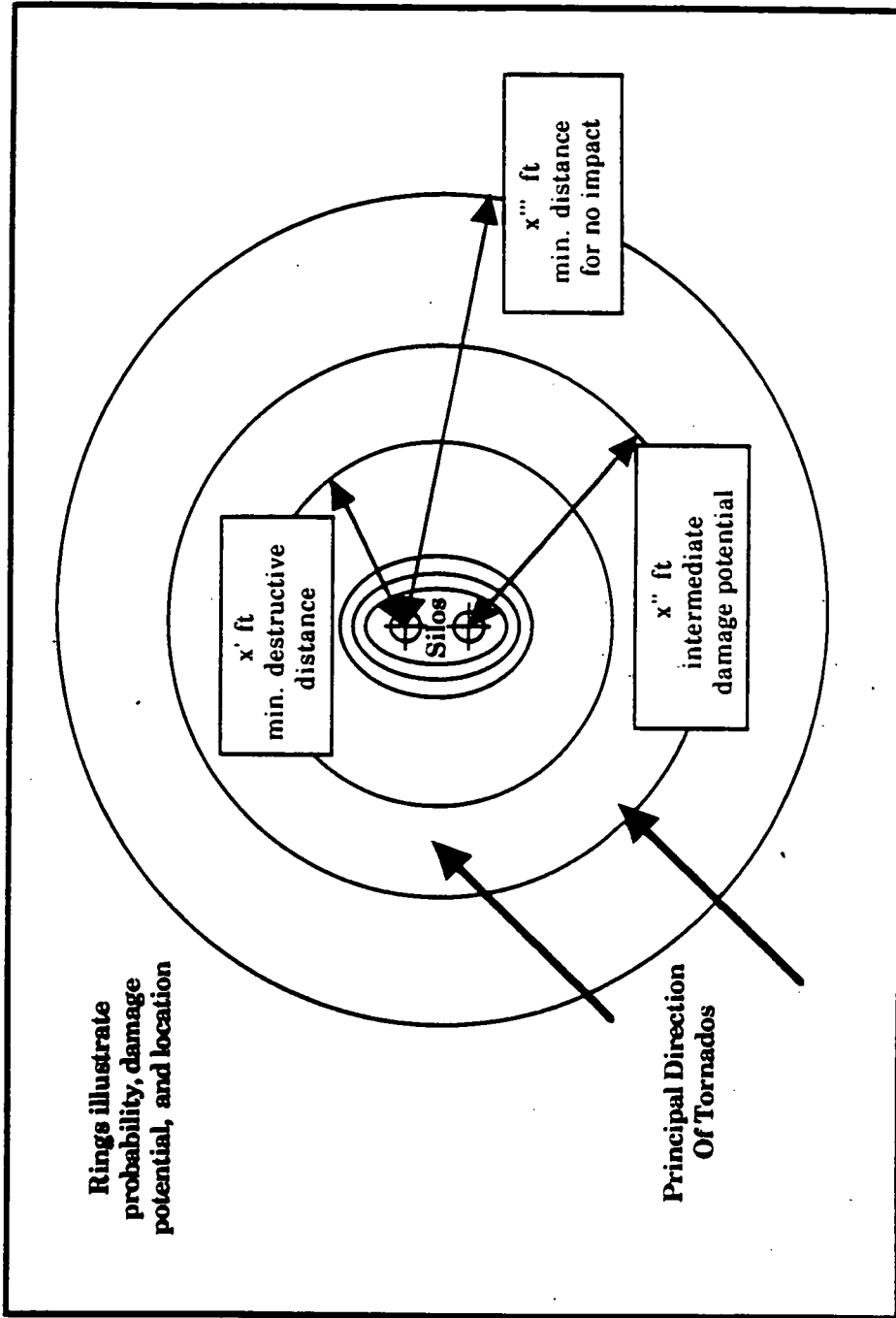
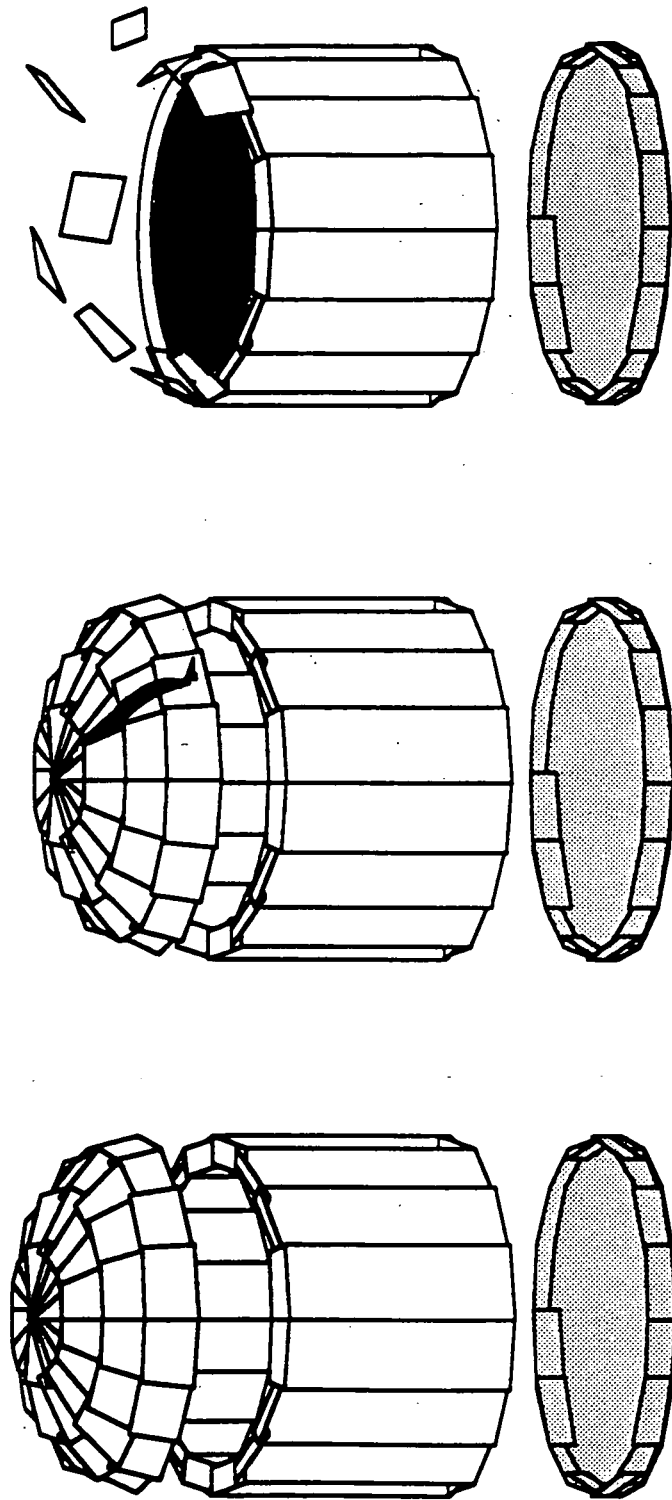


Figure 2.4: Schematic Diagram Of The Silo Structure And Failure Modes



Basic Silo Structure

**Acute Case - A2
Silo Dome Cracks**

**Acute Case - A1
Total Failure Of Silo Dome**

the critical buckling load by a factor of 2, for the outer portion of the dome, and more than a factor of 4, for the inner 20 foot section. This range of damage complicates the analysis of the release term as well as the overall risks. In order to facilitate the risk estimates the maximum damage and therefore the maximum source term released were used in the exposure assessment portion of this study. In this regard no credit was taken for parts of the silo structure falling in and thereby reducing total quantity of residues available for dispersion by the wind.

Summary Of Probabilities And Damage Potential From Severe Weather

As a final point, all of the various probability calculations are presented in Table 2.8. This format enables the reader to view all the various calculations simultaneously. What is not able to be conveyed in a tabular format is the specific meaning for each calculation or probability estimate. This understanding or appreciation is hopefully gained through both the supporting text and the reader's own experiences. Probabilities and especially risks are difficult to grasp in terms of everyday experiences. The more complicated the probability the more difficult the understanding becomes.

It is important to note that the foam and the protective cover to the center portion of the dome were not considered to add strength to the dome structure. The additional weight these modifications impose on the dome were considered to be a detriment and tend to increase the potential for failure. For this reason the loss of the dome during a tornado event was evaluated using only the results of the force and wind loadings as applied to the silo modeled in the Camargo report. The estimated extent of damage in the event of a tornado discussed in this section was taken as a maximum and is not intended to reflect, precisely, the wide range of possibilities for the manner in which the dome structure may fail. The exposure assessment can then be broken down into fewer parts and the complexities associated with what failure mode to use is reduced to using those estimates which reflect the maximum source term and therefore the maximum consequences.

Table 2.8: Summary Of Probabilities Associated With The K-65 Silos

I. Silo Dome Failure Probability

A. Probability Of Failure Due To Natural Degradation

Silo 1	Silo 2	
0.0362	0.0389	per year
0.18124	0.19459	over 5 years

B. Probability Of Failure Due To Natural Degradation Including Tornado As An External Event

Silo 1	Silo 2	Average	
0.0365	0.0339	0.0352	per year
0.1825	0.1695	0.176	over 5 years

II. Tornado Occurrence Probability (per Square Mile)

a.)	Total	per year	over 5 years
	1.186 E - 3	1.248 E - 4	6.24 E - 4

b.) Probability as a function of intensity level

Intensity

F0	1.91 E - 6	9.55 E - 6
F1	3.65 E - 5	1.83 E - 4
F2	2.83 E - 5	1.42 E - 4
F3	1.95 E - 5	9.75 E - 5
F4	1.22 E - 5	6.10 E - 5
F5	2.63 E - 5	1.32 E - 4

**Table 2.8: Summary Of Probabilities Associated
With The K-65 Silos (continued)**

**III. Probability And Risk From Wind Speed Given A Single
Tornado Event In A Five Year Period**

wind velocity (x, mph)	probability $L(x) = 1 - F(x)$	risk factor r (x)
112	2.5 E - 1	3.7 E - 1
135	1.75 E - 2	4.13 E - 2
185	3.34 E - 3	5.78 E - 4
230	2.78 E - 6	6.13 E - 6
290	2.43 E - 7	7.35 E - 8

555

Seismic Activity

There are few places on earth where there is no threat from seismic events. The Ohio valley where the FMPC site is located is at risk from seismic activity. In fact some of the worst earthquakes ever recorded in the United States occurred in the midwest region. Seismic activity as far south as Tennessee, as far north as Minnesota, and as far east as South Carolina have had their effects recorded in the Ohio valley. The return period for earthquakes in this region however is very long indicating that the frequency of occurrence is relatively small.

The details associated with seismic activity in the region affecting the FMPC site have been included in this final report for completeness. The net effect of an earthquake on the K-65 silos is not expected to exceed the critical loads for the dome, floor, and wall portions structure. This conclusion was reached as a direct result of the Camargo study. Due to discrepancies in the Camargo and Bechtel reports the addition of seismic information and a discussion of the structural response was included.

General Information On Seismic Activity

On December 16, 1811, the largest magnitude earthquake man has recorded on the North American continent occurred at New Madrid, Missouri. The intensity of this earthquake was estimated at XII on the Modified Mercalli (MM) scale. Two additional earthquakes of equal intensity occurred on January 23, 1812 and February 7, 1812. These earthquakes were felt over an area of 2,000,000 square miles. Three hundred fifty miles to the northeast, in the vicinity of Cincinnati, these seismic events were felt as intensity VI - VII (MM) (USGS circular 1066, 1990).

Earthquakes occurring within the Eastern United States are of tectonic origin in that they are associated with large-scale strains in the crust of the earth as opposed to earthquakes associated with volcanic sources. Tectonic earthquakes are generally assumed to be caused by slippage along planes of weakness (faults) that separate the large plates forming the earth's crust. The concept of plate tectonics is straight forward: the crust of the earth can be divided into six major plates and many smaller ones that move relative to each other at velocities ranging from a few centimeters per year up to 20 or more (Burchfiel, 1983). Recent estimates of the configuration of the tectonic plates places the Cincinnati area well within what is called the North American Plate.

The FMPC site is located in a seismically quiet region that has experienced ground motion principally due to events in adjacent regions. The low level of seismic activity has resulted in the lack of interest in regional seismicity and the rather small number of instrument recorded events. Most of the knowledge on the seismicity comes from reports in newspapers and other references over the past 200 years.

The great quakes of 1811-1812 located at New Madrid that resulted in ground motions equivalent to Intensity levels of VI or VII are the highest recorded accelerations in the vicinity of what is now the FMPC site. The closest reported earthquakes to the FMPC site occurred near Maysville, Kentucky, approximately 64 miles southeast, and at Cincinnati, Ohio, approximately 10 miles to the southwest. Four earthquakes have been reported in the Maysville area, two Intensity V (MM) events in 1928, one Intensity V in 1933, and one Intensity III event in 1937. Additionally there were approximately 37 earthquakes in the Anna, Ohio area, which is located 75 miles north of the FMPC site. The majority (24) of these 37 events occurred in the 12 year period from 1928 to 1939 with two of the events measuring Intensity VII, one event of Intensity VII - VIII, one at VI+, and one at VI. The epicenters for these events range from 50 to 90 miles from the FMPC site.

The nature of the movement of the tectonic plates determines the effect on structures at the surface. The location of the epicenter and the ground characteristics between this point and the location at the surface being investigated determines a structures response to the event. There are three important parameters in assessing an earthquake: 1) the duration of the earthquake, 2) the velocity of the surface movement, and 3) the rate of change of the surface velocity (ground acceleration).

The basis of seismology is the observation and analysis of elastic energy as it propagates itself through the earth. When mechanical energy is released in a homogeneous earth, it is propagated outward in waves whose fronts are spherical and whose mechanism is alternating compression and rarefaction of the material through they pass. These waves, called P waves, are physically analogous to the the sound waves that spread outward from an explosion in air or water. The P wave travels at a rate of about 5.6 kilometers per second. It is the first wave to reach the surface. A longitudinal wave, the P wave tends to create a "push-pull" effect on rock particles as it passes.

Since the earth is in general not homogeneous, and though imperfectly elastic, it has rigidity or shear strength that is absent in air or water. This rigidity results in a second type of wave to propagate the energy. This second wave action causes the material (through which the wave passes) to move transversely to the direction of the wave motion. These shear waves, called S waves, travel through the solid material at a velocity a little more than half of that of the P waves. The S wave causes the earth to move at a right angle to the direction of the wave.

In addition to the S and P waves, generally referred to as body waves, there is also energy propagation along the surface and at interfaces. At the earth-air interface, waves similar to surface waves in water are propagated. These interface waves are called Rayleigh waves and they cause, as in water, circular vertical motion of the material through which they pass, in the plane containing their direction of propagation. In solid

555

material, surface waves like S waves also occur, and the material moves horizontally in a plane transverse to the direction of motion of the wave. These waves are called Love waves (L waves). These waves are usually only distinguishable at great distances. L waves cause the swaying of tall buildings and slight wave motions in bodies of water at great distances from the epicenter.

Examination of the potential sources of seismic activity and the ground characteristics between the sources and the FMPC area provides a conceptual picture of the wave modes and the eventual response structures on the surface may have. This type of examination was performed by Soil and Material Engineers Incorporated in order to estimate the duration of a hypothetical seismic event, the surface velocity, and the peak ground accelerations. This information collectively provided the basis for the seismic simulation runs for the FMPC site with respect to the K-65 silos.

Seismic Simulation Of K-65 Silos

An earthquake analysis was performed on both of the K-65 silos as part of the Camargo study. Some of the details of this seismic simulation study are presented to provide a basis for final risk evaluations. The following assumptions were made and were considered conservative: 1) the K-65 material stored in the tanks is a solid and is assumed to add mass but not stiffness, 2) damping was neglected, 3) the tank was assumed to be a homogeneous isotropic uncracked concrete structure, 4) all connections between the walls and base slab, and the walls and the dome have enough tendons to cause the system to act as a unit through the majority of the earthquake, and 5) all stresses reported herein are a result of the earthquake and do not account for the compression stresses existing in the tank due to post tensioning and induced by other loads such as self weight, etc.

The peak ground acceleration was taken to be 0.05 g and the ground motion duration was 10.0 seconds. An earthquake with these properties (Intensity V) represents a 90% probability of occurrence within a fifty year period. The results of this seismic analysis for the dome showed that the hoop stresses on both silos was in the range of 97/-95 to 111/-118 psi for the the top of the tank walls. The corresponding longitudinal stresses were on the order of 78/-53 (psi) for silo 2 and 138/0 (psi) for silo 1. The stresses at the middle of the dome were negligible due to the structure's flexibility and therefore does not resist the movement of the earthquake.

The results as indicated in the Camargo report indicate that the dome structures of either silo are not expected to fail as a result of an earthquake in this region. With respect to the K-65 risk assessment the seismic response of the silo domes resulting in structural failure was taken as having a low probability and therefore more time and resources were expended in determining the probability and effect of tornado events on the silos.

The seismic information was included for completeness and to provide an additional level of the potential release mechanisms. Eventhough the risk of a seismic event causing failure of the domes is small the potential release scenario was none the less evaluated. Due to the nature of the forces acting on the structure in the event of failure of the dome structure there is little chance for release of any of the waste material other than the radon in the head volume of the silo. Should this event occur the conservative assumption of a crack forming that will release the entire head space contents within a one hour period was made. In this situation the consequences of an earthquake capable of failing the dome are essentially the same as that of a low intensity tornado or the natural degradation failure mechanisms. The exposure and dose assessment for this event were considered in what is termed the acute A2 release discussed in a later section.

555

Long Term Weathering And Wear

Due to the age and structural condition of the silos, it is possible that the integrity may be significantly reduced to an extent that the silos may no longer be capable of fulfilling their design intent of waste containment. These deterioration processes are time dependent and are continuous. There are no evaluations of quality assurance during construction and hence it is not known if the design specifications were met. Thus the assumption has to be made that at time the time of construction the silo domes were in a structurally perfect condition.

Using the above assumptions and the results of the Non-Destructive Tests (NDT) performed by Muenow and Associates a model was developed to provide numerical values of the condition of the silos. The model developed was used to establish a quantitative basis for estimating the probability of dome failure due to natural degradation. A time dependent degradation rate has been developed assuming an exponential distribution function. This assumption is more accurate than using a linear model and hence compensates for the uncertainty involved with the structural stability at time of construction. Additionally, all modifications made after the Camargo report were not included in the degradation probability model. There is insufficient data available on the relationship between the current and future degradation rates. The models were developed considering only dead loads on the silo structure. Live loads such as wind, rain, or other external forces were not taken into account in the natural degradation process.

There are three primary events which are considered as the contributors to the loss of silo integrity by natural processes; these are:

1. Weathering and Wear.
2. Mesh Support Loss.
3. Concrete Quality.

These basic events are evaluated below, and produce an annual contribution to the probability of dome failure. The contribution of each of these basic events is depicted graphically in Figure 2.5. This figure shows the generalized fault tree representing the possible failure modes associated with the dome unit on the K-65 silos. The basic events are coded by letter and numeric formats. The letter represents the level at which the basic event acts and the numeral indicates the relative number of events on that specific level. The final letter in the designation indicates the type of event. The first basic event discussed is designated as C5e, where the 'C' indicates the third level of the tree, the '5' represents the fifth event, and 'e' designates the event as a basic event.

Failure Analysis

The potential failure of this waste management system can be measured in terms of the potential release of radioactive material to the environment. The purpose of the study, thus far, has been to identify these mechanisms and to provide estimates of the probability of occurrence.

The first step in this analysis has been to identify the hazardous conditions inherent within the present system which have a potential for failure. The information derived from this initial analysis can be used as a basis for the *fault tree analysis*. The fault trees allows the system failures to be quantified in terms of effects and probability of occurrence.

The methodology used in this fault tree analysis involves postulation of a release of waste material and then following the series of component failures which must have occurred to cause the release. Each failure in the fault tree is ultimately traced to one or more initial occurrences. These initial occurrences are collectively defined as the *basic events*. The principal difficulty in developing a fault tree is the determination of the basic events and their relationship to one another.

The evaluation of potential failure of the silos was made by dividing the overall structure into three independent substructures:

- 1. **Dome**
- 2. **Walls**
- 3. **Floor Slab.**

Due to the variance of forces upon the wall, and due to the different potential failure scenarios, the wall was further divided into two regions. The **Upper Wall** refers to the vertical structure between the dome base and the internal waste level. The **Lower Wall** extends from the waste line to the juncture with the floor.

Fault trees have been constructed for each substructure individually; once again the wall section consists of two independent trees for the lower and upper structures. Inter-relationships and inter-dependencies of the substructures have been fully utilized such that a complete silo failure scenario may be evaluated. Although the structure itself is simple, additional complications exist due to the presence of a berm, the addition of a secondary dome, and the lack of evaluated data concerning the condition of the silo floor. Additionally the berm presents a force upon the wall; to a large extent this compressive force is mitigated by the tensile force applied to the wall by the internal wall mass. However, the upper section of the wall has only the compressive stress of the berm as it is above the waste mass. The strength of the dome cannot be assumed to be constant across the dome radius. The center section is believed to be much more susceptible to failure. Hence, failure of the dome is expected to occur in the center 20 feet.

Fault Tree Development

Fault tree analysis is a technique by which many events that interact to produce other events can be related using simple logical relationships (AND, OR); these relationships permit a methodical building of a structure that represents the system, Figure 2.6.

To construct a complete fault tree which best represents the system, it is necessary to fully comprehend the system in question and its function. In addition, all possible events which may cause a potential failure of the system must be fully analysed. Once the system function is fully defined, a fault tree may be constructed.

In fault tree construction, the system failure event that is to be studied is called the *top event*. Successive subordinate (subsystem) failure events which may contribute to the occurrence of the top event are then identified and linked to the top event by a series of logical functions. The subordinate events are subsequently broken down to their logical contributors, and in this manner, a fault tree is constructed.

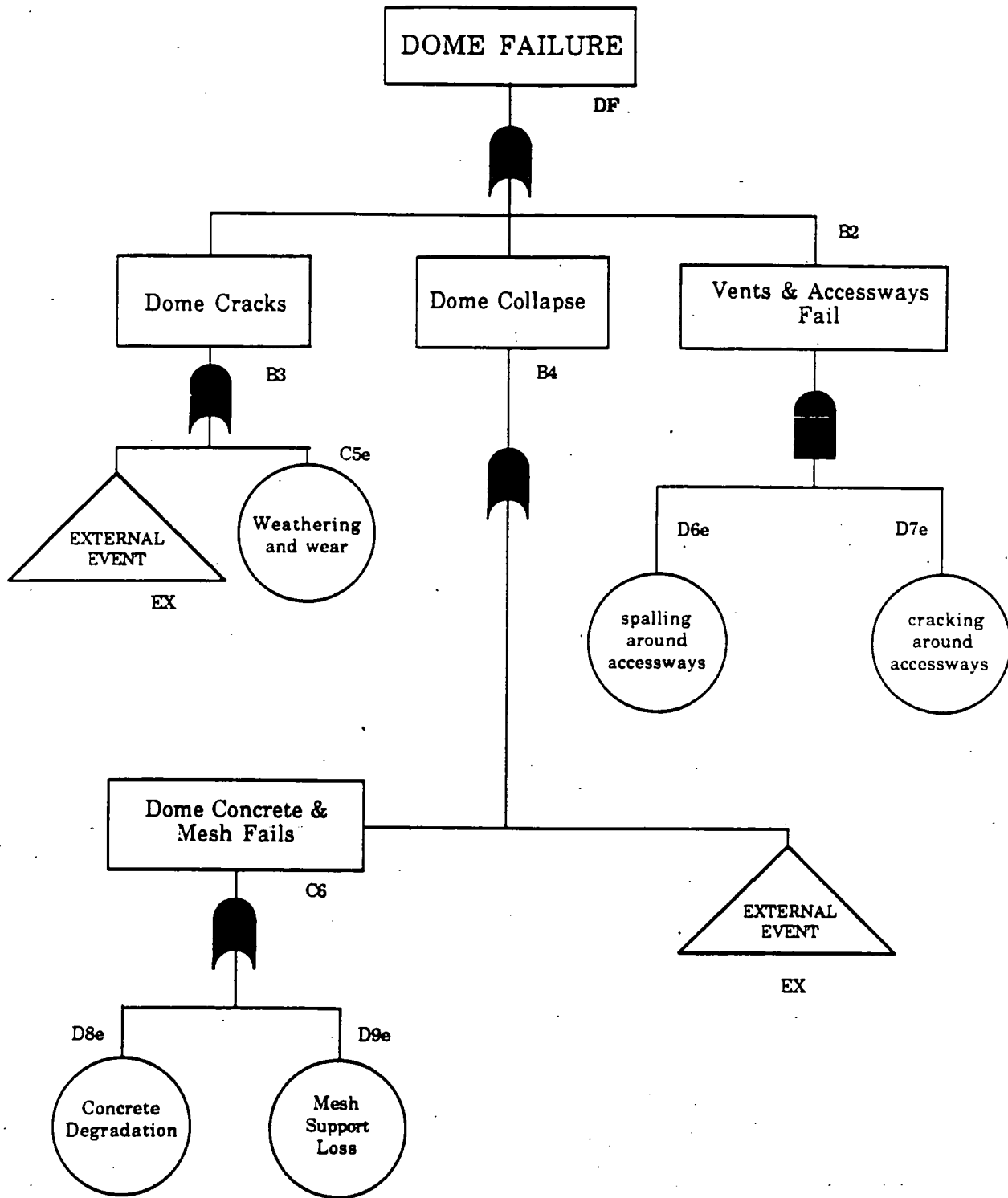
When a contributing event can no longer be further divided, the corresponding branch is terminated with a *basic event*. Basic events are statistically independent unless they are common cause failures. Such failures are those that arise from a common initiating event. Such is the case for the *external events* (seismic activity and tornados) which are to used in this analysis.

Once the tree structure has been established, the subsequent analysis comprises of two forms: 1) **Qualitative Analysis** reduces the tree to its logically equivalent form in terms of the combinations of basic events which will lead to the top event. This will reduce to a minimal cut set of failure modes for the tree; this is accomplished using *Boolean Algebra* and 2) **Quantitative Analysis** of the fault tree consists of transforming the established logical structure into an equivalent probability form, and hence numerically calculating the probability of occurrence of the top event from the probability of occurrence of the basic events.

Once the fault trees for each of the systems have been constructed, the trees are integrated into the one unifying structure; the event tree. The *event tree* is defined by its *initiator* (seismic, tornado, natural degradation, etc.). Figures 2.7 and 2.7a show the fault trees representing the possible failure modes associated with the wall. The basic events are coded by letter and numerical formats. The letter represents the level at which the basic event acts and the numeral indicates the relative number of events on that specific level. The final letter in the designation indicates the type of event. The first basic event discussed is designated as C5e, where the 'C' indicates the third level of the tree, the '5' represents the fifth event, and 'e' designates the event as a basic event.

555

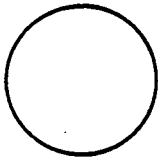
Figure 2.5
Fault Tree For Dome Failures



59
41

Figure 2.6:

Fault Tree Symbols
(NUREG - 0460)



Basic Event - A basic initiating event requiring no further action.



Intermediate Event - A fault event that occurs because of one or more events acting through logic gates



AND - Output fault occurs if all the input faults occur

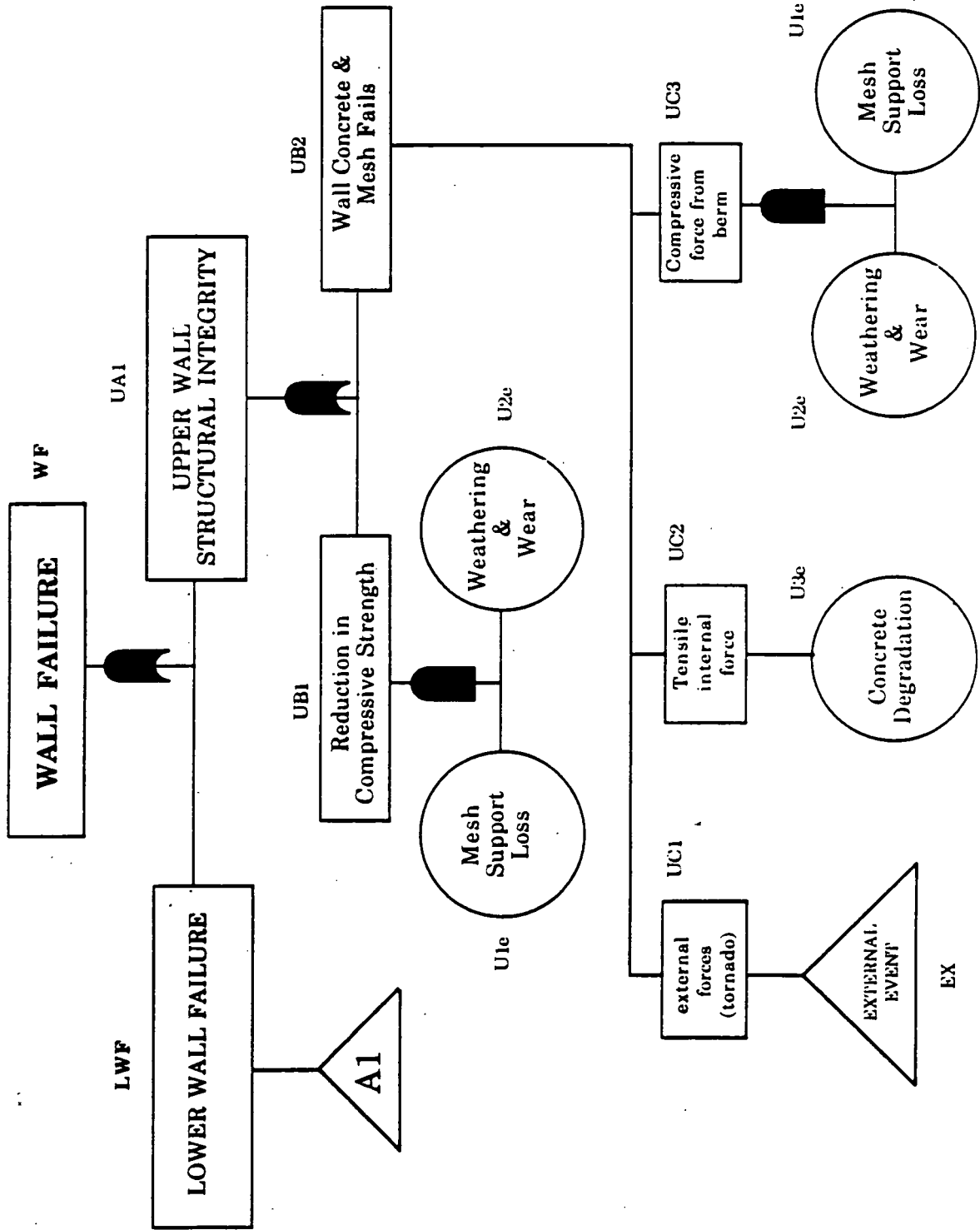


OR - Output fault occurs if at least one of the input faults occur.



TRANSFER - Tree is further developed at another point; avoids repetition.

Fault Tree For Wall Failure : Figure 2.7



Evaluation Methodology

The results of structural testing provide a numerical or qualitative statement of the present day condition of the silo structure. These values need to be statistically evaluated to predict the probability of failure per year. The methodology proposed to accomplish this is to fit an exponential function to the two points of evaluation; 1952, time of construction, and 1986, Camargo non-destructive testing. The function is then extrapolated to the present day, 1990, to produce a predictive condition value. At this time a second exponential function is used to evaluate the fraction of functional time remaining to failure; from this algorithm, an annual probability of failure is calculated. The process of evaluation is described below.

The first step in the process is the evaluation of the Quality Statements (QS) resulting from the non-destructive tests. The QS are presented in terms of either numerical values, such as remaining dome thickness, or in terms of a condition statement, for example as a concrete quality factor for the dome; there are four condition statements assigned to the concrete quality as shown below.

Condition	Quality
1	SOLID
2	AVERAGE
3	MODERATE
4	QUESTIONABLE

An averaged Quality Statement for the entire sub-structure may be evaluated using all the testing locations. This averaged value may be weighted in terms of regions or by critical locations.

The second step is to assess the time dependency of the degradation process. This is accomplished by examining the three principal time periods of concern. The principal times are presented below.

1952	time of construction	t_0	t = 0 (years)
1986	time at testing	t_{ndt}	t = 34
1990	time of evaluation	t_{eval}	t = 38

The assumption is made that at the time of construction (t_0) the condition statement is at the design specification and that there is no loss of integrity. Thus for the case of concrete quality, the condition at time=0, Q_0 is equal to 1 (solid).

The exponential degradation rate, λ , is thus given by Equation 2.16:

$$-\lambda = \frac{\ln \left\{ \frac{Q_{ndt}}{Q_0} \right\}}{t_{ndt}} \quad (2.16)$$

Note: For some cases condition statements are not given; such is the case for concrete thickness, here design values are taken from the original drawings and the 1986 thicknesses are taken from the test results.

The third step in the evaluation process consists of the estimation of the time frame when failure is imminent. This is accomplished by assessing the point at which the integrity of the structure has been compromised. This critical statement Q_{crit} is taken to be the threshold for structural integrity, and marks the value at which failure is imminent. Using the exponential degradation rate it is possible to predict the time taken to reach the critical threshold. This time frame is denoted by T_{crit} and is given by Equation 2.17.

$$T_{crit} = \frac{\ln \left\{ \frac{Q_{crit}}{Q_0} \right\}}{-\lambda} \quad (2.17)$$

The final step is to determine the maximum time before complete structural integrity is lost. The relationship between the time remaining and the time already past provides the basis for estimating the probability per year of further degradation. The fraction of functional time remaining ($T_{crit} - t_{eval}$) can be incorporated into an exponential density function to yield the probability of failure, μ . The functional time remaining is shown graphically by Figure 2.8. The probability of failure per year, μ , is given by:

$$\mu = \left(\frac{\ln \left(1 - \frac{t_{eval}}{T_{crit}} \right)}{t_{eval}} \right) \quad (2.18)$$

Note: $t_{eval} = 38$ years.

Generic Condition Statement Variation

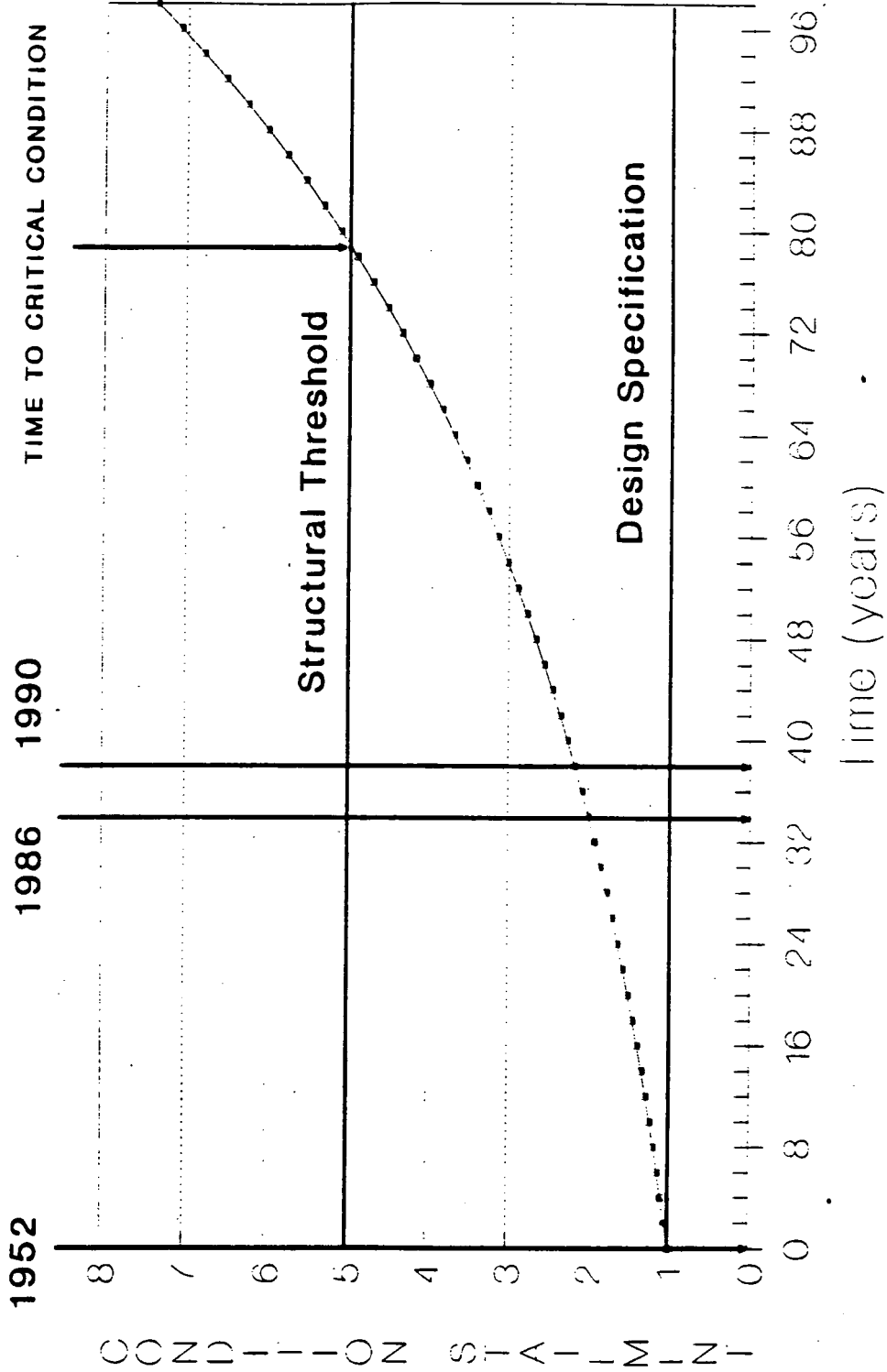


Figure 2.8

555

Failure Event Probabilities: DOME

The fault tree for dome failure show five basic events:

- 1) Basic Event C5e: Weathering and Wear
- 2) Basic Event D9e: Mesh Support Loss
- 3) Basic Event D8e: Concrete Degradation
- 4) Basic Event D6e: Spalling Around Accessways
- 5) Basic Event D8e: Cracking Around Accessways

The annual probability of occurrence of these basic events are evaluated using the methodology described above.

Basic Event C5e: Evaluation of Weathering and Wear

Determination of the wear of the concrete domes can be accomplished using the test values of concrete thickness. The Buckling Stability of the dome is the capacity of the dome to withstand the compressive loads without bending out of plane. Due to the general thinning of the dome, the structural integrity has been significantly reduced. The critical buckling evaluated by Camargo Associates is 284 PSF; this is valid for thickness of 3 inches and greater. A critical buckling of 104 PSF was similarly evaluated for concrete thickness of 2 inches.

Using a linear relationship of critical buckling as a function of concrete thickness an extrapolated value of 1.42 inches is found to correspond to a buckling value of 0 PSF. Thus, 1.42 in presents the lower threshold of integrity; hence any thinning resulting in a dome thickness of 1.42 in, or less, will lead to a breach of the concrete dome integrity.

The values used to compute the magnitude of thinning were taken from the testing regions towards the top of the dome (dome center) as these regions have been deemed by Camargo Associates to be critical. Areas close to the dome/wall intersection were not incorporated into the analysis as the exact testing coordinates were not provided, since it was impractical to attempt to evaluate the value of the original design specification thickness. In addition, the outer regions of the domes are not considered as critical as the inner 20-30 ft. radius, thus to provide an accurate evaluation these values were omitted.

From the remaining test locations, average of the remaining concrete thickness for both silos were evaluated.

Table 2.9: Results Of Concrete Thinning Data

	Average Thickness Reduction (in)	Tested (1986) Average Thickness (in)
SILO 1	0.916	3.084
SILO 2	0.909	3.091

Using the exponential thinning rate (Equation 2.16) of the concrete with time, and assuming that at time T=0 that the thickness was 4 inches (design specification), the thinning rates were calculated to be:

**Table 2.10: Exponential Thinning Rates
(in/year)**

SILO 1	$\lambda_1 = 7.649E-3$
SILO 2	$\lambda_2 = 7.584E-3$

Using these thinning rates it is possible, still using a exponential reduction rate, to predict the time taken for the dome thickness to reduce to the 1.42 in threshold, (Equation 2.17).

Table 2.11: Time to Reach Critical Thickness (years)

SILO 1	$T_1 = 135.40$
SILO 2	$T_2 = 136.59$

Using the fraction of functional time remaining, the annual probability of failure, μ , can be evaluated by Equation 2.18:

Table 2.12: Probability Per Year Of Weathering and Wear

Basic Event C5e

SILO 1	$\mu_1 = 8.669 E-3$
SILO 2	$\mu_2 = 8.579 E-3$

Basic Event D9e: Evaluation of Mesh Support Loss

Pulse echo techniques were employed by Muenow and Associates to determine the quality of the reinforcement steel remaining in the domes. These tests indicate the bonding condition of the concrete to the wire mesh supports. The ability of the steel mesh to provide strength to the concrete structure relates directly to the integrity of the dome. The testing logistics used provided 252 values of steel quality at the 126 test locations. Muenow assigned a Quality Statement to each result. The quality statements are qualitative in nature and are assigned based on the general conditions inferred from the observations at a particular location.

It is important to note that the quality assignments are assigned in such a way that the better the quality the lower the number assigned. A number assignment of '1' indicates that the material is considered to be in the same condition as original design. Similarly, an assignment of quality number '4' indicates that all structural integrity has been lost. This formalism is illustrated through example in the following quality statements.

Quality Statement 1

No pulse reflections noted at reinforcement steel locations and noted depths - indicating no corrosion nor nonbonding of the steel to cement matrix.

Quality Statement 2

Minor and undefined pulse echo reflections noted at reinforcement steel locations and noted depths - indicating some possible slight corrosion and/or lack of bond between steel and cement matrix.

Quality Statement 3

Defined pulse echo reflections noted at reinforcement locations and noted depths - indicating a strong possibility of corrosion product in conjunction with a non-bond condition between steel and cement matrix.

The 252 test results were analysed and weighted to provide a Quality Statement of the reinforced steel for the whole dome. This derived quality statement for the whole dome results in a quasi-continuous distribution. The results of the analysis for this derived quantity in connection to the steel reinforcement is depicted in Table 2.13.

Table 2.13: Reinforced Steel Quality For Entire Dome

SIL0 1	Q₁ = 1.746
SIL0 2	Q₂ = 1.663

It is apparent from the results in Table 2.13 that the overall quality of the steel reinforcement within the dome is less than original design, but still sufficient to provide some support. Continued degradation of the steel supports will eventually result in the total loss of support and this would be designated by a quality number of '4'.

The exponential decay rate of the steel quality can be determined (equation 2.16); assuming at time $t=0$ the quality was 1 over the entire dome.

Table 2.14: Exponential Steel Quality Decay Rates
(year⁻¹)

SILO 1	$\lambda_1 = 0.0164$
SILO 2	$\lambda_2 = 0.0150$

To determine a threshold at which the dome integrity has been compromised, a new Quality Statement 4 is introduced. It is assumed that a Quality Statement of 4 infers that total corrosion has been reached and the reinforcement steel can no longer support the dome.

The time taken to reach the critical condition 4 can be evaluated using the exponential decay rates λ_1 and λ_2 and Equation 2.17.

Table 2.15: Time to Reach Critical Quality 4
(years)

SILO 1	= 84.53
SILO 2	= 92.42

Using the exponential probability density function with the fraction of time to critical quality, the probability of failure due to mesh support loss can be calculated.

Table 2.16: Probability Per Year Of Mesh Support Loss

Basic Event C9e.

SILO 1	$\mu_1 = 0.0157$
SILO 2	$\mu_2 = 0.0139$

Basic Event D8e: Evaluation of Dome Concrete Degradation.

Evaluation of the extent of concrete degradation can be achieved using the Concrete Quality Statement assigned by Muenow and Associates. Cracking is an inherent property of most concrete structures; the extent of such cracking would indicate the ability of the concrete to provide a compressive strength. Four Statements were specified, each of which are listed below. Each statement is set by assigning a threshold for the pulse velocity and a correlated compressive strength for a typical concrete mix.

Concrete Quality Statement

1. SOLID

No Cracks; line of deterioration well defined indicating flat inside surfaces. Pulse velocity in the range of 14,000 ft./sec; compressive strength greater than 4,000 PSI.

2. AVERAGE

Surface cracking; line of deterioration less well defined indicating an undulating inside surface. Pulse velocity range of 13,000 to 14,000 ft./sec; 3250 to 4,000 PSI compressive strength.

3. MODERATE

Surface Cracks and full depth cracks; local sharp undulations indicating areas of deterioration. Pulse velocity range of 12,000 to 13,000 ft./sec; 3250 to 2750 PSI compressive strength.

4. QUESTIONABLE

Surface cracks, full depth cracks and some crack plane offset; grouped or large areas of sharp undulation indicating areas of deterioration. Pulse velocity in the range of less than 12,000 ft./sec; less than 2750 PSI compressive strength.

The methodology to be employed for this analysis has been outlined in the previous two evaluations. The results for each step are shown below. Concrete Quality 5 is the assumed lower threshold for structural integrity

Table 2.17: Concrete Quality For Entire Dome

SILO 1 Q₁ = 2.000

SILO 2 Q₂ = 1.948

Table 2.18: Exponential Degradation Rate For Concrete Quality per Year

SILO 1 $\lambda_1 = 0.0204$

SILO 2 $\lambda_2 = 0.0196$

Table 2.19 Time to Reach Critical Quality 5 (Years)

SILO 1 = 78.89

SILO 2 = 82.11

**Table 2.20: Probability Per Year Of Concrete Degradation
Basic Event D8e.**

SILO 1 $\mu_1 = 0.0173$

SILO 2 $\mu_2 = 0.0163$

Basic Events D6e & D7e: Concrete Degradation Around Accessways

The design specifications show four accessways on the surface of each dome, these inlets were the main input lines for the raffinate into the silos. Information is not available to quantify the degradation around the areas of the inlets. However, the discontinuities of the dome surface at these points will create nodes of high stress and hence there is a possibility that such stresses may lead to failure. To account for this increase in failure probability, these basic events have been assigned the same probability as those for concrete degradation (D8e) and weathering and wear (C5e). Hence;

D6e = C5e

D7e = D8e

It is important to note that the evaluations for weathering and wear and for concrete degradation were performed for the whole dome surface and, in comparison, the areas affected by the degradation around the accessways is minimal. The evaluation of an accessway failure is considered to be a product evaluation, as the logic gate is AND; thus the discrepancy in area is accounted for.

Table 2.21: Probability Per Year Of Accessway Failure

Spalling Around Accessways

Basic Event D6e.

SILO 1 $\mu_1 = 8.669 \text{ E-3}$

SILO 2 $\mu_2 = 8.579 \text{ E-3}$

Table 2.22: Cracking Around Accessways

Basic Event D7e.

SILO 1 $\mu_1 = 0.0173$

SILO 2 $\mu_2 = 0.0163$

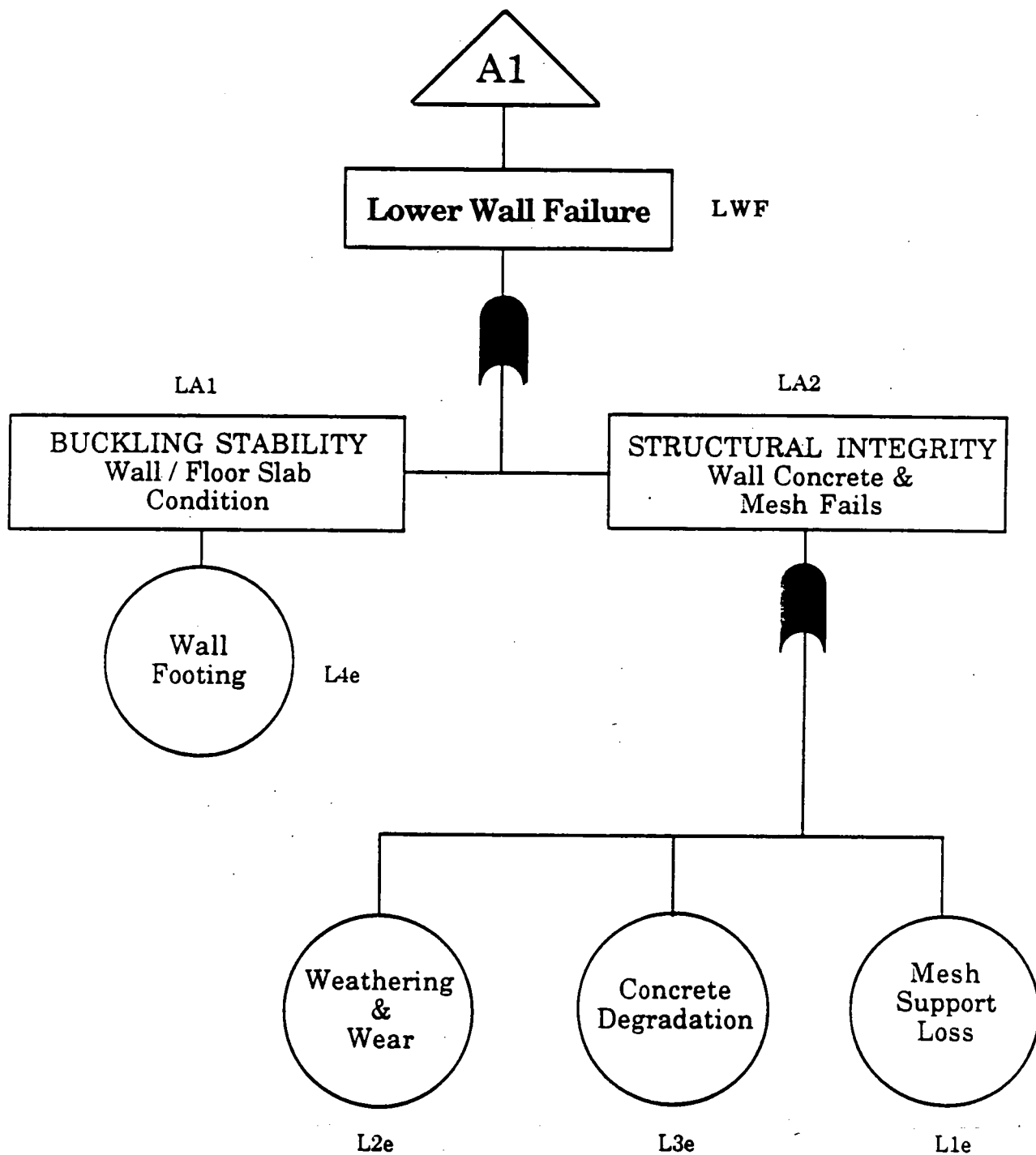
The probabilities for each of the basic events as well as for the total dome failure are listed in summary format in Table 2.23. This table provides for quick reference of all the probabilities associated with the loss of integrity of the silo structure.

Failure Event Probabilities: WALL

The basic events for wall failure are somewhat more complex when compared to those of the dome. Firstly, the wall has been sub-divided for this analysis into two sectors, the upper and lower walls. The field data has been divided so that both wall sectors will have independent basic events. In addition, the data available for the walls is not as complete as that for the domes. The fault tree for wall failure is given by Figures 2.7. and 2.7a.

Fault Tree For Lower Wall Failure

Figure 2.7a



The lower wall failures, as presented in Figure 2.7a, are sub-divided into two potential modes. The structural integrity is governed by the three properties of the concrete, mesh support, weathering and wear (thickness), and concrete degradation (quality, hence compressive strength). The second mode relates to the rigidity of the wall about the floor slab joint.

Lower wall failure is incorporated into the fault tree for total wall failure. Here again, upper wall structural integrity is used to evaluate natural degradation failures.

The fault trees for wall failure show seven basic events:

- 1) Basic Event U1e: Mesh Support Loss, Upper Wall
- 2) Basic Event L1e: Mesh Support Loss, Lower Wall

- 3) Basic Event U2e: Weathering & Wear, Upper Wall
- 4) Basic Event L2e: Weathering & Wear, Lower Wall

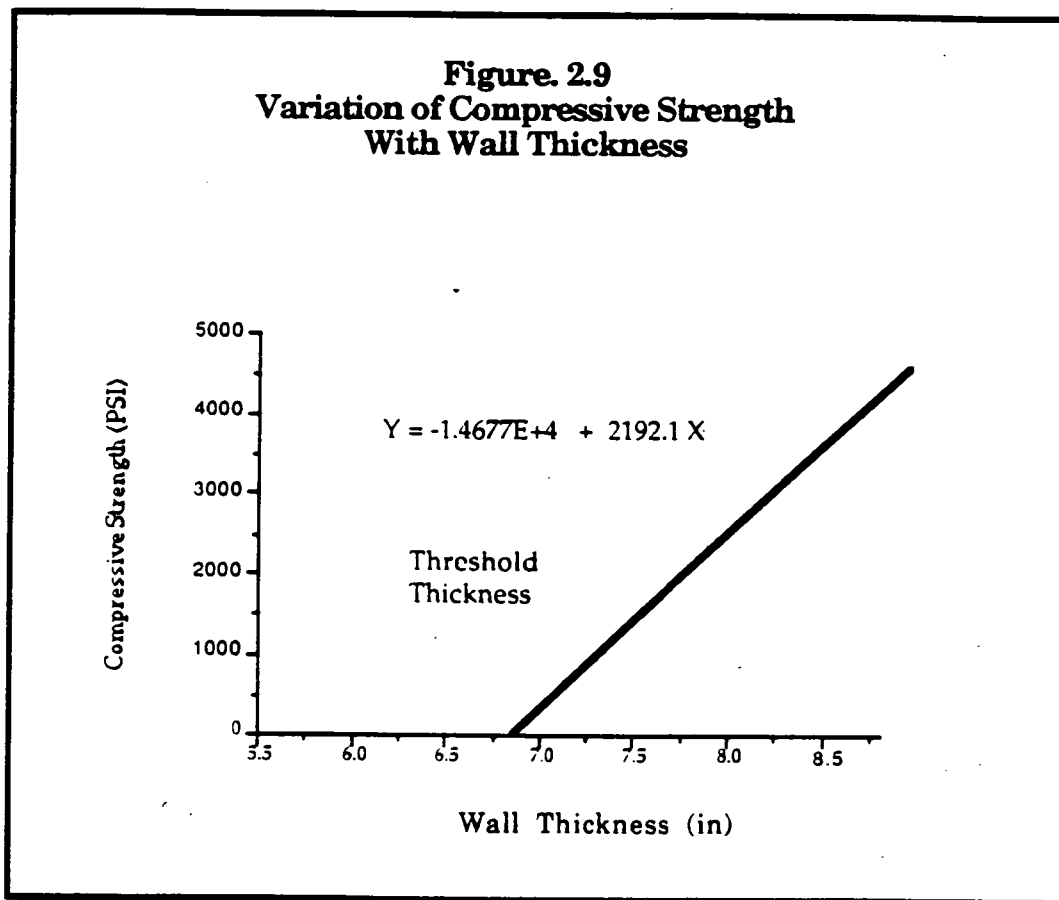
- 5) Basic Event U3e: Concrete Degradation, Upper Wall
- 6) Basic Event L3e: Concrete Degradation, Lower Wall

- 7) Basic Event L4e: Wall Footing Condition

The annual probability of occurrence of these basic events are evaluated using the methodology described above.

Basic Event U2e & L2e : Wall Weathering and Wear.

The wall thickness component of the non-destructive testing, (Camargo, 1986), is used to evaluate the probability of failure due to weathering and wear. The original minimum 28 day compressive strength for the silo walls was 4,500 PSI, (design specification). Correlating the original wall thickness to the design minimum compressive strength allows the extrapolation of a new, present day, compressive strength corresponding to the present day wall thickness. The variation in compressive strength with wall thickness is illustrated in Figure 2.9.



From the above graph, the extrapolated thickness at which the compressive strength is zero, occurs at **6.696 inches**. This value is taken to be the lower threshold of integrity. The average wall thicknesses computed along each test line for both the lower and upper portions of the wall are:

Table 2.24
Average Wall Thickness (in)

SILO 1	
Upper Wall	7.9375
Lower Wall	7.4824

SILO 2	
Upper Wall	7.8780
Lower Wall	7.1382

Using the established methodology to evaluate the exponential degradation rate:

Table 2.25.
Exponential Degradation Rate

SILO 1 (years⁻¹)	
Upper	$\lambda = 2.8663 \text{ E-3}$
Lower	$\lambda = 4.6029 \text{ E-3}$

SILO 2 (years⁻¹)	
Upper	$\lambda = 3.0876 \text{ E-3}$
Lower	$\lambda = 5.9880 \text{ E-3}$

Time to critical thickness, 6.696 in, as expressed by equation 2.2:

Table 2.26
Time to Reach Critical Thickness

SILO 1 (years)	
Upper	$T_{crit} = 93.34$
Lower	$T_{crit} = 58.12$

SILO 2 (years)	
Upper	$T_{crit} = 86.65$
Lower	$T_{crit} = 44.68$

Finally, the annual probability can be evaluated; Equation 2.3:

Table 2.27
Probability Per Year of Wall
Weathering and Wear

Basic Event U2e & L2e

SILO 1 (years⁻¹)	
Upper	$\mu = 0.01376$
Lower	$\mu = 0.02792$

SILO 2 (years⁻¹)	
Upper	$\mu = 0.01519$
Lower	$\mu = 0.05001$

Basic Event U3e & L3e : Evaluation of Concrete Degradation

The extent of internal discontinuities within the concrete matrix can indicate the quality of the structural concrete. These discontinuities include cracks, voids, and the lack of consolidation associated with the reinforcement steel system. Quantification of such discontinuities can be achieved using pulse velocity tests. These values of pulse velocity can be correlated to the uniformity of concrete and thus the in situ compressive strength.

The Camargo test results give values of the pulse velocities at all test locations, these values are converted into compressive strengths for both the upper and lower sections of the walls. The threshold at which the walls may fail is not supplied by Camargo, however, destructive tests conducted on Silo 4 by Bechtel (Bechtel, 1990) show that the remaining strength ranged from 1,463 to 2,531 PSI. This represents an average loss of 60%. In conclusion, the allowable stress quoted by Bechtel is 658 PSI; this value is used as the lower threshold for this evaluation. Using the exponential methodology, the pertinent results are tabulated in Table 2.28.

Basic Event U1e & L1e : Evaluation of Wire Mesh Loss.

Under a critical load combination, the largest stress upon the wires is 114,000 PSI. This case would depict the removal of the earthen berm with the contents of the silos intact. The design stress in the wires was 100,000 PSI and the above value of 114,000 PSI would be above the design limits.

The maximum compressive stress can be assumed to be at locations where wire loss is highest. The highest wire loss reported by Camargo to be 25%. Assuming that at 25% the wire loss is critical, the probability of failure due to wire loss can be calculated. Using the exponential methodology, the pertinent results are tabulated in Table 2.29.

Table. 2.28.
Evaluation of Failure Probability due to
Concrete Degradation
Basic Events U3e & L3e .

	SILO 1		SILO 2	
	Upper	Lower	Upper	Lower
Ave. Pulse Velocity (ft/sec)	14,153	13,332	13,946	13,142
Correlated Comp. Strength (PSI)	4,000	3250	3,500	3,250
Degradation Rate λ (year ⁻¹)	3.4642 E-3	9.5712 E-3	7.3916 E-3	9.5712 E-3
Time to Critical Strength (years)	555.00	200.88	260.12	200.86
Probability of Failure μ (year ⁻¹)	1.866 E-3	5.5184 E-3	4.1560 E-3	5.518 E-3

Table. 2.29.
Evaluation of Failure Probability due to
Wire Mesh Loss
Basic Events U1e & L1e .

	SILO 1		SILO 2	
	Upper	Lower	Upper	Lower
Ave. Wire Loss (%)	0.5208	4.1319	0.4861	6.3141
Degradation Rate λ (year⁻¹)	0.01919	0.04172	0.02121	0.05423
Time to Critical Strength (years)	167.74	77.15	151.76	59.39
Probability of Failure μ (year⁻¹)	6.760 E-3	0.01785	7.584 E-3	0.0269

Basic Event L4e : Wall Footing Condition.

The condition of the joint between the wall and the floor slab may be important from a structural buckling standpoint. Moments which would effect the joint may only be applicable during a seismic applied force. Since such a scenario is regarded as not being an applicable threat, (Camargo, 1986), this basic event is not a primary concern. However, since all inter-dependencies are to be covered, the probability of failure due to wall footing condition are evaluated below.

Condition Statements:

1. GOOD
2. AVERAGE
3. MODERATE
4. QUESTIONABLE
5. THRESHOLD

1986 condition, averaged over all test locations, (Camargo,1986)

Silo 1 2.1667

Silo 2 2.3958

Initial Condition (1952): 1.000

Table 2.30.
Evaluation of Failure Probabilities
Due to Wall Footing Condition
Basic Event L4e.

	SILO 1	SILO 2
Degradation Rate λ (year ⁻¹)	0.0227	0.0257
Critical Condition (years)	70.90	62.62
Probability of Failure (year ⁻¹)	0.0164	0.0131

The probabilities for each of the seven basic events of wall failure are presented in table 2.23. The final annual probability of wall failures are also given for both silo 1 and 2.

Table 2.31.

**Basic Event Contributors
And Total Wall Failure Probability**

Designator	Event Description	SILO 1	SILO 2
Mesh Support Loss:			
U1e	Upper Wall	6.760 E-3	7.584 E-3
L1e	Lower Wall	0.01785	0.0269
Weathering and Wear:			
U2e	Upper Wall	0.01376	0.01519
L2e	Lower Wall	0.02792	0.05001
Concrete Degradation:			
U3e	Upper Wall	1.866 E-3	4.1560 E-3
L3e	Lower Wall	5.5184 E-3	5.51180 E-3
Wall Footing Condition			
L4e	Lower Wall	0.0164	0.0131

2.4 Radionuclide Inventory

The consequence of primary concern that are associated with the failure of the K-65 silos is the exposure of the public to radioactive material. This consequence is dependent on the total radionuclide inventory or source term contained in the silos. The data obtained from WMCO and others clearly shows that the total quantity of radium, thorium, uranium, and radon is not precisely known. The uncertainty associated with the radium inventory also affects the acute and chronic releases of radon and consequently affects the total quantity of the radon daughters. The environmental source term is directly related to the consequences associated with the failure of silos. The failure mode dictates the quantity of material released and the time frame of that release. The objective of this section is to provide the assumptions, results, and analysis for the estimates of the radionuclide inventory and the magnitude of that release.

Estimates Of The Source Term

The total mass of the waste material contained in the K-65 silos is estimated to be on the order of 19,400,000 pounds (NLO, 1968). The total amount of radionuclides residing in this mass is expected to be less than 0.12% by weight. The bulk majority of the waste mass is in the form of silicates (SiO_4), trace metals, various oxides, and residual water. The waste mass is assumed to be approximately 30 to 40 percent water with varying layers that range from hard crust like material to that of a powdery consistency.

A number of estimates and analyses have been conducted in order to arrive at the source term (Battell, 1988);(ASI,1990). To date the most prominent data reflects a total quantity of radium (for both silos) to be in the range of 2,300 to 4,600 curies. The best estimate within this range is on the order of 3,300 curies (≈ 375 nCi/gr). This value was used in this risk assessment to determine the transport and dose resulting from acute releases. The 3,300 Ci estimate also more closely approximates the quantity of radium that would be necessary to yield nearly 600 Ci of radon annually from the silos.

The quantity of radium in the silos has a direct bearing on the production rate of radon (since radium-226 is the parent radionuclide of radon-222). The amount of radium determines in part the quantity of radon available for release. This is true in either a catastrophic failure mode or for the chronic release (radon gas leaking through the pores and cracks of the silo). Radium-226 is called the parent nuclide of radon-222 due to the fact that each time an atom of radium-226 decays an atom of radon-222 is formed. The natural decay mode for radium-226 is the emission of an alpha particle and a gamma ray. The remaining nuclide is then radon-222. The production rate of radon-222 is simply the decay rate of radium-226. There is considerable uncertainty in the radon emission rate from the silos as well as the total inventory available in the free space of the dome,

which is primarily due to two problems: 1) the precise quantity of radium-226 is not available and 2) the rate of diffusion of the radon gas is a nonlinear process and is not known precisely.

The range of values for the inventory of radon in the upper head region range from 30 to 50 curies. The total quantity of radon released per year is also uncertain and values in the range of 167 to over 1100 curies per year have been reported. Estimates of the total source term of radon released each year were made by calculating a range of values that would effectively yield the average values that are measured and by use of the AIRDOS-EPA computer code. As a result of this analysis the acute release of radon was taken to be 50 curies and the chronic annual release was calculated (using best estimates and data that had more than one source) to be 650 curies. In both instances the values were taken as the maximum substantiated values in the given ranges.

Uranium in the silos is estimated (based on records and measurements) to be on the order of 0.41 nCi/gram for the 238 and 234 isotopes, with only 0.02 nCi/gram for uranium-235. This ratio reflects the natural isotopic abundance of uranium-235 and is within the range of the most recent analysis of the residue material (ASI,1990). The estimates of uranium content were taken from early analytical data from NLO. The total quantity of uranium in the silos is taken to be approximately 11,200 kg. This corresponds to a total of approximately 7 curies and is assumed to be distributed uniformly throughout the solid waste material.

The existence of uranium in the silos has been known for some time, but the existence of thorium-230 in the silo residues was not expected. The concentration of thorium within the solid residues has been measured and was found to be both a significant quantity as well as non-uniformly mixed. Three samples analyzed showed a range of concentration of approximately 77 nCi/gram to 483 nCi/gram in the solid waste matrix, for a total inventory of approximately 1,810 Curies. This variation in concentration indicates the non-uniformity and leads to considerable uncertainty in the actual quantity of thorium-230.

The concentration of other radionuclides such as polonium, bismuth, and lead is also expected to be quite large. These elements although significant in their own right were found to be of minimal consequence when compared to the chronic radon dose or the dose resulting from the acute release of residue material. The radon dose calculations were made using dose conversion factors which incorporated the radon decay products. The dose conversion factor assumes a 70% secular equilibrium with the short lived radon progeny. This equilibrium value is probably high by a factor of 1.75. The release rate and the mechanisms affecting the release of radon from the silo can significantly affect the buildup of the daughters. Also the decay products are heavy charged particles and are susceptible to deposition processes more strongly than is radon. Radon that is free of any decay products would require

approximately one hour to reach 60% equilibrium. The time lag would occur simultaneously with the transport of the radon gas. Even with relatively calm winds the dispersion of radon can be over a distance of more than 1500 meters. The transport calculations in the following section show that the dilution of the radon is much more significant than the buildup of the daughter products.

Calculations of long term exposure from the daughter products from ingestion routes are essentially insignificant compared to the direct and inhalation doses from the residue materials. The significant exposure path for the radon daughters is through inhalation and this was taken into account in the dose conversion factor.

The concentration of each of the radionuclides and their isotopes as determined above have a large degree of inherent uncertainty. This stems in part from the possibility that the residue material was processed to some degree. Processing to remove a particular chemical species will disrupt any possibility that there is secular equilibrium. The assumption of natural abundance for the isotopic concentration of uranium-235 is in part a result of the uncertainty in the actual concentrations. There was no way to determine whether there had been any processing to remove uranium-235 therefore the assumption was made to use the natural abundance. Small increases in the concentration of uranium-234 significantly increases the dose to an exposed individual. ASI/IT samples indicate that the concentrations of the uranium isotopes follows the natural abundance within a reasonable range.

2.5 Failure Sequences And Release Potential

Event trees were developed for each phase of the study in order to evaluate, in a stepwise fashion, the contribution of a series of events with the final risk estimates. The preceding discussion centered on specific failure initiators and the methodology for evaluating those initiators. In addition a discussion detailing the forces associated with the wind from a tornado event was presented. The next phase of the study deals with the linking of the failure initiators with the potential for release of the residue material. Figures 2.10 through 2.12 illustrate the comprehensive event trees concerning specifically the failure potential of the silos.

Figures 2.10 through 2.12 illustrate the various events which lead to silo failure as a result of each of the initiators considered. In each of the figures the basic components of the silo structure are examined with attention focused on the potential for release of residue material. In the case of the tree describing the loss of silo integrity due to a tornado event the silo components are the upper wall, the dome, and the lower wall. The basis for using these three elements as the top events in this tree stem from the interaction of the tornado event on the silo. The upper wall is expected to have stresses imposed on it from the high winds, the pressure gradient, and the stress induced by the other structural units. Similarly the dome structure is acted upon by the wind and the upper and lower wall units. The order of the units is intended to aid in the elimination of unnecessary events and sequences.

In each scenario, which is described by an event sequence, the outcome is expected to be either the integrity of the silo is maintained or is lost. The tree depicted in Figure 2.12 has three 'failure' sequences and one 'success' sequence. The successful sequence is labeled by 'TI' which represents the probability that a tornado event will occur in any given year in any given square mile. This sequence is considered a success due to each outcome, the upper and lower wall units as well as the dome, results in a success. If the tornado event occurs and the result is no loss of structural integrity to the silo then the sequence is a success. The other three sequences in this tree each yield a failure by resulting in at least one path through which radioactive residue material can escape. The upper wall failure will lead to a path for radon in the head space, the lower wall failure may lead to a path via leaching, and the loss of the dome is a direct path for both the radon and the residue material. This tree is not used for determining the actual release but only the probability of structural failure as a result of the tornado initiator. The numbers contained in the right hand column indicate the respective sequence probability. The very small probabilities for the sequences involving the upper and lower wall failures indicate the extreme forces necessary to fail these units. The tornado events required in order to have any possibility of failing these substructures are in the range of the F4 to F5 intensity class. The probability of the maximum wind speed coincident with the required tornado event is used to represent the probability of the structural failure.

Figure 2.10: Loss Of Structural Integrity (Concrete Degredation) Event Tree For K-65 Storage Silos

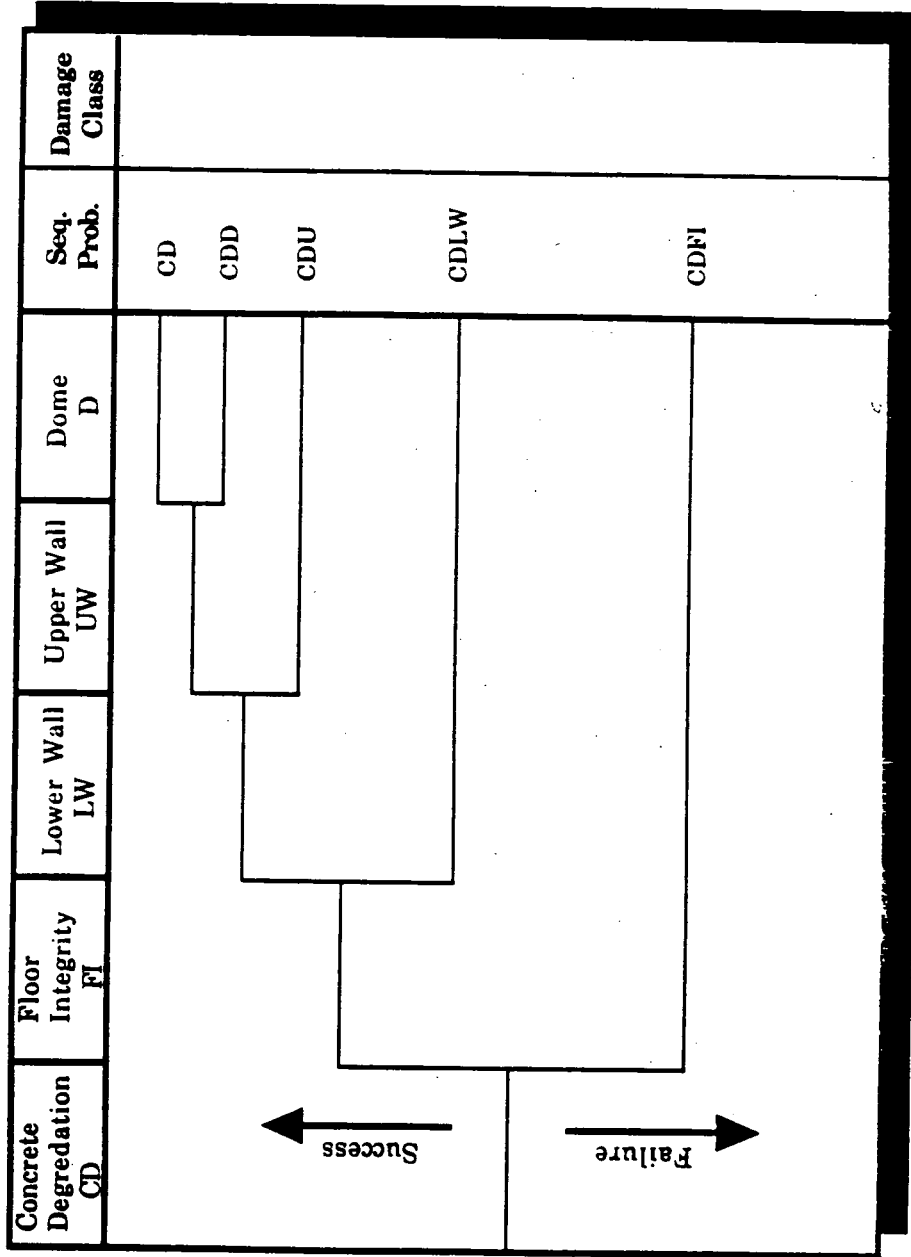


**Figure 2.11: Loss Of Integrity From Natural Forces (Seismic) Event Tree
For K-65 Storage Silos**

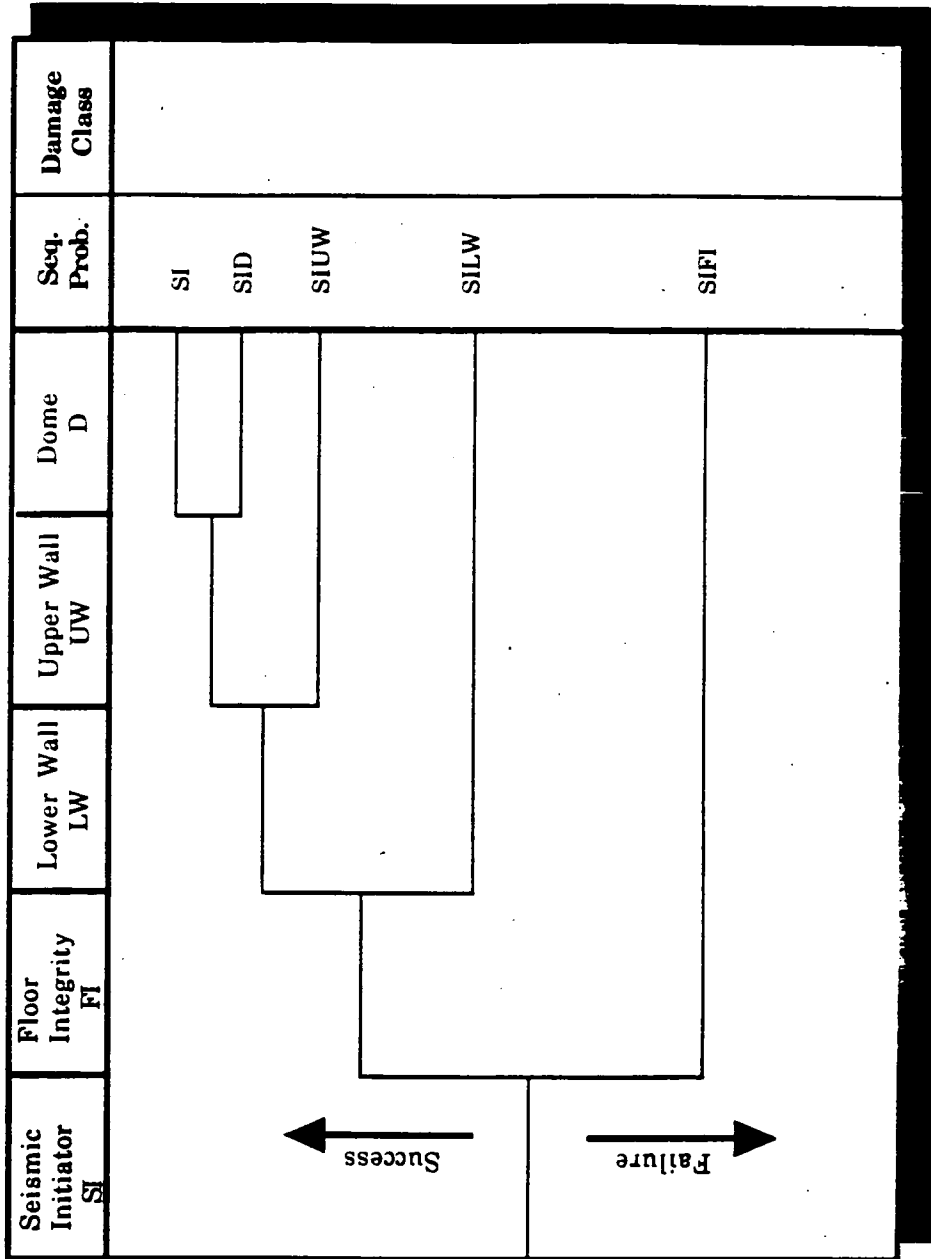
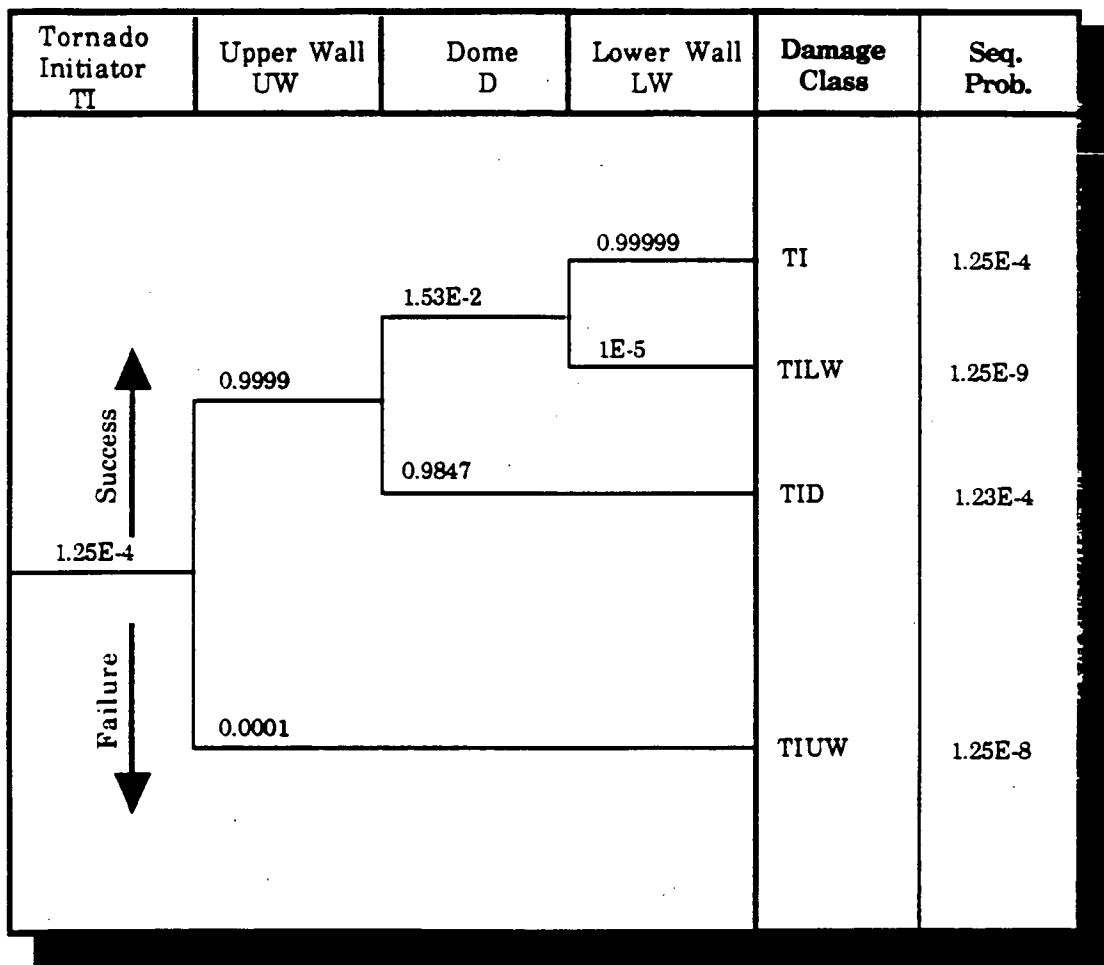


**Figure 2.12: Loss Of Integrity
From Natural Forces (Tornado)
Event Tree For K-65 Storage Silos**



98

The silo failure trees were then linked to event trees which describe the mechanisms and scenarios leading to a release of the waste material. These trees, called release trees, are illustrated in Figures 2.13 and 2.14. Figure 2.13 illustrates the release events associated with the seismic and degradation initiators while Figure 2.14 depicts the release sequences resulting from the tornado event. For the purposes of this study the tornado release event tree has been developed to illustrate the wide range of possible release scenarios.

The five events after the initiator are intended to describe the specific scenarios which are a result of the action of tornadic winds on the silo structures. The first event indicates the potential for only minor dome cracks which would release radon. This first event is considered to be associated with a tornado of intensity F1. The second event describes the potential for partial dome collapse as a result of an F2 or F3 tornado. The fourth and fifth events relate to complete dome collapse and removal that are expected to be associated with the F4 and F5 tornado intensities. The classification of tornado intensity with specific structural response was determined as a result of the forces associated with the tornado events and the critical loading estimated for the silo structure. The last event is intended to represent the force needed to remove the residue material. The last event is a link to the next stage of the overall analysis which is the transport and exposure assessment. This tree then presents the probability of release after a silo failure. These numbers are listed in the right hand column of Figure 2.14.

The final stage was to incorporate event trees describing the connection or series of events related to the transport and ultimate exposure of the waste material in the environment. An example of this tree, for the 'Tornado Event', is illustrated in Figure 2.15. This tree is intended to serve as the bridge between the failure and the ultimate exposure scenario. The events in this tree describe the manner in which the wind forces act on the residue material. There are pressure gradients, translational winds, and finally the ability for the wind to carry residue particulates for both short and long distances. The probability estimates listed in this figure illustrate the extreme uncertainties and variabilities in the transport and exposure calculations. The exact nature of the wind action on the residue material is not clearly understood. The possibility exists that the residue material is extremely rigid and unyielding to the eroding and lifting capabilities of the wind.

The completion of similar trees for the seismic and degradation scenarios was eliminated due to the trivial results that would have been obtained. The overall connection between the phases of the study (and the various event trees) is depicted in Figure 2.16. This figure illustrates the functions used to pass both probabilities and consequences from one phase of the study to another.

**Figure 2.13: Seismic - Degradation Event Tree
For Release From K-65 Storage Silos**

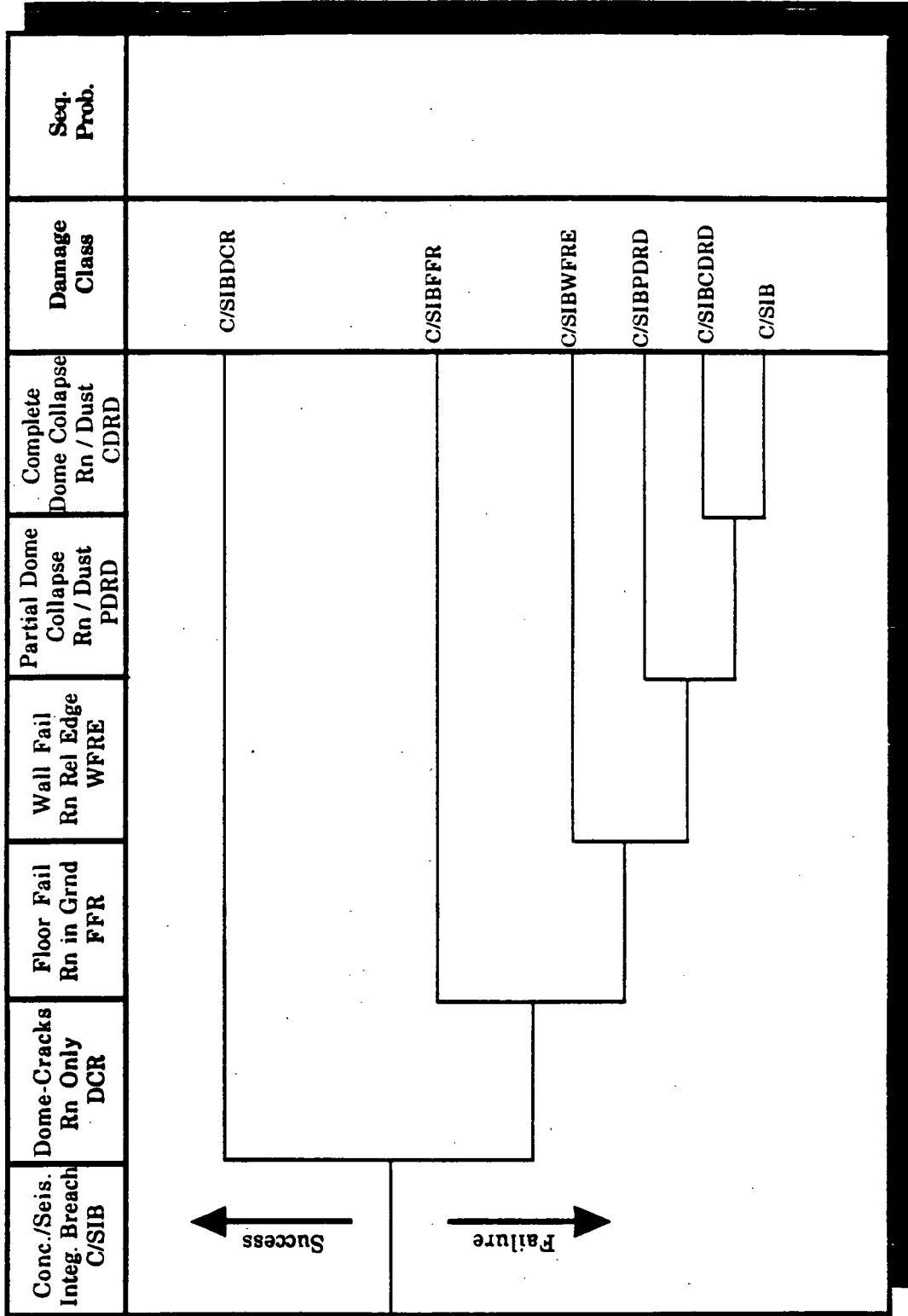


**Figure 2.14: Natural Forces (Tornado) Event Tree
For Release From K-65 Storage Silos**

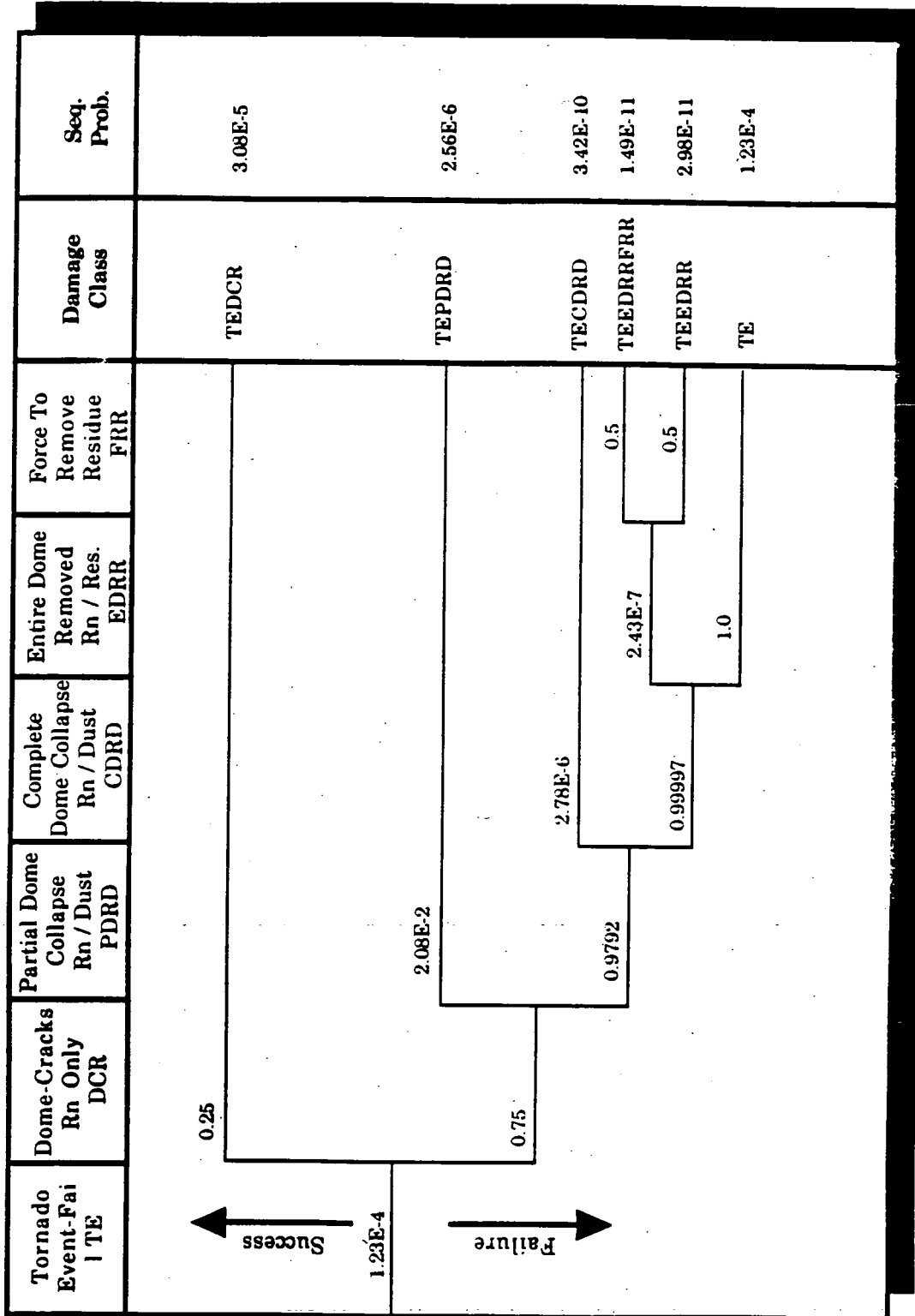


**Figure 2.15: Tornado Transport / Exposure
Event Tree For K-65 Storage Silos**

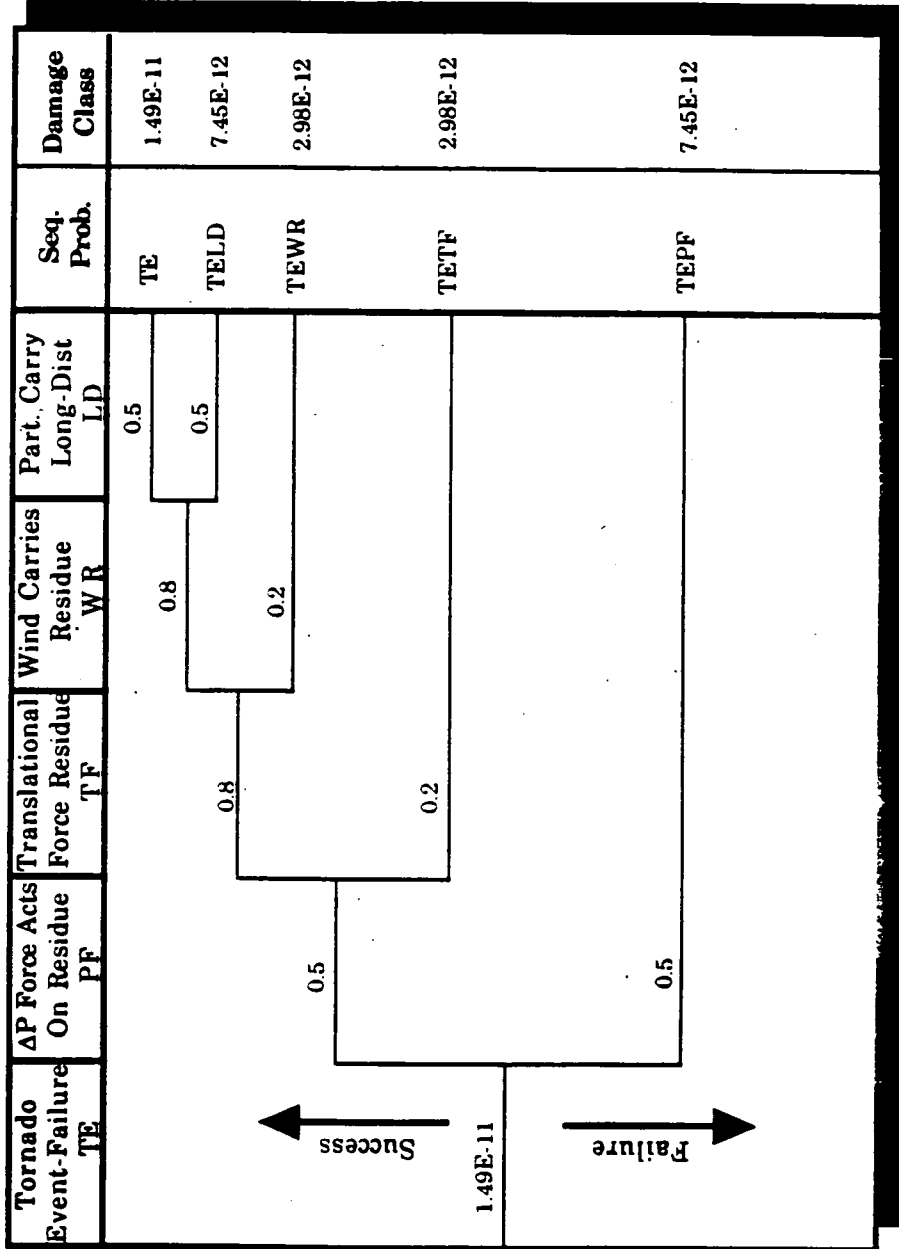
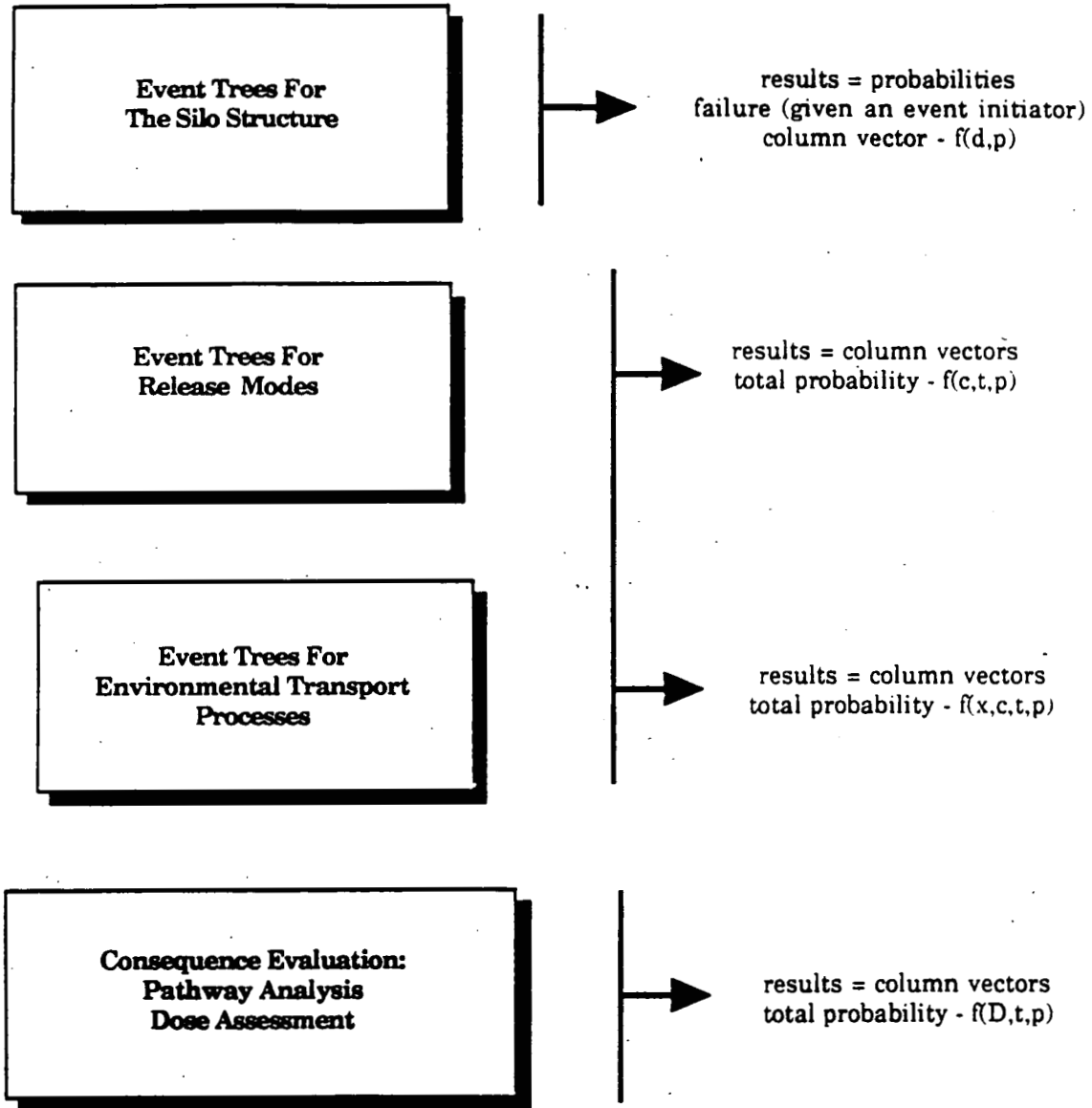


Figure 2.16: Event Tree Relationships Applied In The K-65 Risk Assessment



$$R = [\text{fail}] \times [\text{release}] \times [\text{transprt}] \times \{\text{consequences}\}$$

The potential (probability following silo failure) for release of radionuclides to the environment is related to the physical characteristics of the waste material or residue as well as the probability of the silo failure mechanism. The probability of the failure mechanism was covered in Section 2.3. Since the total radionuclide inventory accounts for less than 1% of the total mass, the residue material must act as a carrier for the radioactive particulates. This fact then reduces the problem of determining the source term to one of estimating (qualitatively and/or quantitatively) the total mass of residue material that can be released from the silo structure. In the case of atmospheric release the dispersion of material will be determined in part by the chemical form, the particle size, and the scale of turbulence in the environment. The waste material was assumed to be composed predominantly of silicates (sand). The exact water content although not known precisely has been estimated to be approximately 30 to 40 percent which may significantly influence the impact of the wind forces on the material. The water is expected to act as a binder for the solid material thus reducing the tendency for distribution, however measurements and sampling data indicate that the upper layers of the residue material may be dry and available for dispersion.

The failure modes addressed for applicability to the release terms are: 1) catastrophic failure leading to an acute release of radon, radium, uranium, and thorium, 2) partial failure resulting in an acute release of radon, and 3) chronic failure resulting in the continuous emission of radon gas.

Magnitude of Maximum Release

The model used for evaluating the source term for an acute release where only radon-222 is released is straight forward and consists primarily of the estimation of the total quantity of radon gas in the upper free space of the silo. The model for the source term associated with an acute release where a significant amount of the residues are exposed to the atmosphere is much more difficult to evaluate. As previously stated the damage to the silo in the event of a tornado was assumed to be the complete removal of the dome structure. The total surface area of the residue material is then left exposed to the full force of the wind and pressure forces.

The total force associated with a tornado event is composed of two parts: 1) the lift and drag forces resulting from the high tangential and translational wind velocities, and 2) the uplifting forces associated with the pressure drop accompanying the funnel cloud. These forces can in many cases act in concert for the total load on an object. As a result of these two force components the dome structure is assumed to be completely removed and the residue material is allowed to experience the full effect of the wind and pressure forces. In order to estimate the effect of the wind on the removal of radioactive contaminants both the density of the residue (which is approximately 100 pounds per cubic foot) and the maximum compressive and tensile forces (which are greater than 390 pounds per square foot each)

555

were considered. The radionuclides were assumed to be distributed homogeneously throughout the residue material and the problem of evaluating the source term released is reduced to evaluating the total quantity of residue material removed and dispersed.

The depth of residue material available for redistribution can be estimated by using the ratio of the pressures to the dead weight of the material. In this case the force of the wind would be capable of lifting an amount of residue material approximately 4 feet in depth and 1 foot wide. The weight of 4 cubic feet of residue material would therefore be about 400 pounds. Even though the wind forces are acting over an surface area the net effect of the continued wind and pressure forces for the duration of the tornado event is assumed to be capable of lifting nearly the 4 foot depth of material. The calculations made for this study assumed, for convenience, a total depth of 1 meter (which is approximately 3.28 feet) over the area of a single silo. Since the silo being approximately 80 feet across (24.5 meters) the total volume of residue material that would be potentially removed is calculated to be approximately 468 m³. The density of the residue material is calculated to be nearly 100 lbs/ft³. At this density and with the concentration of radium of 375 nCi/g the total quantity of radium released is approximately 281 Ci. This is in turn approximately 8.5% of the total radium inventory.

This analysis method provides the total quantity of residue material released and therefore the magnitude of the radioactive source term, which has already been divided by radionuclide and by the specific isotope. The next phase of the analysis requires an estimate of the quantity of the released material which is airborne and the amount which is deposited on the ground near the failed silo. The best estimates on the fraction of the airborne and ground deposited material come from measurements of particle sizes and distributions resulting from explosions of sand, gravel, and other similarly related materials (LLNL, 1985). In most cases the distribution of size is taken to follow a 90-9-1% ratio. The net result is that 90% of the released material is deposited within close proximity to the structure (within 300 feet of the point of release), then about 9% is deposited within about 2500 feet, and the remaining 1% is available for atmospheric dispersion. Figure 2.17 depicts the magnitude of the release and the distribution in the environment. Table 2.32 provides the magnitude and type of the source term as a function of the failure mode.

The mechanism of dispersing the residue material as a result of tornadic winds may be different from that of sand and other materials that are in explosions. The problem however was further evaluated by investigating photographs of damage done to a variety of structures by tornado events. Additionally calculations using the wind speeds and pressure drops were used to estimate the net impact on the residue material. Figures 2.18 through 2.20 help to illustrate the effect of the wind on the silo material. Figure 2.18 shows the possibility of the wind as an erosion force on the residues. This possibility assumes that the residue

Figure 2.17: Magnitude And Distribution Of The Source Term

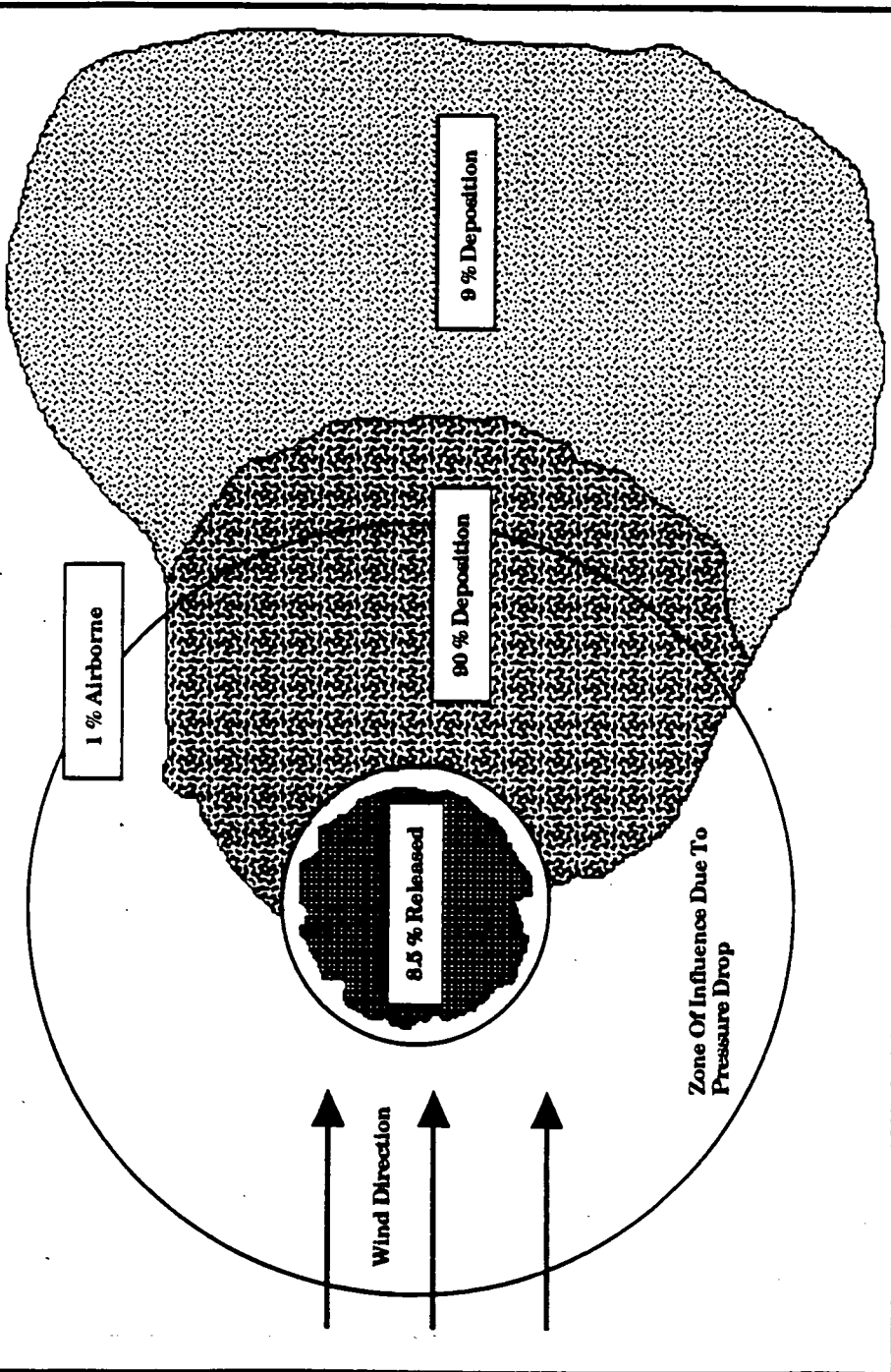


Figure 2.18: Diagram Illustrating Translational Wind Forces On Residue Material

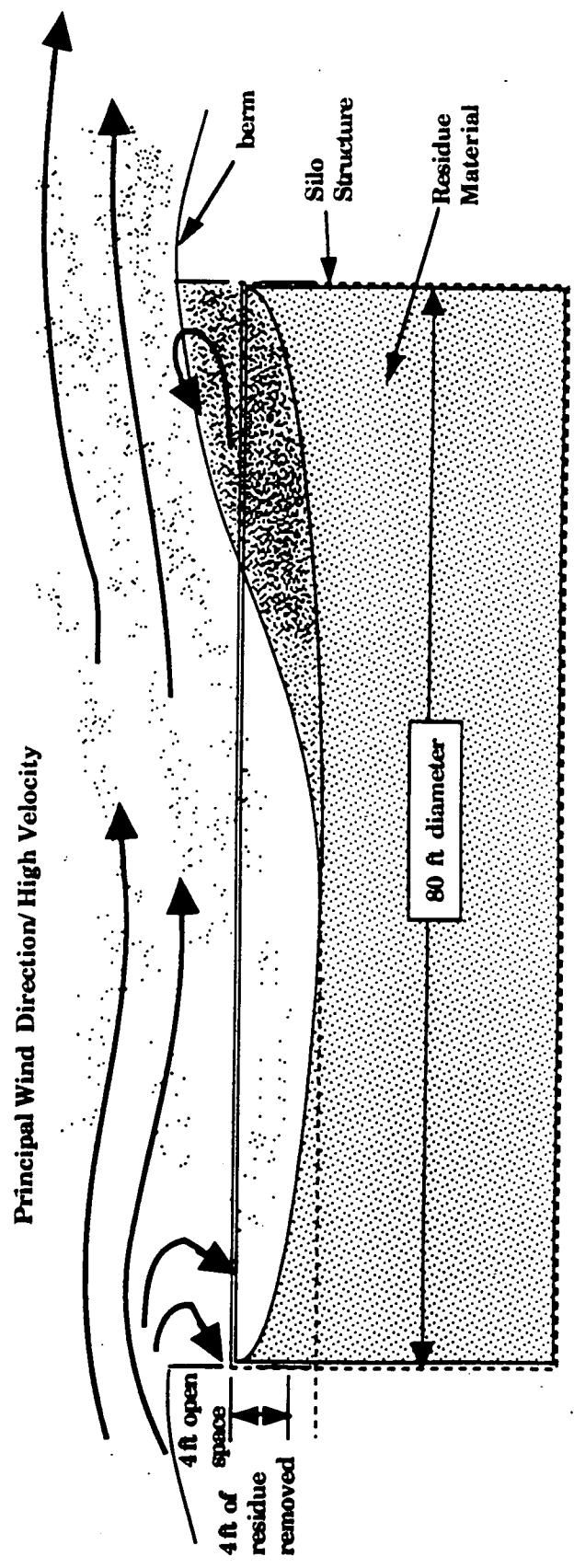


Table 2.32: Source Term Released Relative To Failure Mode

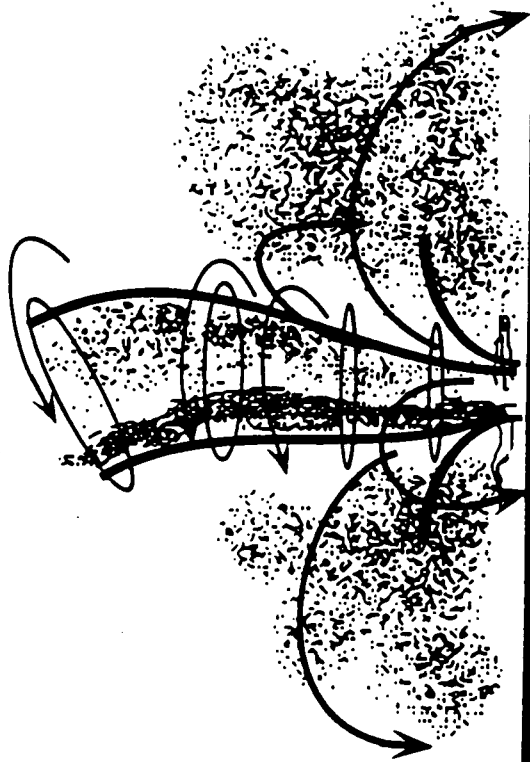
Failure Mode	Source Term (Curies)		
	Airborne	(100 - 300 ft.)	Ground Deposition (300 - 2500 ft.)
Acute			
uranium (238, 234)	5.96 E-3	0.536	0.0536
uranium (235)	7.3 E-5	6.5 E-3	6.8 E-4
thorium-230	1.54	138.6	13.86
radium-226	2.81	252.9	25.29
radon-222	50.0	-	-
Chronic			
radon-222	650.0	-	-

material is loose and mostly sand like. Figures 2.19 and 2.20 are intended to illustrate the possible trajectories and paths that particles will follow when caught in tornadic winds. These diagrams calculations and related references were used to substantiate both the maximum residue material that could be removed and the distribution in the environment.

This analysis was arrived using conservative assumptions and estimates whenever possible. The conservative factors are intended to overestimate the source term and the eventual distribution in order that the maximum effects (risks) can be characterized. The release and transport trees were then developed to add perspective to the overall risk assessment.

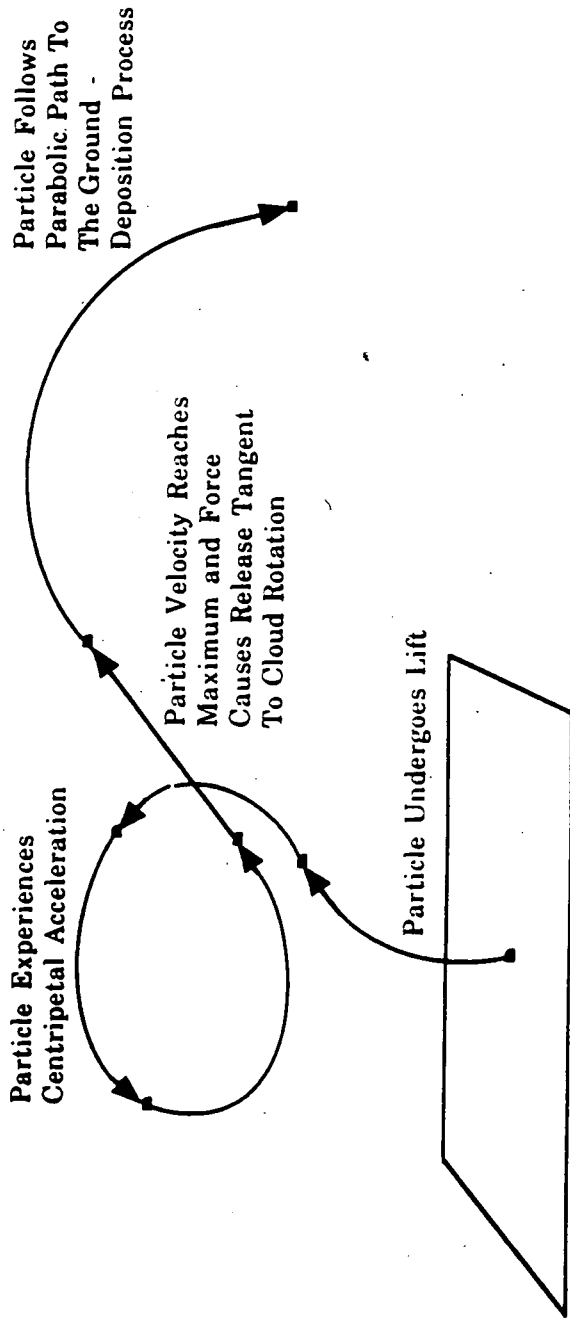
The source term estimates were based on both analytical work and references to other reports and documents concerning the K-65 silos. The calculations made include estimates of the volume of free space available in the dome portion of the silos and the approximation of the radon release rate using analytical and calculational techniques as well as data from actual measurements to relate the production and loss terms. This work was employed in an attempt to consolidate and compare the various estimates of the quantity of radium in the silos. The uncertainty of the radium concentration is considered a dominant limitation of the risk assessment.

Figure 2.19: Diagram Illustrating Tornado Effect On Surface Material Such As Sand, Dirt, Leaves, Etc.



The turbulent forces associated with the cyclonic winds tends to pick up objects from the surface. Once an object is fully involved in the cyclonic wind the release and deposition is dependent on the mass of the object and the shape. Small particles such as that associated with the residue material tend to be picked up easily and deposited within a close proximity due to the extreme resistance to the high velocities and the drag effects.

Figure 2.20: Schematic Representation Of Particle Path And Trajectory As A Result Of Tornado



3.0 EXPOSURE AND DOSE ASSESSMENT

This section details the environmental transport, exposure scenarios, and the pathway analysis associated with the dose assessment. Essentially this section of the report considers everything after silo failure and the corresponding release has occurred. The extent of the dispersion or distribution of radionuclides in the atmosphere, soil, and water were analyzed. Exposure scenarios were postulated and evaluated and the dose was assessed. This section of the report also covers the probability aspects of the release sequences and the environmental transport as described in Section 2.6.

3.1 Environmental Transport Considerations

Atmospheric, terrestrial and biotic, and water routes constitute the available pathways through which radioactive material released to the environment can ultimately result in the exposure of the public. The terrestrial and biotic pathways included ingestion of contaminated food as well as the redistribution of the contaminants through processing and shipment. The water routes include surface water and groundwater sources which are typically used for everything from irrigation to drinking water. The atmospheric routes eventually impact the water and biotic pathways through precipitation, winds, and fallout.

The pathways considered in this study were limited to the atmospheric routes. The limitation of transport paths was due to the time frame of the risk assessment (5 years) and to the nature of the release and transport mechanisms following silo failure. The dominant exposure pathway for the radionuclides of concern was found to be inhalation.

Environmental Transport Models

The transport of the radioactive material in the environment is a component of the pathway analysis and exposure assessment phase. The details of the analysis, including the basic assumptions, will be discussed in this section with the results (concentrations in the air and on the ground) will be presented in Section 3.

There are essentially two types of release modes considered in this analysis. These are considered as acute and chronic. This terminology refers primarily to the time frame of the release, but also to the type of failure mechanism and therefore the magnitude of the release. The chronic refers to the continuous release of radon gas, while the acute release can be either entirely radon or a combination of radon, radium, thorium, and uranium. With this convention there are a total of three exposure assessments and three source terms to be evaluated for transport in the environment.

The principal transport mechanism is atmospheric dispersion, including the ground deposition processes. Other potential transport mechanisms generally require time frames longer than a few years to assess completely. For this reason only the atmospheric transport of contaminants released from the silos was considered.

Atmospheric transport of contaminants is typically modeled using a standard Gaussian plume dispersion equation, which relates the distribution of contaminants in the atmosphere to the point of release by means of a dispersion coefficient. The dispersion coefficients are developed as a result of empirical correlations from experimental data. The best known model is that which is contained in the AIRDOS-EPA computer code. This code utilizes the Pasquill-Gifford parameter system for evaluating the dispersion coefficients.

The Gaussian plume model is applicable, in many situations, to both short term (one hour) and continuous releases and transport times. The data base containing the wind direction, velocity, and stability frequencies can be manipulated to approximate both of these release modes. For the purposes of this study the acute releases were assumed to occur over a one hour period, while the chronic release was taken as an average release rate over a one year period. The principal difference between the two modes, in terms of atmospheric transport, is the number of sectors over which the concentration calculations are made. The one hour release (acute cases) uses only one 22.5 degree sector at 100% frequency (for wind direction, velocity, and stability class) for the concentration calculations. The chronic case on the other hand utilizes the time averaged wind frequency data which is accumulated over an entire year along with all 16 of the 22.5 degree sectors. Additional changes to the input data, to account for the short term release, concern the magnitude of the source provided to the code and the buildup time (for ingrowth from radioactive decay as well as scavenging and deposition processes). Depending on the specific scenario considered there are a number of options, in the input data file, that can be selected in order that the computer results best reflect the physical scenario.

The following assumptions were used to evaluate the concentrations of radionuclides in the atmosphere resulting from a hypothetical tornado event and from the continuous release of radon from the K-65 silos. As mentioned previously two types of release modes were considered: 1) acute release of radon gas and residue material, due to severe weather (tornado) and 2) the chronic release of radon gas due to the current situation of the silos. The time frames considered for the AIRDOS-EPA computer runs were taken to be 1) one hour release for the acute case and 2) one year average for the continuous case.

The continuous case was evaluated using the FMPC site specific meteorological data which includes time averaged wind speeds, stability classes, and wind directions. This method corresponds to the typical use of

the AIRDOS code with the exception that the doses were evaluated with both the radionuclide data base contained in the code and by using the more recent values for dose conversion factors (DCF's) as provided by Kocher. The radionuclide data base for the DCF's contained in the AIRDOS code does not contain the most recent and accepted values. The AIRDOS code was, therefore, essentially used to evaluate the concentrations of the four radionuclide species in the atmosphere. The dose estimates provided by the AIRDOS code were useful as a reference values or for a magnitude comparison for each of the exposure scenarios considered.

The acute release was modeled using a single sector and a single stability class (F) for the most conservative estimate. The direction considered depended on the population distribution and the predominant wind direction. The population center used in this analysis was considered to be within 14 kilometers, of the release point, and is located essentially East Northeast of the site. This would correspond to a principal wind direction from the West Southwest. Using the AIRDOS code in this manner is consistent with the basic theory of the Gaussian diffusion model since the time scale considered must be compatible with the turbulent diffusion mechanism. The translational wind speeds typically accompanying the tornado event are in the range of 30 to 70 mph and thereby providing the wind force sufficient to disperse particulates as far away as 30 miles in a one hour period.

The concentration in the atmosphere for both the population dose and the nearest resident were estimated using the sector average option in the AIRDOS code. Although this results in a lower dose the sector average concentration is the more realistic value and is comparable with fence line radon measurements at the FMPC site. Table 3.0 lists several of the key input parameters and the values used in the assessment. The annual rainfall and the heights of the plume and lid were taken to provide a better representation of a storm situation for the single sector one hour release model used.

Table 3.0: AIRDOS-EPA Input Data

Parameter	Input Value
source height (PH)	27 feet (accounting for silo wall height)
plume height (PR)	50 meters (high winds)
lid height (LID)	1000 meters
annual rain (RR)	100 inches
average temperature (TA)	285.3 K
scavenging coefficient (SC)	1E - 5
deposition velocity (VD)	1.8E - 3

The source terms used depended on the specific release mode considered. The concentration in the atmosphere is linearly related to the source term, therefore to evaluate the concentrations resulting from greater source terms new concentrations are simple multiples of the previous concentrations. The results of the atmospheric transport models are listed in Table 3.1 and are discussed in Section 3.1.

Table 3.1: Results Of Environmental Transport For Acute And Chronic Release Modes

Radionuclide	Distance (m)	Acute		Chronic	
		Conc. Air (Ci/m ³)	(pCi/g) Conc. ground	Conc. Air (Ci/m ³)	Conc. Air (Ci/m ³)
uranium	100	2.8E-09	1.069	-	-
	500	1.4E-10	0.049	-	-
	2,500	6.3E-12	0.002	-	-
	14,500	1.8E-15	0.0	-	-
thorium	100	9.8E-08	35.3	-	-
	500	4.6E-09	1.64	-	-
	2,500	2.1E-10	0.0756	-	-
	14,500	5.9E-14	7.56E-06	-	-
radium	100	1.4E-07	50.0	-	-
	500	6.5E-09	2.34	-	-
	2,500	3.0E-10	0.11	-	-
	14,500	8.5E-14	1.1E-05	-	-
radon	100	3.3E-05	-	8.4E-09	-
	500	1.5E-06	-	4.8E-10	-
	2,500	7.3E-08	-	4.1E-11	-
	14,500	2.7E-09	-	2.6E-12	-

3.2 Probability Of Release And Transport

The consideration of the probability of a given release and the probability of the resulting dispersion in the environment was considered extensively for the final PRA of the K-65 silos. The transport models and analysis discussed previously were utilized in the evaluation of this phase of the study. A significant amount of energy and time were expended in determining the methodology and the analysis techniques for evaluating this portion of the PRA.

Several diagrams have been added to this section to provide some insight to the type of modeling undertaken. The first three illustrations, Figures 3.1 through 3.3 indicate the potential for variation in radon concentration from atmospheric dispersion as a result of building wakes. The uncertainty in the coefficients for building wakes and the inherent limitations in the AIRDOS and GENII dispersion models restricted the usefulness of the building wake analysis. The variation in the measured values of radon and the values predicted by the AIRDOS code help to illustrate the difficulty in assessing the exact concentration a large distances from the source.

A number of areas have been investigated in and around the FMPC production area in order to evaluate the occupational exposure. The tool used to accomplish this type of modeling was limited to the Gaussian plume model with primary emphasis on the AIRDOS and GENII codes. Figures 3.4 through 3.6 represent the extent of the 100 and 500 meter exposure points discussed later and the extent of the influence from the maximum release of residue material.

Additional analysis was made of the chronic radon release by using the AIRDOS code and actual data taken from both onsite and offsite locations. Figure 3.7 shows the locations where actual radon measurements were taken. Straight line distances, from the silos to the monitoring point, were estimated for these locations using site maps. The distances were then input into the AIRDOS code and the predicted concentrations were determined. The result of this modeling is summarized in Table 3.2. The measured values along with the net value after subtracting for background are presented. The statistical results for the measured values and the background values is presented in the 1988 Environmental Monitoring Report. The measured and predicted values are seen to compare favorably in light of the limitations inherent in the Gaussian Plume model.

The distances of the measured values are near the limit of acceptability for the Pasquill-Gifford system of dispersion coefficients, which is assumed to be at 1 to 2 kilometers. Additionally the AIRDOS code is not extremely flexible for evaluation of regions where the terrain is as varied as it is near the FMPC. In spite of the limitations the predicted values are generally within an order of magnitude and for those critical

Figure 3.1: Diagram Showing An Overview Of The FMPC Production Area And The Assessment Region For Chronic Radon

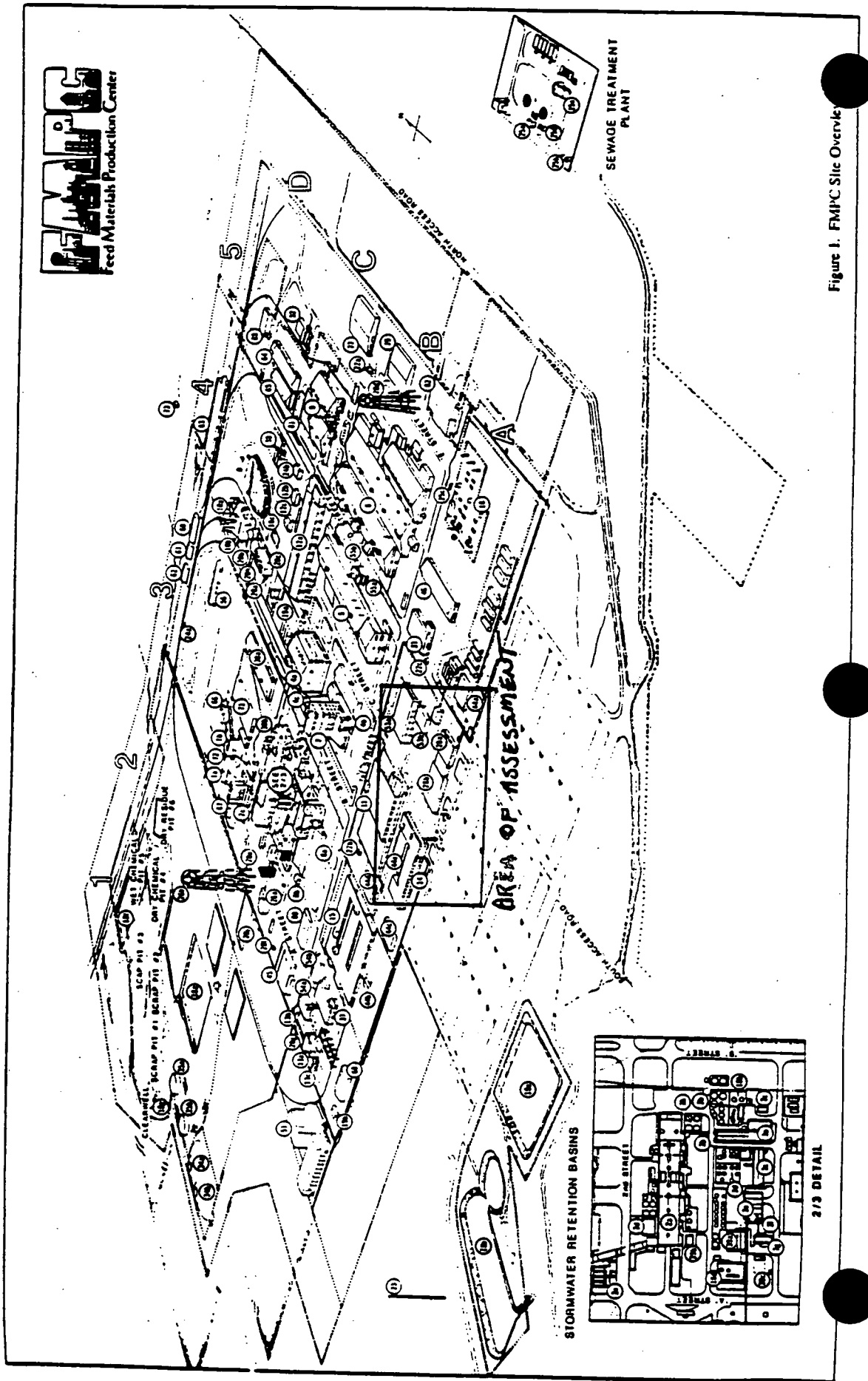


Figure 1. FMPC Site Overview

Figure 3.2: Diagram Of The Preliminary Assessment Of Wind Patterns In The Production Area

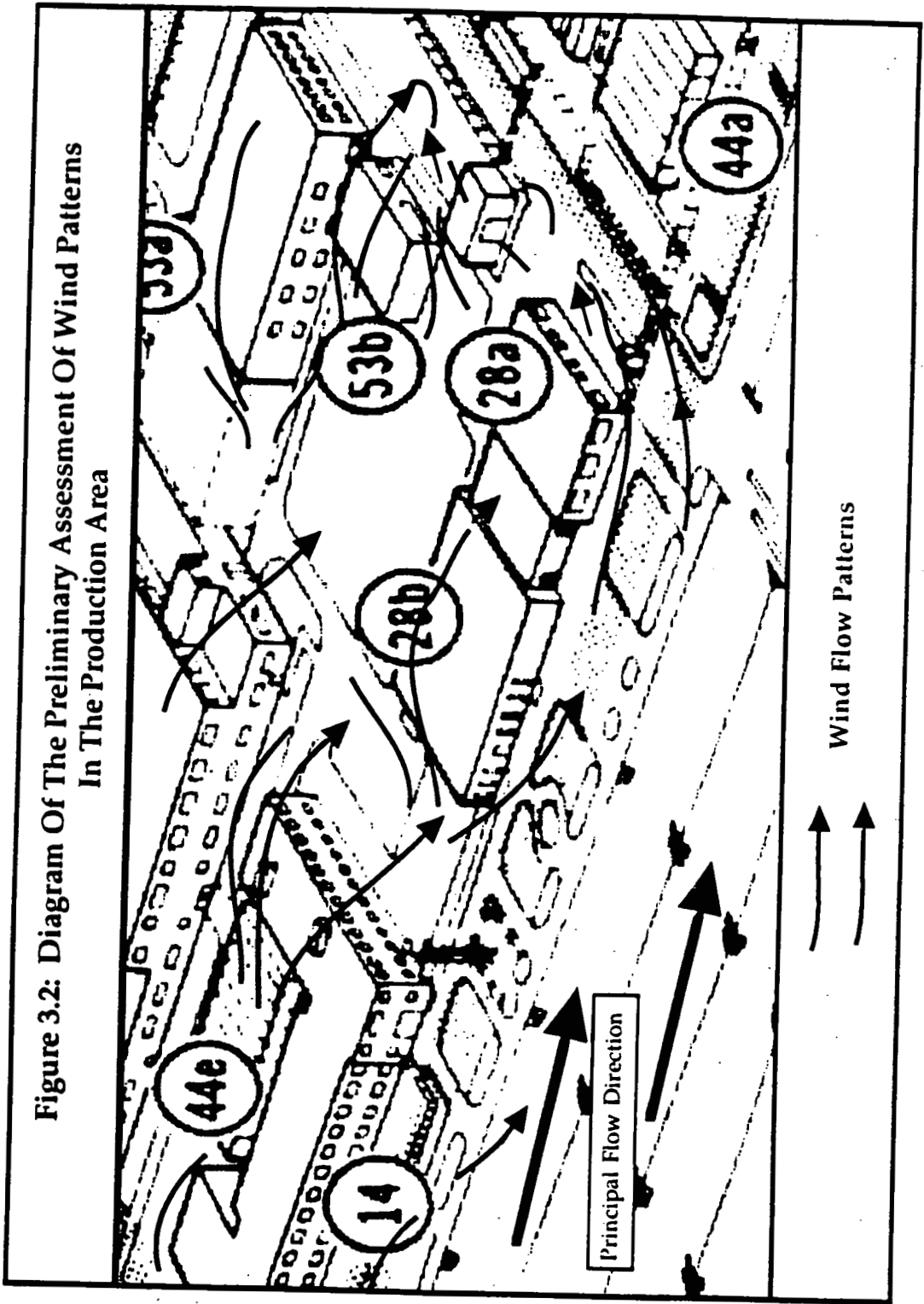


Figure 3.3: Diagram Of The Preliminary Assessment Of Radon-222 In The Production Area

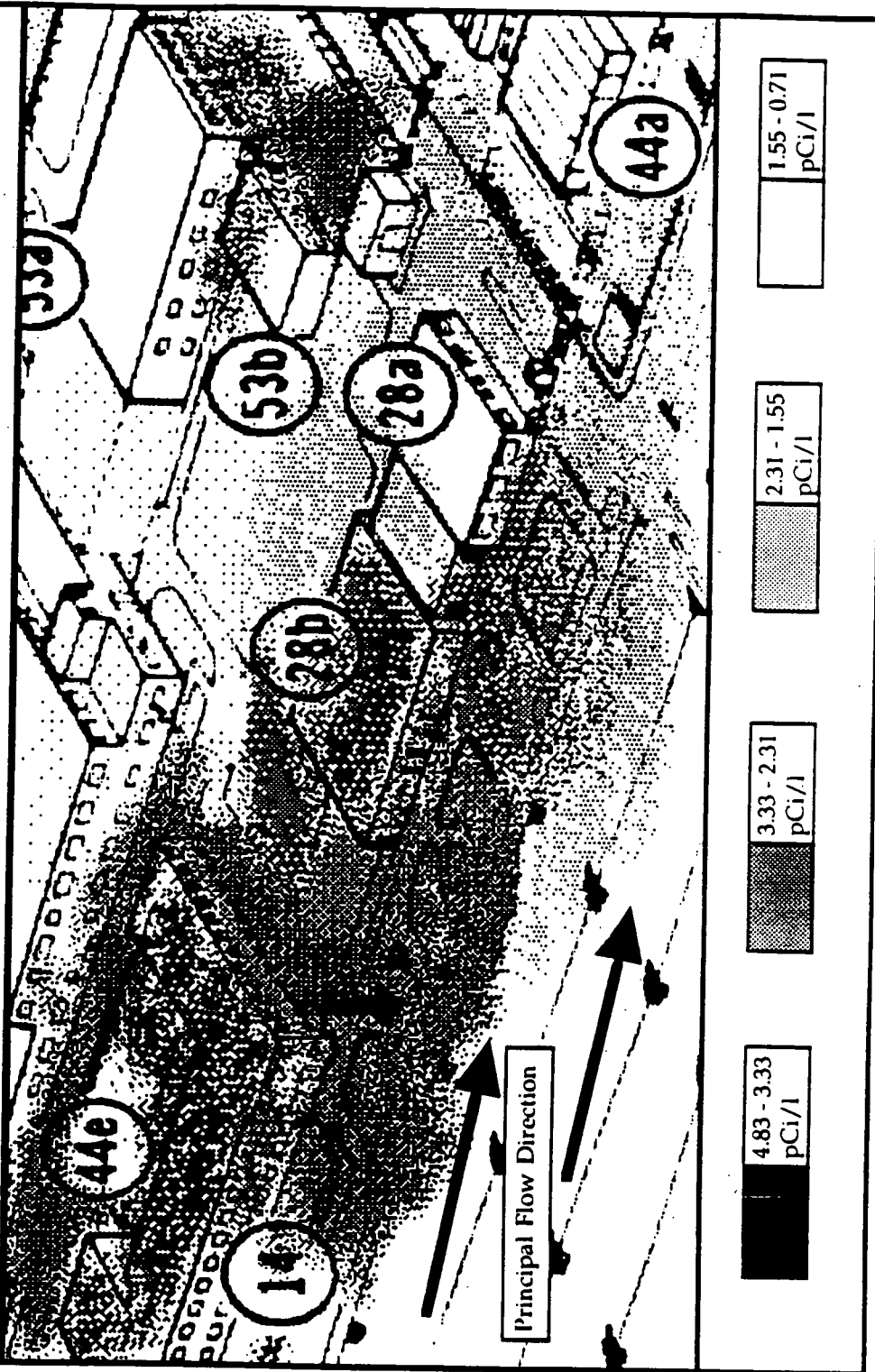


Figure 3.4: Schematic Representation Of The 100 Meter Occupational Exposure Point

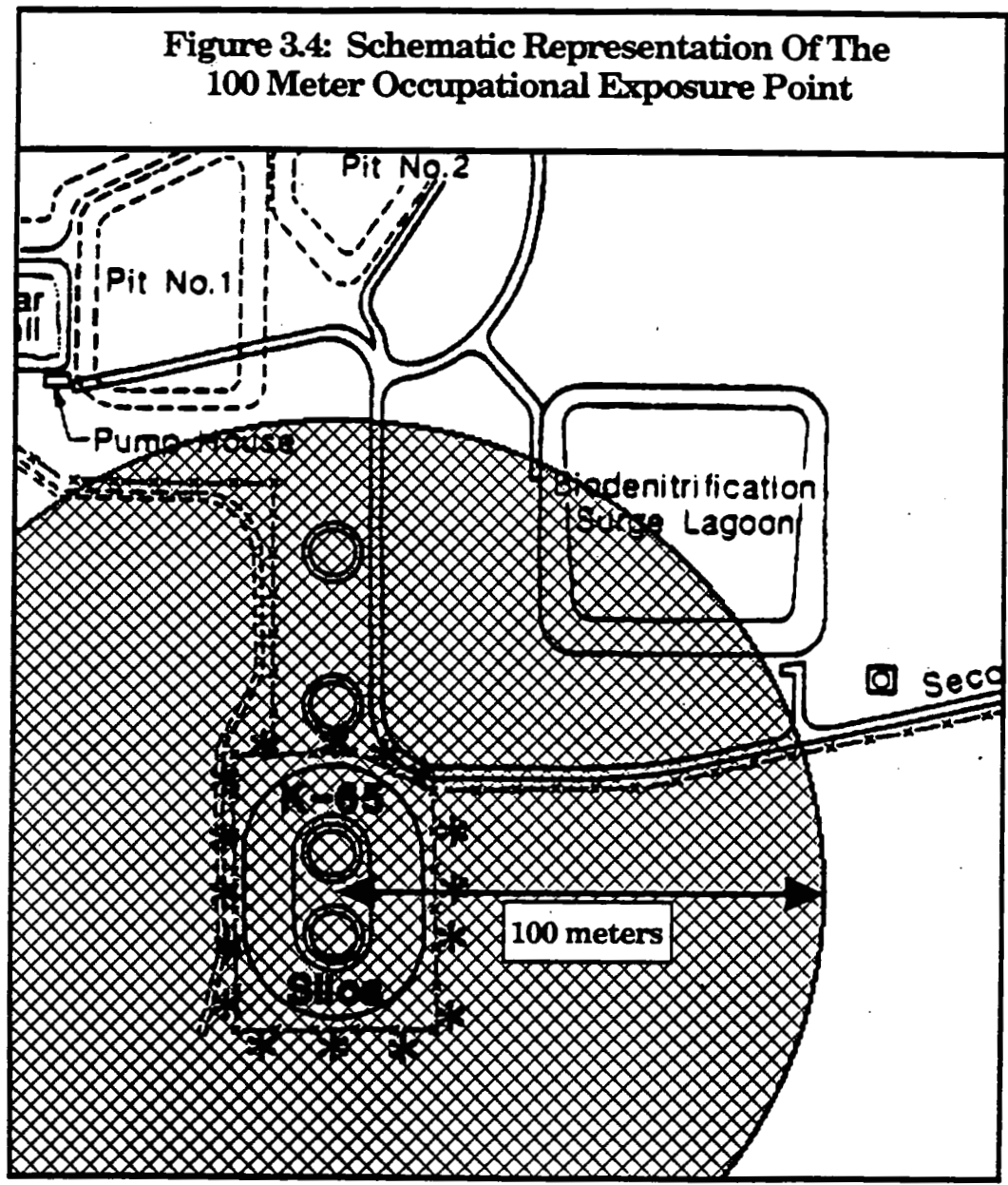
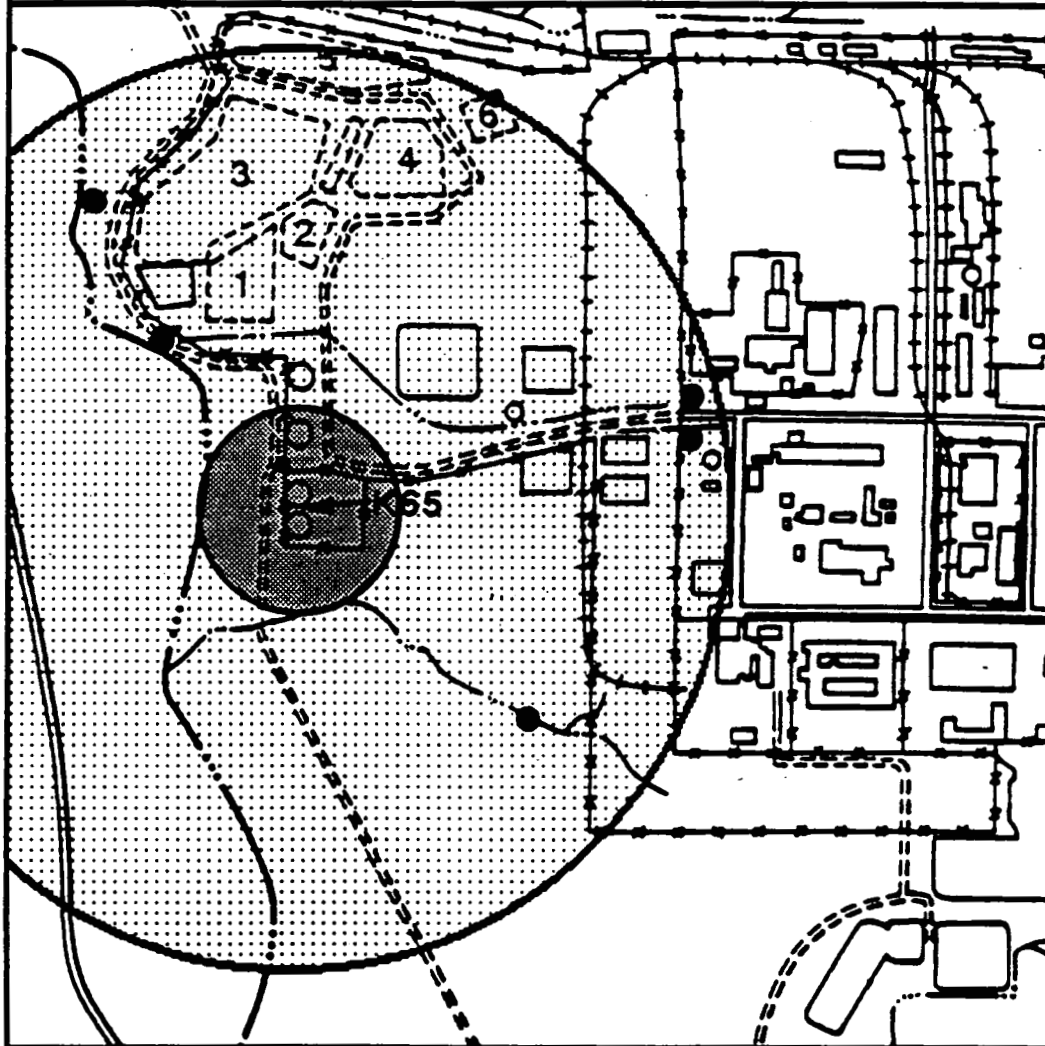


Figure 3.5: Schematic Representation Of The 100 And 500 Meter Exposure Areas For The K-65 Risk Assessment



**100
meter
area**



**500
meter
area**

44

Figure 3.6: Illustration Of The Range Of Influence For The Acute AI Source Term

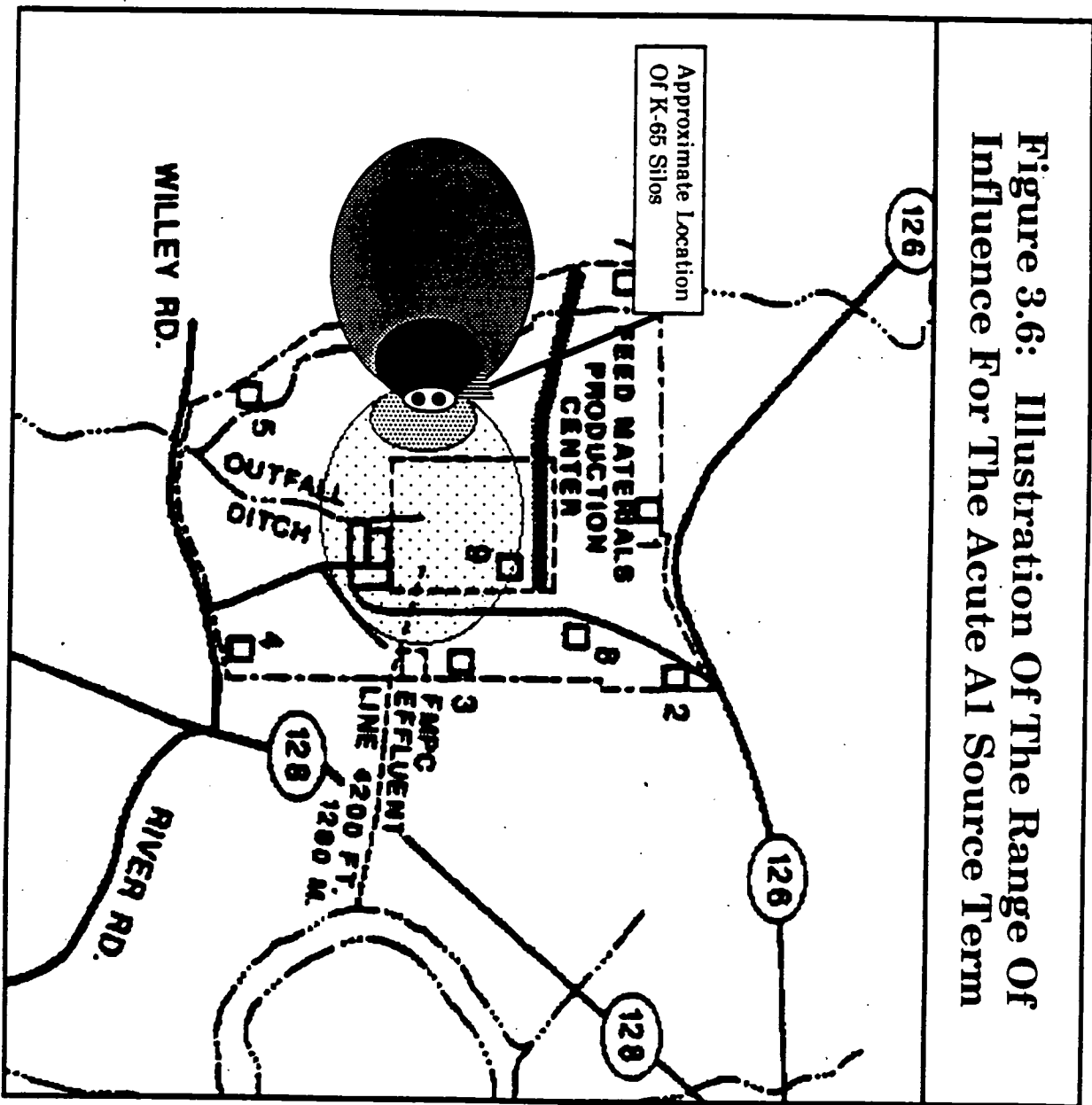
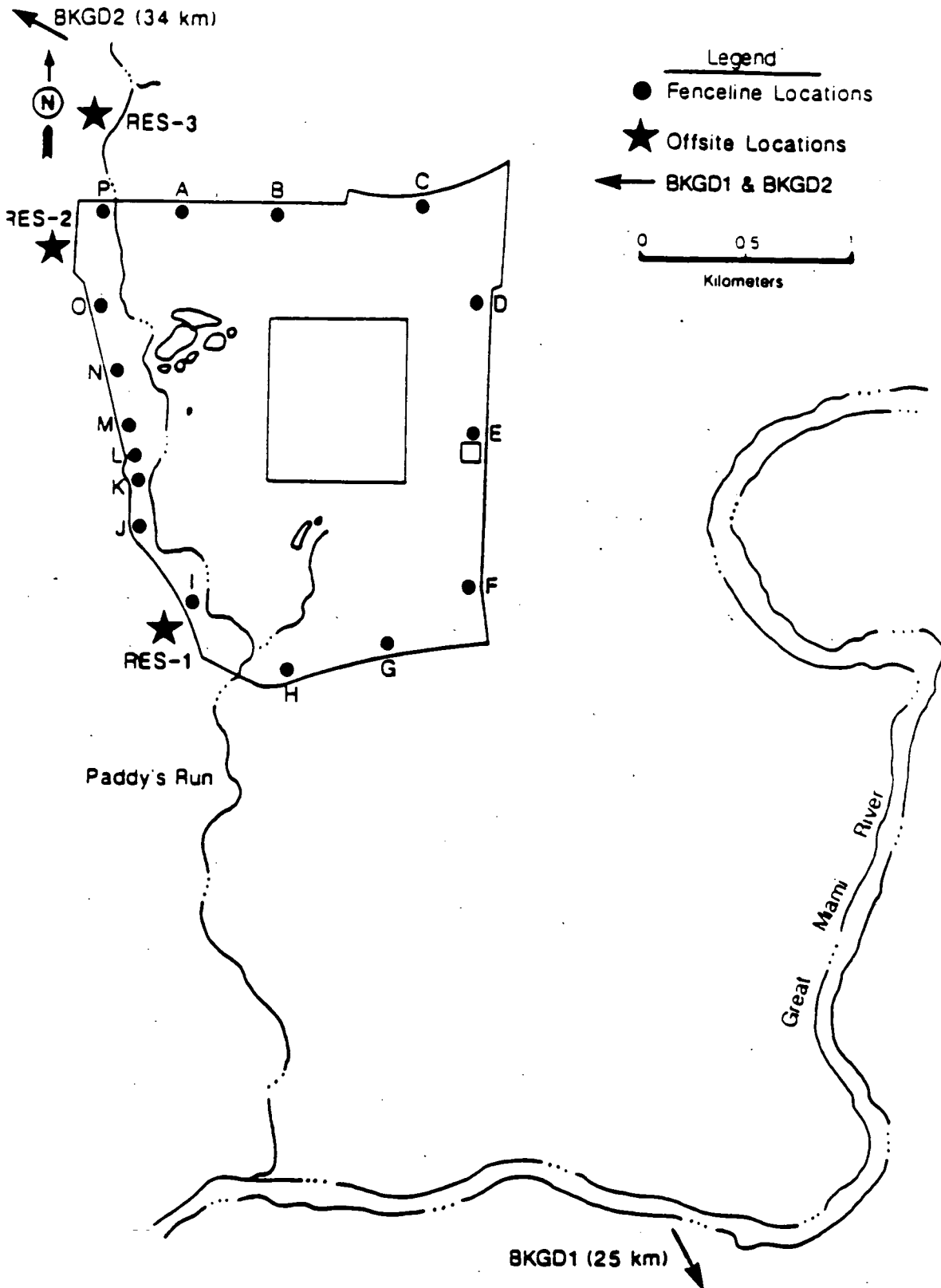


Figure 3.7: Offsite And Fenceline Radon Monitoring Locations



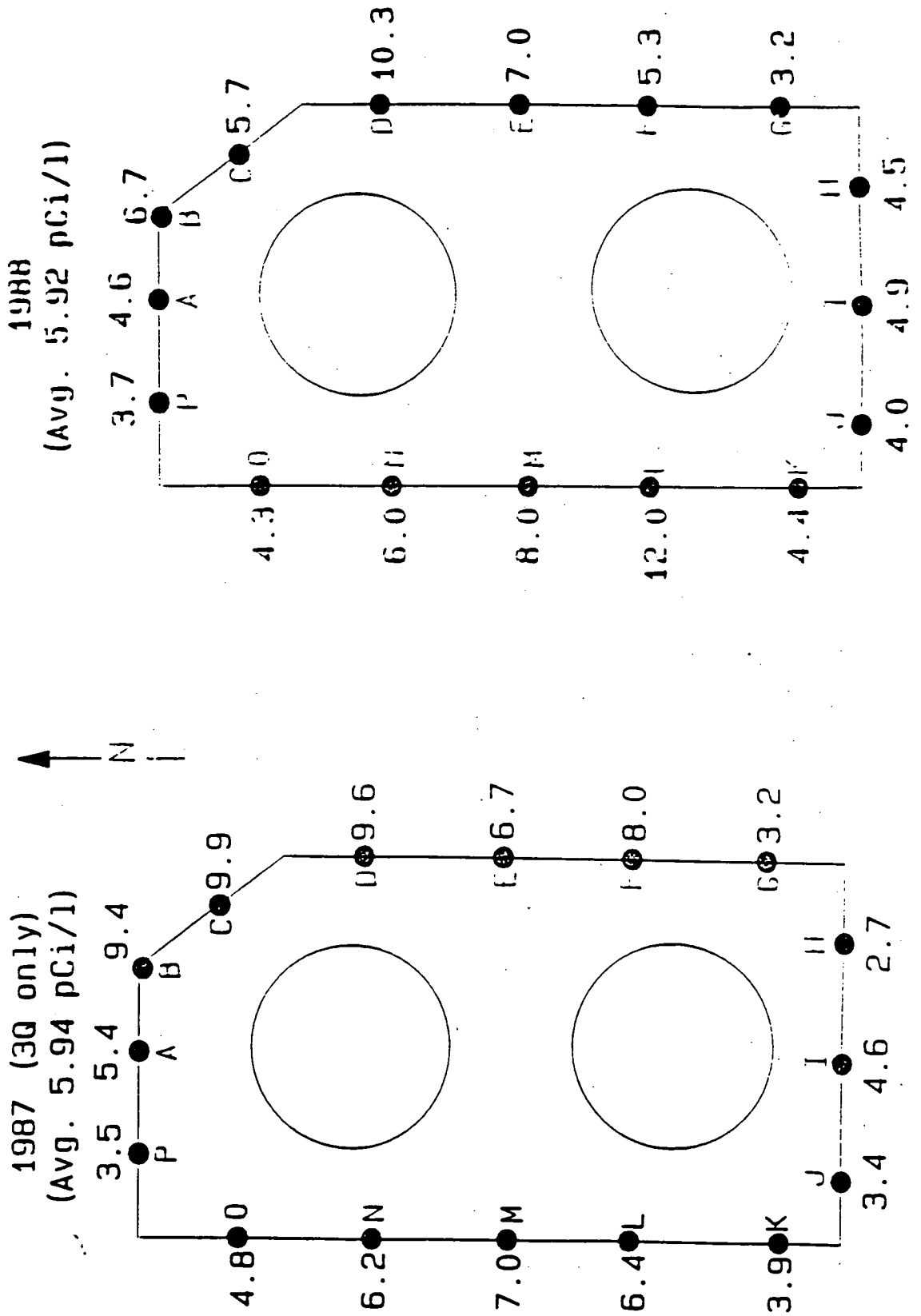
directions is nearly the same. The critical directions are considered to be those where the measured concentrations were the highest. Figures 3.8 and 3.9 show 1987, 1988, and 1989 average radon concentrations at the exclusion fence surrounding the K-65 silos. Table 3.2 presents the predicted values corresponding to north, N, east, E, south, S, and west, W at approximately the same distance as the exclusion fence. Again the predicted and measured averages compare favorably.

The AIRDOS code was used with meteorological data from on site. The results in general show reasonable agreement with the average of actual measured values. Example input and output for the AIRDOS modeling is provided as an appendix. The net effect of the more detailed modeling of the radon concentrations is to substantiate the concentration, dose, and resulting risk estimates for the nearest resident, and the population. An analysis of specific locations for the representative population center, a specific worker, and the nearest resident would have yielded only marginally different results, therefore in order to keep the study tractible and on schedule the compilation of these results was eliminated. The radon concentration for a range of distances, from 25 meters to 2500 meters, is included in the example output in Appendix A.

Table 3.2: Results Of Radon Concentration Modeling

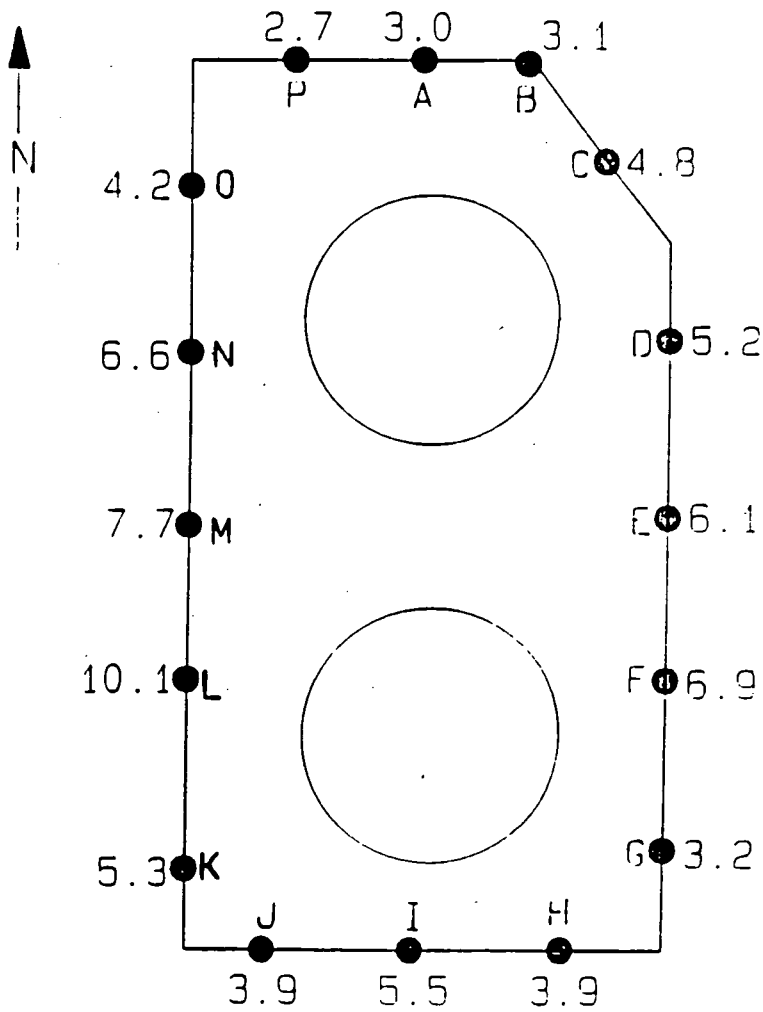
Loc.	Dist. (m)	Direct.	Conc. (pCi/l)			
			measured			predicted
			1988	1987	87 - Bkgr	AIRDOS
A	925	N	1.3	1.5	0.88	0.07
B	1000	NNE	1.7	1.3	0.68	0.047
C	1500	NE	1.4	1.3	0.68	0.03
D	1500	ENE	1.1	1.1	0.48	0.034
E	1250	E	1.2	0.9	0.28	0.06
F	1600	ESE	1.1	1.3	0.68	0.043
G	1500	SE	0.9	0.7	0.08	0.031
H	1200	SSE	1.0	0.9	0.28	0.037
I	1000	S	1.7	2.1	1.48	1.7
J	550	SSW	0.9	1.0	0.38	0.12
K	450	SW	2.1	2.9	2.28	3.52
L	300	SW	1.3	0.7	0.8	5.29
M	300	WSW	2.0	1.8	1.18	0.489
N	375	WNW	0.8	0.9	0.28	0.45
O	650	NW	1.3	1.9	1.28	0.31
P	1000	NNW	0.9	0.7	0.08	0.12
RES1	1100	S	1.3	1.2	0.58	0.078
RES2	1000	NW	0.9	0.9	0.28	0.165
RES3	1500	NNW	1.3	1.2	0.58	1.43
			1987	1988	1989	
A	25	N	5.4	4.6	3.0	5.02
B	25	NNE	9.4	6.7	3.1	4.2
C	25	NNE	9.9	5.7	4.8	----
D	25	NE	9.6	10.3	5.2	2.92
E	25	E	6.7	7.0	6.1	7.87
F	25	ESE	8.0	5.3	6.9	7.01
G	25	SE	3.2	3.2	3.2	4.46
H	25	SSE	2.7	4.5	3.9	4.88
I	25	S	4.6	4.9	5.5	57.4
J	25	SSW	3.4	4.0	3.9	5.72
K	25	SW	3.9	4.4	5.3	147.0
L	25	WSW	6.4	12.0	10.1	10.9
M	25	W	7.0	8.0	7.7	12.9
N	25	WNW	6.2	6.0	6.6	15.2
O	25	NW	4.8	4.3	4.2	13.8
P	25	NNW	3.5	3.7	2.7	0.69

Figure 3.8: Radon Monitoring Locations And Results At The Exclusion Fence Of The K-65 Silos For 1987 And 1988



**Figure 3.9: Radon Monitoring Locations
And Results At The Exclusion Fence Of The
K-65 Silos For 1989**

1989 (3Q only)
(Avg. 5.13 pCi/l)



3.3 Characterizing The Exposure Setting

The objective of the exposure assessment is to estimate the type and magnitude of exposures which may result due to the release of the various radionuclides present in the waste material of the K-65 silos. This information, in the form of doses and exposure levels at the significant exposure points, will be combined with the probabilities of silo failure, risk coefficients, and EPA slope factors in order to fully characterize the potential risk to each significant exposure point.

The exposure assessment process is composed of basically three steps: 1) characterizing the exposure setting, 2) identifying the exposure pathways, and 3) quantifying the exposure. The step of characterizing the exposure setting involves analyzing the physical setting around the silos and identifying the potentially exposed populations. The process of identifying the exposure pathways involves determining the source terms, defining the exposure points, and identifying the exposure routes. The final step, quantifying the exposure, involves determining the exposure point concentrations and doses.

For this investigation, the characterization of the physical setting around the silos primarily involves being able to predict, as a function of time and distance, the ultimate fate and distribution of the materials in the K-65 silos as a result of an accident or the continued degradation of the silos leading to the excessive release of radon. In order to perform the exposure assessment, three significant exposure points were assumed. These three exposure points represent the potentially exposed populations should a release occur from the silos.

The first significant exposure point assumed is an occupational work shift at the FMPC. This work force is assumed to be within 100 meters of the silos when the accident occurs. Furthermore, the work force is assumed to number 50 people. The second potential exposure point is the nearest resident. This person is located a distance of 500 meters from the site. The final potential exposure point is a small population, assumed to be located approximately 14.5 kilometers away.

3.4 Identification of Exposure Pathways

The principal objective of this task is to identify those pathways by which the identified populations may be exposed. Each exposure pathway describes a mechanism by which a population (or individual) may be exposed to the contaminants originating from the silos. These exposure pathways were identified based on the consideration of the sources and mechanisms of release of the radionuclides; the most likely environmental transport route; and the location and activities of the potentially exposed populations.

An exposure pathway consists of four elements: 1) source and mechanism of radionuclide release, 2) retention or transport medium, 3) point of potential human contact with the contaminated medium (referred to as an exposure point), and 4) an exposure route (for example, inhalation) at the contact point. Table 3.3 illustrates the pathway analysis methodology.

Source And Mechanism Of Radionuclide Release

The source of the radioactive material for all the exposure scenarios considered is the contents of the K-65 silos. The mechanisms involved with the potential for release are dependent on the specific failure mode of the silo and they are coupled with anticipated environmental processes. The nature and magnitude of the source term was discussed and presented in Section 2.4 and will not be specifically addressed here. The mechanisms for transport of the residue material were also discussed in Section 2.3. The specific mechanism involved with the release and transport of the waste material from the silos is the wind. This study considered atmospheric turbulence as the primary mechanism that can lead to the catastrophic failure of the silo structures and the subsequent dispersal of the contents. The wind or more appropriately the weather is both the initiator and the basic phenomenon involved in the silo degradation over time.

The action of the wind and weather on the components of the structure continue to degrade the integrity through weathering, wear, freezing and thawing, and severe dynamic and static loadings. The temperature changes when water is present significantly increases the forces associated with the expansion and contraction processes. The long term affect from these forces and processes is the steady increase in the probability of failure and ultimately the release of radioactive material. As previously discussed the failure mode is directly related to the quantity and time frame of a release.

The source and mechanism can be stated simply as acute and chronic release rates and types. The acute release has the larger source term and the shorter time frame, and the chronic release is characterized

by the continuous release of radon gas.

Table 3.3: Pathway Analysis Methodology for the Acute and Chronic Cases

Acute Case - Catastrophic Release (A1)

Radionuclides Released: Uranium-238, Uranium-234, Thorium-230,
Radium-226, and Radon-222.

Pathways Analyzed: Inhalation of gaseous plume (1 hour exposure).
Inhalation of resuspended dust.
External Exposure from radionuclides.

Exposure Points: Worker (100 meters).
Nearest Resident (500 meters).
Population Center (14.5 kilometers)

Acute Case - Total Release of Radon (A2)

Radionuclide Released: Radon-222

Pathway Analyzed: Inhalation of radon plume (1 hour).

Exposure Points: Worker (100 meters).
Nearest Resident (500 meters).
Population Center (14.5 kilometers)

Chronic Case - Daily Release of Radon-222

Radionuclide Released: Radon-222

Pathway Analyzed: Inhalation of radon-222

Exposure Points: Worker (100 meters).
Nearest Resident (500 meters).
Population Center (14.5 kilometers)

Acute Releases

The first type of acute release is designated as A1 and is characterized by the catastrophic failure of the silo structure permitting the direct link between the environment and the radionuclide inventory. The specific type of silo failure will determine the size of the release and ultimately the impact. This study characterized the acute release as resulting from the action of tornado strength wind loadings on the structure. Assuming the turbulent forces are sufficiently strong to cause complete or partial dome failure then these winds can be expected to be capable of significant dislocation and transport of the radioactive waste. In this case the total release of the available radon will be dispersed by the wind. Additionally, the solid radionuclide particulates are assumed to be distributed outside the silo structure. The quantity released was evaluated in Section 2.3.

The second type of acute release is designated as A2 and is characterized as a partial silo failure which results in the total release of radon from the head-space of each silo. The AIRDOS-EPA computer code was used to model the atmospheric dispersion of the radon and predict the exposure point concentrations. It was assumed that the exposure time for each acute case was one hour. The total volume of radon released over the one hour period is assumed to be 50 Ci and represents the available volume in the head space and the space above the residue but below the top of the wall.

Chronic Release

This case is characterized by the chronic release of radon. The chronic case is caused by existing cracks or holes in the concrete. These openings will readily permit transfer of the radon gas but generally will not permit the transport or loss of significant quantities of the heavier isotopes. As indicated previously the actual mass of the radioactive waste is small and is homogeneously mixed in the bulk mass of the silo's contents which is primarily composed of silicates and water. The release of the elements of radium, thorium, and uranium would require large openings and an additional transport mechanism other than the wind.

Environmental Transport Medium

The time frame considered for this study was five years for the failure potential, the radionuclide release, and the subsequent transport in the environment. The possible transport processes available to distribute the waste material after failure of the structure are: 1) atmospheric distribution, 2) the hydrologic cycle, and 3) the distribution as a result of biotic uptake. Atmospheric distribution would involve both resuspension of contaminated dust and atmospheric distribution as a result of plume

migration. Radionuclides deposited in the surface soil slowly migrate through the vadose zone where they may in turn reach the water table and travel large distances rapidly. Distribution of contaminants in the environment can also occur as a result of biotic uptake. Radionuclides can enter plants through primarily two routes: roots (root uptake) and leaves (foliar deposition). Of these three mechanisms for transport, the biotic uptake route is the least significant for the failure scenarios addressed in this study. The processes involved overlap and are interdependent. For purposes of this study the hydrologic cycle was not evaluated in detail due to predominantly long time frames and the large distances, to significant exposure points, involved. The exposure point discussion is addressed in a later section.

Atmospheric turbulence results in relatively rapid transport of contaminants. This transport mechanism is also characterized as having potentially significant effects or impacts over large distances. Significant concentrations can result as far away as several kilometers from the point of release. The transport of radioactive material from the silos for both cases of the acute release and the chronic release mode was estimated using the AIRDOS-EPA computer code. This code is based on the Gaussian Plume Equation and utilizes the Pasquill-Gifford system for the evaluation of the dispersion coefficients. This formulation is not specifically applicable to the transport of contaminants as postulated in this study. The model does, however, provide a basis for estimating the possible effects from the release of the material in the K-65 silos.

The use of the AIRDOS-EPA code required data on the population distribution, agricultural production and use, and site specific meteorological conditions. The analysis, however, did not rely solely on the results from the code. The models developed were also evaluated using hand calculations and other numerical codes as supplemental material and for verification.

The AIRDOS-EPA code is designed to model continuous long term releases and was assumed to be adequate in regards to the chronic release of radon. The acute releases are not as straight forward. The direction for the release was taken to be that of the most prominent wind direction. The wind speed and stability class used were also not easily determined. The result of applying the Gaussian Plume equation to atmospheric transport is that the distribution of the contaminant is averaged based on the specific input. The application to long time frames is justified based on the averaging affect of the wind direction, speed, and stability class. For those situations when the release time is short to intermediate the wind conditions are required to be nearly constant over the time frame considered. Any significant change in the wind direction, speed, or stability class will result in different results and uncertainties. The time frame for the acute releases was therefore taken to be approximately one hour. This duration is also consistent with the duration of severe weather phenomena. Table 3.1 provides the results of the atmospheric transport

analysis for the radionuclides considered.

Significant Exposure Points

The three potentially significant exposure points previously discussed (work force, nearest resident, and nearest population) were hypothetically established to represent three types of reasonable maximum exposure points. Detailed information on these exposure points was lacking, such as the work force population, the nearest population center and estimate of its size, and other values related to the activity patterns for each of the exposure points. Therefore, information on each exposure point was assumed.

As detailed in the previous discussion of the environmental transport medium, the primary transport route in the event of a silo failure is the wind. Therefore, atmospheric transport was assumed to be the only transport medium. Furthermore, through the atmospheric transport of the silo's material, it was determined that the principal pathways of exposure would be the inhalation of the gaseous plume, the inhalation of resuspended dust (after the source term has been spread across the surface soil), and the external radiation dose (again, due to the source material acting as a volume source from the ground). The inhalation dose from the plume release was determined using AIRDOS - EPA (EPA, 1979); while, the inhalation of resuspended dust was modeled atmospherically using AIRDOS with the dose assessment being determined using the methodology expressed in RESRAD (Gilbert, 1989). The external radiation dose to each exposure point was modeled in a similar fashion using both AIRDOS and RESRAD.

3.5 Pathway Analysis And Dose Assessment

The final step in characterizing the exposure assessment process is to quantify the pathway analysis in terms of magnitude, frequency, and duration of exposure for each of the significant exposure points based on either the acute releases or the chronic release. Exposure is defined as the contact of an exposure point with the radionuclide (either by inhalation or external radiation dose). The information previously discussed detailing the atmospheric distribution of the material will be used directly to calculate the exposure point doses and exposure levels. Table 3.4 illustrates the exposure point concentrations for each radionuclide as a result of an acute release, except for radon-222 which is only used in the calculation of the plume inhalation pathway. Table 3.2 listed the concentrations for radon 222 as a result of a chronic release.

**Table 3.4: Surface Soil Exposure Point Concentrations for each Radionuclide
(Based on the Atmospheric Distribution of Source Material from the K-65 Silos)**

<u>Exposure Point</u>	<u>Radionuclide</u>	<u>Concentration (pCi/g of soil)</u>
Work Force (100 meter Distance)	U-238	1.07
	U-234	1.07
	Ra-226	50.0
	Th-230	35.3
Nearest Resident (500 meter Distance)	U-238	0.049
	U-234	0.049
	Ra-226	2.34
	Th-230	1.6
Nearest Population (14,500 meter Distance)	U-238	0.002
	U-234	0.002
	Ra-226	0.041
	Th-230	7.56 x 10 ⁻⁶

External Radiation Pathway

The calculation of exposure point doses for the external radiation pathway is based on the methodology contained in the RESRAD manual (Gilbert, 1989). Equation 3.1 shows the basic formula used to calculate the external radiation dose. These doses are based on the acute catastrophic release, as may occur in a severe weather event.

$$\text{Dose}_{i1} = \frac{\text{Conc.}_i \left(\frac{\text{pCi}}{\text{g}}\right) \times \text{DCF}_{i1} \left(\frac{\text{mrem/yr}}{\text{pCi/g}}\right) \times \rho_b \left(\frac{\text{g}}{\text{cm}^3}\right) \times \text{FO}_1}{1000 \text{ mrem/rem}} \quad (3.1)$$

Dose_{i1} = Dose from the *i*th radionuclide over the external radiation pathway, 1, in units of rem per year.

Conc._i = Concentration of the *i*th radionuclide in units of picocurie per gram of soil.

DCF_{i1} = Dose Conversion Factor of the *i*th radionuclide with units of millirem per year per picocurie per gram of soil.

ρ_b = Bulk density of soil with units of grams per cubic centimeter.

FO₁ = Occupancy factor for direct radiation pathway, 0.6.

This pathway is based on an accidental release of material from the silos during a severe weather event. During a tornado, for instance, a certain percentage of material will be blown from the silos and will remain suspended in air as fine particulate matter and result in a plume inhalation dose, while the majority of the material will settle in decreasing quantities with the increasing distance from the silos. The dose calculated in Equation 3.1 is the annual effective dose equivalent for external radiation from this deposited material. The concentration refers to the radionuclide concentration in the surface soil with units of picocuries per gram of soil. The bulk density of the soil is given by ρ with units of grams per cubic centimeter. The final term of Equation 3.1 is the occupancy and shielding factor, defined as 0.6 in RESRAD. Table 3.5 lists the doses calculated for the exposure points from the external radiation pathway. In Table 3.5 the total dose, abbreviated EDE for effective dose equivalent, refers to the summation of all four radionuclides for each exposure point.

555

**Table 3.5: Exposure Point Doses for the External Radiation Dose
(Acute Case A1)
(Based on the Atmospheric Distribution of
Source Material from the K-65 Silos)**

<u>Exposure Point</u>	<u>Radionuclide</u>	<u>Dose (rem/yr)</u>
Work Force (100 meter Distance)	U-238	8.1×10^{-5}
	U-234	8.1×10^{-7}
	Ra-226	0.46
	Th-230	4.0×10^{-5}
Total Dose (EDE)		0.46
Nearest Resident (500 meter Distance)	U-238	3.7×10^{-6}
	U-234	3.7×10^{-8}
	Ra-226	0.022
	Th-230	1.8×10^{-6}
Total Dose (EDE)		0.022
Population (14,500 meter Distance)	U-238	1.5×10^{-7}
	U-234	1.5×10^{-9}
	Ra-226	1.0×10^{-3}
	Th-230	8.4×10^{-12}
Total Dose (EDE)		1×10^{-3}

Inhalation of Resuspended Dust (Acute Release)

The inhalation of resuspended dust pathway also follows the methodology contained in the Gilbert manual. This pathway is also based on the release of material from the silos during a severe weather event. During a tornado a certain percentage of material will be blown from the silos and will remain suspended in air as fine particulate and result in a plume inhalation dose, while the majority of the material will settle in decreasing quantities with the increasing distance from the silos. This deposited material, whose distribution was determined by the AIRDOS-EPA code, was used to calculate the inhalation of resuspended dust dose.

Equation 3.2 illustrates the dose calculation for the inhalation of resuspended dust pathway. The term ASR refers to the air-to-soil concentration ratio (dust loading), a RESRAD default value of $2 \times 10^{-4} \text{ g/m}^3$ was used. The term FI refers to the annual inhalation rate (7300 m^3 per year). The value of 0.6 is used as an occupancy factor (Gilbert, 1989). Table 3.6 lists the exposure point doses for this pathway.

$$\text{Dose}_{i21} = \text{Conc.}_i \left(\frac{\text{pCi}}{\text{g}} \right) \times \text{DCF}_{i2} \left(\frac{\text{mrem}}{\text{pCi}} \right) \times \text{FI}_2 \left(\frac{\text{m}^3}{\text{yr}} \right) \times \text{FO}_2 (0.6) \times \text{ASR} \left(\frac{\text{g}}{\text{m}^3} \right) \quad (3.2)$$

Dose_{i21} = Dose to an individual at each significant exposure point from the i^{th} radionuclide over the inhalation pathway, 2, and subpathway of resuspended dust, 1, with units of mrem per year (converted to rem/yr).

Conc._i = Concentration of the i^{th} radionuclide in the surface soil, with units of picocuries per gram of soil (pCi/g).

DCF_{i2} = Dose Conversion Factor for the i^{th} radionuclide with units of millirem per picocurie.

FI₂ = Inhalation rate of 7300 cubic meters per year ($20 \text{ m}^3/\text{day}$).

FO₂ = Occupancy Factor for the inhalation pathway, 0.6.

ASR = Air-to-Soil Concentration Ratio or dust loading factor, with units of grams per cubic meter (g/m^3).

**Table 3.6: Exposure Point Doses for the Inhalation of
Resuspended Dust Pathway
(Acute Case A1)
(Based on the Atmospheric Distribution of
Source Material from the K- 65 Silos)**

<u>Exposure Point</u>	<u>Radionuclide</u>	<u>Dose (rem/yr)</u>
Work Force (100 meter Distance)	U-238	7.7×10^{-5}
	U-234	8.3×10^{-5}
	Ra-226	2.4×10^{-4}
	Th-230	<u>6.8×10^{-3}</u>
Total Dose (CEDE)		7.2×10^{-3}
Nearest Resident (500 meter Distance)	U-238	5.2×10^{-6}
	U-234	5.6×10^{-6}
	Ra-226	1.6×10^{-5}
	Th-230	<u>4.6×10^{-4}</u>
Total Dose (CEDE)		4.9×10^{-4}
Population (14,500 meter Distance)	U-238	2.1×10^{-7}
	U-234	2.3×10^{-7}
	Ra-226	7.6×10^{-7}
	Th-230	<u>2.1×10^{-9}</u>
Total Dose (CEDE)		1.2×10^{-6}

Inhalation of Gaseous Plume Pathway

The plume inhalation pathway is based on the quantity of suspended particulates resulting from a severe weather event disrupting the silo's integrity. As with the other two pathways, this pathway's results are based on the release of four significant radionuclides: uranium-238, uranium-234, radium-226, thorium-230, and radon-222. The calculations for this pathway were determined using AIRDOS EPA to model the atmospheric transport of the puff release and the methodology described by Gilbert to calculate the dose. The models utilized in the AIRDOS code were previously described. Equation 3.3 illustrates the calculation of the plume inhalation dose. Table 3.7 lists the doses at each exposure point which were determined for this pathway. The total dose refers to the summation of doses for each of the five radionuclides, with the abbreviation of CEDE referring to the annual committed effective dose equivalent.

$$\text{Dose}_{i22} = \text{Air Conc.} \left(\frac{\text{pCi}}{\text{m}^3} \right) \times \text{FI}_2 \times \text{ED} \times \left(\frac{10^{-6} \mu\text{Ci}}{\text{pCi}} \right) \times \text{DCF}_{i2} \quad (3.3)$$

where the terms of Equation 3.3 are defined as follows:

Dose_{i22} = Dose from the *i*th radionuclide to an individual at a significant exposure point over the inhalation pathway, 2, and the subpathway of the gaseous plume release, 2, with units of rem per year.

Air Conc. = Air Concentration of *i*th radionuclide at significant exposure point with units of picocuries per cubic meter. Modeled using the AIRDOS-EPA code.

FI₂ = Inhalation intake rate for individual at significant exposure point with units of cubic meters per hour (0.833 m³/hr).

ED = Exposure Duration for an individual at each significant exposure point (1 hour).

DCF_{i2} = Dose Conversion Factor for the *i*th radionuclide with units of (rem/μCi) or (rem/pCi).

**Table 3.7: Exposure Point Doses for the Inhalation of an
Acute Atmospheric Release of Material from the K-65 Silos
(Acute Case A1)
(Based on 1 Hour Exposure Period)**

<u>Exposure Point</u>	<u>Radionuclide</u>	<u>Dose (rem/yr)</u>
Work Force (100 meter Distance)	U-238	2.8×10^{-1}
	U-234	3.0×10^{-1}
	Ra-226	9.2×10^{-1}
	Th-230	2.6×10^1
	Rn-222	<u>2.8</u>
Total Dose (CEDE)		3.05×10^1
Nearest Resident (500 meter Distance)	U-238	1.4×10^{-2}
	U-234	1.5×10^{-2}
	Ra-226	4.3×10^{-2}
	Th-230	1.2×10^0
	Rn-222	<u>1.3×10^{-1}</u>
Total Dose (CEDE)		1.43
Population (14,500 meter Distance)	U-238	1.8×10^{-7}
	U-234	2.0×10^{-7}
	Ra-226	5.6×10^{-7}
	Th-230	1.6×10^{-5}
	Rn-222	<u>2.3×10^{-4}</u>
Total Dose (CEDE)		2.5×10^{-4}

Summation of Doses for each Exposure Point (Acute Case A1)

The final task of the exposure assessment phase for the acute release case A1 is to determine the total dose to each exposure point based on the summation of the applicable pathways. The three pathways analyzed for the dose assessment, external radiation, inhalation of plume release, and inhalation of resuspended dust, are complete pathways given silo failure for each of the exposure points. Table 3.8 lists the total doses for each exposure point based on the acute release of uranium-238, 234, radium-226, thorium-230, and radon-222.

**Table 3.8: Total Doses at each Exposure Point -
for the Acute Case A1
(Based on the Plume Inhalation Dose, Inhalation of Resuspended Dust, and
External Radiation Dose)**

<u>Exposure Point</u>	<u>Radionuclides</u>	<u>Dose</u> (rem - 1 year)
Work Force (100 meter Distance)		
Total Dose (CEDE)	U-238, 234, Ra-226, Th-230 Rn-222	3.1 x 10¹
Nearest Resident (500 meter Distance)		
Total Dose (CEDE)	U-238, 234, Ra-226, Th-230 Rn-222	1.5
Population (14,500 meter Distance) (individual of Population)		
Total Dose (CEDE)	U-238, 234, Ra-226, Th-230 Rn-222	1.3 x 10⁻³

Exposure Assessment of the Acute Total Release of Radon-222 - Case A2

The exposure assessment of the acute total release of radon-222, designated as case A2, is a subset of the gaseous plume inhalation dose which is designated as case A1. Therefore, the methodology used to determine the acute radon-222 dose at each exposure point is the same as that which was previously discussed in Equation 3.3. This pathway is based on the partial failure of the silo's structure to the extent that only radon-222 can escape. Table 3.9 lists the doses determined for the acute case A2, the total release of radon-222.

**Table 3.9: Doses at each Exposure Point for the Acute Case A2
(Based on the Total Release of Radon-222)**

<u>Exposure Point</u>	<u>Radionuclide</u>	<u>Dose (rem)</u>
Work Force (100 meter Distance)		
Total Dose (CEDE)	Rn-222	2.8
Nearest Resident (500 meter Distance)		
Total Dose (CEDE)	Rn-222	0.13
Population (14,500 meter Distance) (individual of Population)		
Total Dose (CEDE)	Rn-222	2.3 x 10 ⁻⁴

Exposure Assessment of the Chronic Release

Exposure to individuals at each of the significant exposure points from radon-222 occurs on a daily basis. The details of the chronic case were previously described. The environmental transport modeling, the exposure points, and the pathways are the same as the acute cases and as a result will not be discussed here. The primary difference is in the source term available, since only radon will be available for the chronic case. Table 3.10 lists the exposure point doses for the chronic case.

Table 3.10: Exposure Point Doses for the Chronic Case - Radon-222 Release

<u>Exposure Point</u>	<u>Dose</u> <u>(rem/yr)</u>
Work Force (100 meter Distance) (CEDE)	2.57
Nearest Resident (500 meter Distance) (CEDE)	0.21
Population (14,500 meter Distance) (CEDE)	1.2×10^{-3}

Summary of Exposure Assessment

The exposure assessment process is composed of three components: 1) the characterization of the exposure setting, 2) the identification of the exposure pathways, and 3) the determination of exposure point doses. The characterization of the exposure setting consisted of identifying the physical characteristics of the region around the K-65 silos which would lead to the transport of contaminants from the silos to the potential exposure points. Three significant exposure points were identified as reasonable maximum exposure points. The principal contaminant transport route identified was that of atmospheric transport. The atmospheric distribution of radionuclides from the silos to the surrounding region results in three pathways which contribute to the dose assessment of each significant exposure point. The three exposure pathways are inhalation of the puff release, inhalation of the resuspended dust after radionuclides have been deposited on the surface soil, and the external radiation resulting from the atmospherically deposited radionuclides. Quantifying the exposure assessment consisted of determining the exposure point concentrations for each radionuclide in the air and surface soil. The principal radionuclides which were investigated: uranium-238, uranium-234, radium-226, thorium-230, and radon-222. Dose conversion factors from the Department of Energy (DOE, 1988) and the AIRDOS EPA computer code were used to calculate the doses to an individual at each exposure point.

Table 3.8 lists the total doses to an individual at each exposure point for the acute case A1. These doses reflect an individual's total dose, given the assumptions of the A1 case of silo failure, for the first year. Table 3.9 lists the doses for the acute A2 case of silo failure. These doses represent both the first year dose and the five year dose since the probability of silo failure is based on one occurrence in the next five years. Table 3.10 lists the doses for the chronic radon-222 case at each of the exposure points. These doses are in units of rem per year since they represent the annual dose that an individual at each of the three exposure points could receive, given the assumptions, each year.

4.0 RISK CHARACTERIZATION

This section of the investigation deals with the final step of the baseline health risk assessment process, the risk characterization phase. In this step the exposure assessments are summarized and integrated into quantitative and qualitative expressions of risk. In the following sections the risk characterization methodology is developed for each exposure point from the perspective of the acute case and the chronic case. The acute case has two subcategories which are either the catastrophic release of the silos contents from natural forces, such as a tornado, or a total release of radon resulting from the ultimate failure of the silos due to their continued structural degradation.

In the preceding draft report, "A Baseline Risk Assessment for the K-65 Silos Using EPA Methodology for Applicability to the EE/CA," the risk characterization step was performed by multiplying the ICRP risk coefficient, 2×10^{-4} risk per rem of exposure, by each of the particular exposure point doses in order to determine annual risks. These risks were then coupled with the probabilities associated with the two classes of failure modes which are severe weather conditions and natural degradation of the concrete structure in order to quantify the annual risks.

The following paragraphs present a revision of the risk characterization methodology detailed in the draft report. Also contained in the following discussion is a risk characterization using the newly acquired Environmental Protection Agency's methodology for determining risks from radionuclides. The Office of Radiation Programs (ORP) has recently issued these radionuclide carcinogenic slope factors for the purpose of conducting health risk assessments. The "Slope Factors" were obtained directly from ORP in the form of the Health Effects Assessment Summary Table C (HEAST Table C). The methodology presented in this report for using these slope factors is contained in Chapter 10 of the Human Health Evaluation Manual (EPA, 1989) which details the EPA method for performing radiation risk assessments. Table 4.0 presents a summary of the pathway analysis methodology for the acute and chronic cases. Table 4.1 presents a summary of the risk characterization methodologies.

The risk characterization methodologies outlined in Table 4.1 are based on the effective dose equivalent risk coefficient and the EPA lifetime, age-averaged slope factors. The risk coefficient method expresses the risk as an annual risk. The annual risk can be multiplied by 70 years to give the lifetime risk. Slope factors were derived to represent the lifetime risk. Both methodologies will be presented in this investigation in order to compare the results from the draft study with the results obtained by using the updated risk information obtained from the Environmental Protection Agency.

Table 4.0: Pathway Analysis Methodology for the Acute and Chronic Cases

Acute Case - Catastrophic Release (A1)

Radionuclides Released: Uranium-238, Uranium-234, Thorium-230,
Radium-226, and Radon-222.

Pathways Analyzed: Inhalation of gaseous plume (1 hour exposure).
Inhalation of resuspended dust.
External Exposure from radionuclides.

Exposure Points: Worker (100 meters).
Nearest Resident (500 meters).
Population Center (14.5 kilometers)

Acute Case - Total Release of Radon (A2)

Radionuclide Released: Radon-222

Pathway Analyzed: Inhalation of radon plume (1 hour).

Exposure Points: Worker (100 meters).
Nearest Resident (500 meters).
Population Center (14.5 kilometers)

Chronic Case - Daily Release of Radon-222

Radionuclide Released: Radon-222

Pathway Analyzed: Inhalation of radon-222

Exposure Points: Worker (100 meters).
Nearest Resident (500 meters).
Population Center (14.5 kilometers)

Table 4.1: Risk Characterization Methodologies

<u>Release Case</u>	<u>Risk Coefficient Methods</u>	<u>Slope Factor Methods</u>
Acute Catastrophic Release (A1)	$\sum_p EDE_{ipq} \times RC \times PA_1$	$\sum_p EL_{ipq} \times SF_{ip} \times PA_1$
	$\sum_p EDE_{ipq} \times RC$	$\sum_p EL_{ipq} \times SF_{ip}$
Acute Total Rn-222 Release (A2)	$EDE_{ipq} \times RC \times PA_2$	$EL_{ipq} \times SF_{ip} \times PA_2$
	$EDE_{ipq} \times RC$	$EL_{ipq} \times SF_{ip}$
Chronic Rn-222 Release	$EDE_{ipq} \times RC$	$EL_{ipq} \times SF_{ip}$

Where the terms of Table 4.1 are defined as follows:

EDE_{ip} = Effective Dose Equivalent for pathway p, exposure point q, and radionuclide i (rem/year).

RC = Risk Coefficient, 2×10^{-4} risk per rem of exposure.

PA₁ = Probability associated with the acute case of catastrophic release, designated by subscript A1.

EL_{ip} = Exposure Level for pathway p, exposure point q, and radionuclide i (pCi).

SF_{ip} = EPA Slope Factor for pathway p and radionuclide i with units of either $(pCi)^{-1}$ or $(pCi/m^2/yr)^{-1}$.

PA₂ = Probability associated with the acute case of total radon release, designated by subscript A2.

Defining the Risk Coefficient. RC

Risk is synonymous with a hazard or peril and appears as a loss or injury. Risk analysis addresses the probability related to this loss or injury. This view of risk, although simplified, provides a measure of the hazard. In everyday life risk is often expressed as a probability. This probability is often stated in very general terms. For example, the risk of being killed in a car accident is 1 in 4000. The EPA recently issued warnings regarding radon gas in the home. The EPA established an action level at 4 pCi/liter of air. This was based on the risk to individuals breathing this air. The risk to individuals from radon gas (its daughter products) is lung cancer incidence. EPA radon data indicates that radon gas at a level of 4 picocuries per liter would result in 13-50 lung cancer deaths per 1000 people exposed over their lifetime. This would be considered a lifetime risk of 50/1000 or 5×10^{-2} .

Evaluating the risk from chronic low level exposure to ionizing radiation has been the subject of countless research papers and prestigious scientific committee evaluations. Excellent discussions of the effect of low level ionizing radiation on humans can be found in the United Nations Scientific Committee on the Effects of Atomic Radiation (UN, 1977) and National Academy of Sciences / National Research Council Advisory Committee on the Biological Effects of Ionizing Radiation (known as BEIR III)(NAS, 1972). Both reports contain risk estimates for exposure to chronic low level ionizing radiation. These risk estimates vary and are the subject of much scientific discussion.

It is now widely acknowledged that the "risk" from low level exposure to ionizing radiation is the risk of a fatal cancer. Thus, the current discussion focuses on the risk coefficient associated with the induction of a fatal cancer. Most scientists (BEIR III, ICRP, and NCRP) now use a risk coefficient of 2×10^{-4} per rem of exposure. This means that if 10,000 people were exposed to 1 rem of radiation, there is a probability that 2 fatal cancers would be induced. Since the national cancer rate is about 21%, a cohort of 10,000 people will have 2100 "natural" cancer deaths.

Defining the EPA Slope Factors. SEip

In the draft investigation the risk characterization step was performed by multiplying the dose equivalents for each exposure point by the ICRP risk coefficient of 2×10^{-4} risk per rem of exposure. This method yielded an estimate of risk but was not completely applicable for members of the general public. A better estimate of risk can be determined by using age averaged coefficients for individual organs receiving the radiation doses (EPA, 1989). This EPA method uses organ-specific dose conversion factors to derive slope factors that represent the age-averaged lifetime excess cancer incidence per unit intake for the radionuclides of concern. The Integrated Risk Information System (IRIS) is currently being updated to include these slope factors for various radionuclides over the principal pathways of exposure (EPA, 1989). At the time of the draft report, the IRIS network could not be accessed which is why the conventional method of using dose equivalent risk coefficients was used. Since the draft report carcinogenic slope factors for the radionuclides of concern have been obtained from the Office of Radiation Programs in Washington, D.C (EPA, 1990). The following sections define the equations associated with both the EPA slope factor method and the risk coefficient method.

Risk Characterization of Acute Case A1

The risk assessment methodology for the acute case A1 was outlined in Table 4.1. The two methodologies for characterizing risk which are described in Table 4.1 are the risk coefficient method and slope factor method. The results of the risk coefficient method will be illustrated first.

Risk Coefficient Method

Table 4.2 lists the total doses to an individual of each exposure point for the acute case A1. The doses are in units of rem per year and represent the annual contribution to the 50 year committed effective dose equivalent from a one year intake. If the exposure duration for each exposure point were a lifetime, a lifetime dose could be determined by multiplying these total doses by a lifetime of 50 or 70 years. The Environmental Protection Agency assumes a lifetime is 70 years. However, this assessment assumed exposure over the inhalation of resuspended dust and the external radiation pathways would occur for the period of one-to-five years. The puff release pathway was assumed to have an exposure period of one hour. Therefore, the doses from the inhalation of resuspended dust and the external irradiation pathways are multiplied by 5 years to represent their total dose contribution to each exposure point over the five year exposure duration.

Risk Characterization of Acute Case A1 (continued)

Table 4.2: Total Doses to an Individual of each Exposure Point for the Acute Case A1

<u>Exposure Point</u>	<u>Total Dose (first year) (rem)</u>	<u>Total Dose (five year) (rem)</u>
Work Force	30.9	32.8
Nearest Resident	1.45	1.54
Population	1.3×10^{-3}	5.3×10^{-3}

Risk Coefficient Method (continued)

The risk coefficient methodology is expressed in Equation 4.0. The risk coefficient (RC) is 2×10^{-4} risk per rem of exposure and the dose ($D_{case,EP}$) is the total dose for each particular case and exposure point.

$$Risk_{case,EP} = RC \times D_{case,EP} \quad (4.0)$$

Table 4.3 lists the risks determined using the risk coefficient method for first year exposure and also the risk for the total five year exposure duration.

Table 4.3: Risks to an Individual of each Exposure Point for the Acute Case A1 Based on the Risk Coefficient Method

<u>Exposure Point</u>	<u>Risk (first year)</u>	<u>Risk (five year)</u>
Work Force	6.2×10^{-3}	6.6×10^{-3}
Nearest Resident	2.9×10^{-4}	3.1×10^{-4}
Population	2.5×10^{-7}	1.1×10^{-6}

Risk Characterization of Acute Case A1 (continued)

Risk Coefficient Method (continued)

Risks were also developed using the risk coefficient method and the probability of silo failure for the acute case A1. The general formula for determining risk by incorporating the probability of silo failure is shown in Equation 4.1, where P defines the probability associated with the particular case. Table 4.4 lists the risks as reflected by including the probability of silo failure for the acute case A1. This probabilistic risk assessment methodology is included since it reflects a more realistic assessment of the risk associated with the failure of the silos by a severe weather event. The development of the probabilities was discussed in Section 2.0 and Table 4.4a lists the probabilities for the acute case A1: probability per year and probability over the 5 year exposure duration.

$$\text{Risk}_{\text{case,EP}} = \text{RC} \times \text{D}_{\text{case,EP}} \times \text{P}_{\text{case}} \quad (4.1)$$

Table 4.4a: Probabilities for the Acute Case A1 - Severe Weather Event

<u>Probability Description</u>	<u>Silo 1</u>	<u>Silo 2</u>	<u>Average</u>
Probability per year	1.25 x 10 ⁻⁴	1.25 x 10 ⁻⁴	1.25 x 10 ⁻⁴
Probability over 5 years	6.25 x 10 ⁻⁴	6.25 x 10 ⁻⁴	6.25 x 10 ⁻⁴

**Table 4.4: Risks to an Individual of each Exposure Point for the Acute Case A1
Based on the Risk Coefficient Method and the Associated Probability**

<u>Exposure Point</u>	<u>Risk (five year)</u>	<u>Risk (Probability)</u>
Work Force	6.6 x 10 ⁻³	4.1 x 10 ⁻⁶
Nearest Resident	3.1 x 10 ⁻⁴	1.9 x 10 ⁻⁷
Population	1.1 x 10 ⁻⁶	6.7 x 10 ⁻¹⁰

Risk Characterization of Acute Case A1 (continued)

Carcinogenic Slope Factor Method

The carcinogenic slope factor method is based on the United States Environmental Protection Agency's risk assessment methodology for radionuclides (EPA, 1989). The EPA classifies all radionuclides as Group A carcinogens based on their property of emitting ionizing radiation and on the extensive weight of evidence provided by epidemiological studies of ionizing radiation induced cancers in humans (EPA, 1990). The U.S. EPA use data derived from both human epidemiological studies and animal experiments to construct mathematical models of exposure, dose, and risk in order to estimate radionuclide slope factor values. The complex models utilized by the EPA consider pathways of exposure, the distinct metabolic behavior of each element by compound and the radiological characteristics of each nuclide of concern, the time and duration of exposure, the radiosensitivity of each target organ in the body, the latency period for cancer expression in these organs, and the age and sex of individuals in the exposed population. The radiation risk models extrapolate cancer risks due to low dose exposures from risks observed at higher doses using linear, dose-response relationships.

Slope factors for radionuclides are characterized as best estimates (maximum likelihood estimates) of the age-averaged total lifetime excess cancer incidence, total cancers, per unit intake or exposure. Quantitative carcinogenic slope factors for radionuclides estimate the risk per unit intake or exposure. More specifically, they represent the risk per picocurie inhaled or ingested or as the risk per picocurie per square meter per year due to external exposure.

The acute case A1 is based on an individual at each exposure point receiving a dose of radiation from three pathways: 1) external radiation pathway, 2) inhalation of resuspended dust pathway, and 3) inhalation of gaseous plume pathway. The following paragraphs detail each of these pathways as they are developed using the EPA's radionuclide slope factors.

External Radiation Pathway

The EPA derived risk associated with the external radiation pathway is defined by Equation 4.2.

$$Risk_{ipq} = Conc_{is} \times FO_1 \times pb \times 1000 \text{ g/kg} \times SF_{ip} \times ED \quad (4.2)$$

Risk Characterization of Acute Case A1 (continued)

Carcinogenic Slope Factor Method (continued)

External Radiation Pathway (continued)

The terms of Equation 4.2 are described as follows:

Risk_{ipq} = EPA based age-averaged, lifetime risk for *i*th radionuclide, pathway *p*, and exposure point *q*.

Conc_{is} = Concentration of *i*th radionuclide in surface soil with units of pCi/g of soil.

FO₁ = Occupancy Factor for the direct radiation pathway.

ρ_b = Bulk Surface Density of contaminated soil with units of kg/m².

ED = Exposure Duration, 5 years.

SF_{ip} = Slope Factor for radionuclide *i* and pathway *p* with units of (pCi)⁻¹ or (pCi/m²/yr)⁻¹.

Table 4.5 lists the risks determined for the external radiation pathway using the EPA methodology of the carcinogenic slope factors. As one would expect the highest risk exists for an individual of the work force exposed to radium-226, since it emits a high energy gamma-ray.

Risk Characterization of Acute Case A1 (continued)

Carcinogenic Slope Factor Method (continued)

Table 4.5: Risks Determined for the External Radiation Pathway of the Acute Case A1 - Based on the EPA Slope Factor Methodology

<u>Exposure Point</u>	<u>Radionuclide</u>	<u>Risk</u>
Work Force	Uranium-238	2.7 x 10 ⁻⁸
	Uranium-234	3.3 x 10 ⁻⁸
	Radium-226	1.1 x 10 ⁻⁵
	Thorium-230	<u>1.1 x 10⁻⁶</u>
Total Risk		1.3 x 10⁻⁵
Resident	Uranium-238	1.2 x 10 ⁻⁹
	Uranium-234	1.5 x 10 ⁻⁹
	Radium-226	5.3 x 10 ⁻⁷
	Thorium-230	<u>5.2 x 10⁻⁸</u>
Total Risk		5.9 x 10⁻⁷
Population	Uranium-238	5.0 x 10 ⁻¹¹
	Uranium-234	6.2 x 10 ⁻¹¹
	Radium-226	2.5 x 10 ⁻⁸
	Thorium-230	<u>2.4 x 10⁻¹³</u>
Total Risk		2.5 x 10⁻⁸

Inhalation of Resuspended Dust Pathway

The inhalation of resuspended dust pathway is based on the same environmental transport properties as those discussed in Section 3 which characterized the dose assessment. Equation 4.3 illustrates the methodology used to characterize the inhalation of resuspended dust pathway using the EPA based risk techniques.

Risk_{ipq} = Conc_{is} x FO₂ x ASR x FI₂ x ED x EF x SF_{ip} (4.3)

Risk Characterization of Acute Case A1 (continued)

Carcinogenic Slope Factor Method (continued)

Inhalation of Resuspended Dust Pathway (continued)

The terms of Equation 4.3 are defined as follows:

Risk_{ipq} = EPA based age-averaged, lifetime risk for *i*th radionuclide, pathway *p*, and exposure point *q*.

Conc_{is} = Concentration of radionuclide *i* in surface soil with units of pCi/g of soil.

FO₂ = Occupancy Factor for the inhalation pathway, 0.6.

ASR = Air-to-Soil Concentration Ratio, 2×10^{-4} g/m³.

FI₂ = Air Intake Rate, 20 m³/day.

ED = Exposure Duration, 5 years.

EF = Exposure Frequency, 365 days/year or 250 days/year.

SF_{ip} = Slope Factor for radionuclide *i* for the inhalation pathway *p*, with units of (pCi)⁻¹.

Table 4.6 lists the risks for the inhalation of resuspended dust pathway determined using the EPA based methodology. The highest risk for this pathway is contributed by thorium-230.

Risk Characterization of Acute Case A1 (continued)

Carcinogenic Slope Factor Method (continued)

Table 4.6: Risks Determined for the Inhalation of Resuspended Dust Pathway of the Acute Case A1 - Based on the EPA Slope Factor Methodology

<u>Exposure Point</u>	<u>Radionuclide</u>	<u>Risk</u>
Work Force	Uranium-238	7.7 x 10 ⁻⁸
	Uranium-234	8.7 x 10 ⁻⁸
	Radium-226	4.5 x 10 ⁻⁷
	Thorium-230	<u>3.3 x 10⁻⁶</u>
Total Risk		3.9 x 10⁻⁶
Resident	Uranium-238	5.2 x 10 ⁻⁹
	Uranium-234	5.8 x 10 ⁻⁹
	Radium-226	3.1 x 10 ⁻⁸
	Thorium-230	<u>2.2 x 10⁻⁷</u>
Total Risk		2.6 x 10⁻⁷
Population	Uranium-238	2.1 x 10 ⁻¹⁰
	Uranium-234	2.4 x 10 ⁻¹⁰
	Radium-226	1.5 x 10 ⁻⁹
	Thorium-230	<u>1.0 x 10⁻¹²</u>
Total Risk		1.9 x 10⁻⁹

Inhalation of Gaseous Plume Release

The inhalation of the gaseous plume release is characterized by Equation 4.4. This pathway is based on a puff release from the silos, which is initiated by a severe weather event, with the exposure period at each exposure point being one hour.

Risk_{ipq} = Conc_{ia} x FI₂ x ED x 1 x 10¹² pCi/Ci x SF_{ip} (4.4)

Risk Characterization of Acute Case A1 (continued)

Carcinogenic Slope Factor Method (continued)

Inhalation of Gaseous Plume Release Pathway (continued)

The terms of Equation 4.4 are defined as follows:

Risk_{ipq} = EPA based age-averaged, lifetime risk for i^{th} radionuclide, pathway p, and exposure point q.

Conc_{ia} = Concentration of radionuclide i in air with units of Ci/m³ of air (modeled using AIRDOS).

FI₂ = Air Intake Rate, 0.833 m³/hour.

ED = Exposure Duration, 1 hour.

SF_{ip} = Slope Factor for radionuclide i for the inhalation pathway p, with units of (pCi)⁻¹.

Table 4.7 lists the risks determined for the acute case A1 of the gaseous plume release pathway. Observe that the exposure duration for this pathway is one hour, based on the estimated length of time of the severe weather event. The most critical radionuclide is the thorium-230.

Risk Characterization of Acute Case A1 (continued)

Carcinogenic Slope Factor Method (continued)

Table 4.7: Risks Determined for the Inhalation of Gaseous Plume Release Pathway of the Acute Case A1 - Based on the EPA Slope Factor Methodology

<u>Exposure Point</u>	<u>Radionuclide</u>	<u>Risk</u>
Work Force	Uranium-238	5.6 x 10 ⁻⁵
	Uranium-234	5.6 x 10 ⁻⁵
	Radium-226	3.5 x 10 ⁻⁴
	Thorium-230	2.5 x 10 ⁻³
	Radon-222	<u>2.0 x 10⁻⁵</u>
Total Risk		3.0 x 10⁻³
Resident	Uranium-238	2.8 x 10 ⁻⁶
	Uranium-234	2.8 x 10 ⁻⁶
	Radium-226	1.6 x 10 ⁻⁵
	Thorium-230	1.2 x 10 ⁻⁴
	Radon-222	<u>9.2 x 10⁻⁷</u>
Total Risk		1.4 x 10⁻⁴
Population	Uranium-238	3.6 x 10 ⁻¹¹
	Uranium-234	3.6 x 10 ⁻¹¹
	Radium-226	2.1 x 10 ⁻¹⁰
	Thorium-230	1.5 x 10 ⁻⁹
	Radon-222	<u>1.6 x 10⁻⁹</u>
Total Risk		3.5 x 10⁻⁹

The Total Risk for each Exposure Point - Acute Case A1

The total risk for each exposure point is defined by Equation 4.5. Each exposure point, under the acute case A1, is assumed to be exposed through the three previously discussed pathways.

$$Risk_q = \sum_{ip} EL_{ipq} \times SF_{ip} \tag{4.5}$$

Risk Characterization of Acute Case A1 (continued)

Carcinogenic Slope Factor Method (continued)

The Total Risk for each Exposure Point - Acute Case A1 (continued)

Table 4.8 lists the total risks for each exposure point for the acute case A1. These risks represent the Environmental Protection Agency's methodology for determining the lifetime cancer risk from the intake or exposure to radionuclides.

**Table 4.8: Total Risks Determined for the Acute Case A1
Based on the EPA Slope Factor Methodology**

<u>Exposure Point</u>	<u>Risk</u>
Work Force	3.0×10^{-3}
Resident	1.4×10^{-4}
Population	3.0×10^{-8}

In a similar fashion, the total risks for the acute case A1, expressed above, can be modified to reflect the probability of silo failure under the acute case A1 and in the process present a more realistic estimate of the risk associated with the failure of the K-65 silos. These enhanced risks are listed in Table 4.9. The average probability of silo failure over the 5 year exposure duration was used to determine the risks in Table 4.9. The probabilities for the acute case A1 are listed in Table 4.4a.

**Table 4.9: Total Risks Determined for the Acute Case A1 - Based on the
EPA Slope Factor Methodology and the Probability of Silo Failure**

<u>Exposure Point</u>	<u>Risk</u>
Work Force	2.0×10^{-6}
Resident	8.9×10^{-8}
Population	1.9×10^{-11}

Risk Characterization of Acute Case A2

Risk Coefficient Method

Table 4.10 lists the doses from radon-222 for the acute case A2 at each exposure point. The acute case A2 is similar to the acute case A1. The difference is manifested in the type of event which leads to the silo failure. The failure of the silos for the acute case A2 is based on the natural or continued degradation of the silo's structure. The risks for this case were developed in a similar fashion as for the acute case A1. First, the risks at each exposure point will be estimated using the risk coefficient method and then the risks at each exposure point will be estimated again but with the additional influence of the acute case A1 probability. Equation 4.6 illustrates the risk calculation for the conventional method of simply multiplying the risk coefficient by the dose equivalent. Equation 4.7 illustrates the risk calculation for the risk coefficient method using the probability of silo failure given the natural degradation case.

$$\text{Risk}_q = \sum_{ip} \text{Dose}_{ipq} \times \text{RC} \tag{4.6}$$

$$\text{Risk}_{qp} = \sum_{ip} \text{Dose}_{ipq} \times \text{RC} \times \text{PA2} \tag{4.7}$$

The terms of Equations 4.6 and 4.7 are defined as follows:

Risk_q = Risk to Exposure Point q based on the risk coefficient method.

Risk_{qp} = Risk to Exposure Point q based on risk coefficient method and Probability A2.

Dose_{ipq} = Dose for radionuclide i, pathway p, and exposure point q.

RC = Risk Coefficient, 2×10^{-4} risk per rem of exposure.

Table 4.11 illustrates the risks determined from the doses in Table 4.10 using the risk coefficient value.

Risk Characterization of Acute Case A2

Risk Coefficient Method (continued)

Table 4.10: Doses at each Exposure Point for the Acute Case A2

<u>Exposure Point</u>	<u>Dose (rem)</u>
Work Force (100 meter Distance)	2.8
Nearest Resident (500 meter Distance)	0.13
Population (14,500 meter Distance) (Individual of Population)	2.3×10^{-4}

Table 4.11: Risks at each Exposure Point for the Acute Case A2 Based on the Risk Coefficient Method

<u>Exposure Point</u>	<u>Risk</u>
Work Force (100 meter Distance)	5.7×10^{-4}
Nearest Resident (500 meter Distance)	2.6×10^{-5}
Population (14,500 meter Distance) (Individual of Population)	4.6×10^{-8}

The risks in Table 4.11 can be enhanced by multiplying by the probability of silo failure for the acute case A2. These modified risks are listed in Table 4.12. Table 4.12a lists the probabilities for the acute case A2.

Risk Characterization of Acute Case A2 (continued)

Risk Coefficient Method (continued)

Table 4.12a: Probabilities for the Acute Case A2 - Natural Degradation

<u>Probability Description</u>	<u>Silo 1</u>	<u>Silo 2</u>	<u>Average</u>
Probability per year	0.036	0.0336	0.0348
Probability over 5 years	0.180	0.168	0.174

Table 4.12: Risks at each Exposure Point for the Acute Case A2 Based on the Risk Coefficient Method and the Probability of Silo Failure

<u>Exposure Point</u>	<u>Risk</u>
Work Force (100 meter Distance)	1.0×10^{-4}
Nearest Resident (500 meter Distance)	4.5×10^{-6}
Population (14,500 meter Distance) (Individual of Population)	8.1×10^{-9}

Risk Characterization of Acute Case A2 (continued)

Slope Factor Method

The slope factor risk method for the acute case A2 is similar to the risk coefficient method, except instead of determining the exposure point dose one determines an *Exposure Level*. The exposure level is then multiplied by the pathway and radionuclide specific slope factor in order to characterize the lifetime, age-averaged cancer risk for an individual at each exposure point. Equation 4.8 describes the risk determined by using the slope factor methodology. Equation 4.9 illustrates the slope factor risk but with the addition of the acute case A2 probability of silo failure.

$$\text{Risk}_q = \sum_{ip} \text{EL}_{ipq} \times \text{SF}_{ip} \quad (4.8)$$

$$\text{Risk}_{qp} = \sum_{ip} \text{EL}_{ipq} \times \text{SF}_{ip} \times \text{PA}_2 \quad (4.9)$$

The terms of Equations 4.8 and 4.9 are defined below.

Risk_q = Slope Factor Risk for exposure point q.

EL_{ipq} = Exposure Level for radionuclide i, pathway p, and slope factor of radionuclide i and pathway p. This case is only for radon-222 and the inhalation pathway.

SF_{ip} = Slope Factor for radionuclide i and pathway p with units of (pCi)⁻¹ or (pCi/m²/yr)⁻¹.

Risk_{qp} = Slope Factor Risk for exposure point q with the Probability (A2) of silo failure included.

PA₂ = Probability of Silo Failure for the natural degradation case.

The exposure Level, EL_{radon-222q}, is defined by Equation 4.10.

$$\text{EL}_{\text{radon-222}q} = \text{Concair} \times \text{FI}_2 \times \text{ED} \times \text{CF} \quad (4.10)$$

Risk Characterization of Acute Case A2 (continued)

Slope Factor Method (continued)

The terms of Equation 4.10 are defined as follows:

EL_{radon-222q} = Exposure Level for the acute A2 case considering radon-222 over the inhalation pathway.

Con_{air} = Air Concentration modeled using AIRDOS EPA, Ci/m³.

FI₂ = Inhalation Rate, 0.833 m³/hr.

ED = Exposure Duration for acute case A2, 1 hour.

CF = Conversion Factor, pCi/Ci.

Table 4.13 lists the risks at each exposure point for the acute case A2 determined by using the slope factor methodology. Table 4.14 lists the slope factor risks at each exposure point for the acute case A2 with the addition of the probability of silo failure, P_{A2}. These probabilities were listed in Table 4.12a.

Table 4.13: Total Risks Determined for the Acute Case A2 Based on the EPA Slope Factor Methodology

<u>Exposure Point</u>	<u>Risk</u>
Work Force	2.0 x 10 ⁻⁵
Resident	9.2 x 10 ⁻⁷
Population	1.6 x 10 ⁻⁹

Risk Characterization of Acute Case A2 (continued)

Slope Factor Method (continued)

Table 4.14: Total Risks Determined for the Acute Case A2 - Based on the EPA Slope Factor Methodology and the Probability of Silo Failure

<u>Exposure Point</u>	<u>Risk</u>
Work Force	3.5×10^{-6}
Resident	1.6×10^{-7}
Population	2.9×10^{-10}

Risk Characterization for the Chronic Radon-222 Case

Risk Coefficient Method

The final case examined in this investigation are the risks associated with the ongoing radon emissions from the K-65 silos. This case is not based on silo failure, but rather on the fact that radon-222 is emanating from the silos, primarily the dome, on a daily basis. Equation 4.11 illustrates the risk calculation for the chronic case using the risk coefficient method. The subscript q refers to the exposure point.

$$\text{Risk}_q = \text{Dose}_{\text{Rn-222}q} \times \text{RC} \quad (4.11)$$

Table 4.15 lists the doses for the chronic radon case. Also listed in Table 4.15 are the risks at each exposure point for the chronic case. Note that the risks illustrated are annual risks and total risks which were determined by multiplying the annual risks by the 5 year exposure period.

Risk Characterization for the Chronic Radon-222 Case (continued)

Risk Coefficient Method (continued)

Table 4.15: Doses and Risks at each Exposure Point for the Chronic Radon Case Based on the Risk Coefficient Method

<u>Exposure Point</u>	<u>Annual Dose (rem/year)</u>	<u>Total Dose (rem)</u>	<u>Annual Risk</u>	<u>Total Risk</u>
Worker	2.57	12.9	5.14 x 10 ⁻⁴	2.57 x 10 ⁻³
Resident	0.21	1.07	4.29 x 10 ⁻⁵	2.14 x 10 ⁻⁴
Population	1.16 x 10 ⁻³	5.81 x 10 ⁻³	2.37 x 10 ⁻⁷	1.16 x 10 ⁻⁶

Slope Factor Method

The risk characterization of the chronic radon case using the slope factor methodology is described by Equation 4.12. The subscript q refers to the exposure point and the EL refers to the exposure level. The exposure level for the chronic case is defined by Equation 4.13.

$$\text{Risk}_q = \text{EL}_{\text{Rn-222}q} \times \text{SF}_{\text{inhalation}} \quad (4.12)$$

$$\text{EL}_{\text{Rn-222}q} = \text{Conc}_{\text{air}} \times \text{FI}_2 \times \text{ED} \times \text{EF} \times \text{FO} \quad (4.13)$$

The terms of Equation 4.13 are defined as follows:

EL_{Rn-222q} = Exposure Level, pCi.

FI₂ = Air Intake Rate, 20 m³/d.

ED = Exposure Duration, 5 years.

EF = Exposure Frequency, 250 days/year or 365 days per year.

FO = Occupancy Factor, outdoors 60% of time, 0.6.

Risk Characterization for the Chronic Radon-222 Case (continued)

Slope Factor Method (continued)

Table 4.16 lists the risk at each exposure point for the chronic radon case using the slope factor methodology. These risks represent the EPA's risk characterization methodology for determining the age-averaged, lifetime cancer risk from the chronic release of radon over the five year exposure period.

Table 4.16: Total Risks Determined for the Chronic Radon Case Based on the EPA Slope Factor Methodology

<u>Exposure Point</u>	<u>Risk</u>
Work Force	9.1×10^{-5}
Resident	7.6×10^{-7}
Population	4.1×10^{-8}

Summary of the Risk Characterization Results

The approach to this risk assessment involved both a probabilistic risk assessment methodology and a conventional Superfund based risk assessment methodology. The objective of the investigation was to quantify the risks for the baseline case and also to quantify the risks associated with the most probable cases of silo failure. In characterizing the risks for the cases of silo failure, probabilistic risk estimates were calculated as well as risk estimates for the more conventional approach which determines risk based on conditional estimates given a considerable number of assumptions about the source terms and exposure scenarios.

More specifically, risks were determined for two separate cases of silo failure: 1) the acute failure of the K-65 silos 1 and 2 due to a severe weather event (Acute Case A1) and 2) the acute failure of the K-65 silos 1 and 2 resulting from the continued structural deterioration leading to the total release of radon-222 (Acute Case A2). Risks were also determined for the baseline case of chronic radon emission. Risks were determined for the three Reasonable Maximum Exposure points for each case of silo failure and the chronic radon emission case. Two separate risk characterization methodologies were utilized in the determination of the risks for each case of silo failure and the chronic case as well. The first risk methodology analyzed was termed the risk coefficient method (RC) and was based on the effective dose equivalent risk factor of 2×10^{-4} risk per rem of exposure. The second risk method investigated was the Environmental Protection Agency's carcinogenic slope factor approach for radionuclides. Radionuclide slope factors are characterized as best estimates (maximum likelihood estimates) of the age-averaged total lifetime excess cancer incidence per unit intake or exposure.

Table 4.8 lists the risks determined for the acute case A1 based on the EPA slope factor methodology. A lifetime excess cancer incidence risk of 3×10^{-3} is shown in Table 4.8 for an individual of the work force. This means that under the exposure assumptions of the acute A1 case an individual of the work force has 3 chances in 1000 of developing cancer in his or her lifetime. Similarly a resident under the exposure assumptions of the acute A1 case has 1.4 chances in 10,000 of developing a cancer in his or her lifetime.

Table 4.13 lists the risks determined for the acute case A2 based on the EPA slope factor methodology. A lifetime excess cancer incidence risk of 2×10^{-5} is shown in Table 4.13 for an individual of the work force. This means that under the exposure assumptions of the acute A2 case an individual of the work force has 2 chances in 100,000 of developing cancer in his or her lifetime. Similarly, a resident under the exposure assumptions of the acute A2 case has 9.2 chances in 10 million or roughly 1 chance in 1 million of developing a cancer in his or her lifetime.

Finally, Table 4.16 lists the risks determined for the chronic radon case based on the EPA slope factor methodology. A lifetime excess cancer incidence risk of 9.1×10^{-5} is shown in Table 4.16 for an individual of the work force. This means that under the exposure assumptions of the chronic radon-222 case an individual of the work force has 9.1 chances in 100,000 of developing cancer in his or her lifetime. Similarly, a resident under the exposure assumptions of the chronic radon case has 7.6 chances in 10 million of developing a cancer in his or her lifetime.

5.0 DISCUSSION OF UNCERTAINTY

The quantification of uncertainty is a process by which a measure of the confidence of the results can be weighed against the wide range of possible outcomes of a particular event or series of events. This section will provide where possible both quantitative and qualitative results of the uncertainty analysis associated with the failure potential and consequences of failure of the K-65 silos.

This section discusses the inherent problems and limitations with the data and models used in the risk assessment. The problems and limitations are due to difficulties in data collection, record keeping, modeling, and any number of other areas. These limitations lead directly to a lack of confidence in the final results. The evaluation of these limitations and confidence problems is covered by the more general topic of uncertainty analysis. This analysis should be performed on both a qualitative and quantitative level. The ability to conduct the uncertainty analysis is also in part limited by the limitations and problems that created the uncertainties in the first place. In the situations where little or no data is available the uncertainty in the results is quite large and furthermore the ability to evaluate the uncertainty on a quantitative level is limited.

The uncertainty analysis associated with this risk assessment is primarily on a qualitative level. The uncertainties in the data and analysis associated with the probability calculations are much easier to quantify than for instance the uncertainties in the source term estimates. The intent of this section is to present the general qualitative uncertainties of this study. These uncertainties are presented for each phase of the risk assessment project from the evaluation of the structural integrity and calculation of failure probabilities to the final stages of the risk estimates.

Uncertainty In Silo Structural Integrity

The structural integrity of the silos was evaluated using previous reports, of studies performed on the silos, by Both Camargo Associates Limited and Bechtel National Incorporated. The data available from these previous studies was derived from both destructive and non-destructive testing. The use of this data has induced a certain amount of uncertainty in the probability of failure due to a number of factors. The Camargo study, which provided the data used for determining the decay rates, was finished prior to the addition of the foam cover or the wood and steel protective covering in the center of each silo. These additions therefore could not be considered in the probability estimates of dome failure. The uncertainty imposed by the omission of these additions can be evaluated on a qualitative level by addressing the physical nature of the degradation process and the critical loadings of the silo structure.

The results of both the Bechtel report and the Camargo study showed that the structural integrity of the silo dome structure was not sufficient to provide any estimate of life expectancy. The results also showed that the dead load capacity of the dome was small and was subject to failure from any significant additional dead or live loads. Taking this information into account the additional protective measures made to the silo domes can be considered to have a negligible affect on the structural integrity. The ability for these modifications to prohibit or at least retard the weathering process however is more difficult to address.

Clearly there is a degree of uncertainty in this area, however, the magnitude of the effect on the probabilities is expected to be small due in part to the time frame with which the modifications were made. The silos were nearly 30 years old by the time the foam covering and the protective wood and steel section was added. Considerable weathering and wear had taken place by this time. The additional modifications will only retard the weathering processes on the outside of the structure. Since the silo is not an airtight structure air is permitted to be exchanged between the inside and the outside. This exchange process will continue to degrade the dome from the inside. Given the above discussion the magnitude of the uncertainty in the probability of failure, due to natural degradation, is considered to be small.

Uncertainty In Tornado Related Probabilities

The uncertainty analysis associated with the probability of the external 'tornado' event can be evaluated on both a quantitative and qualitative level. The errors and uncertainties are basically quantified when the statistical analysis is performed on the data. The probability distributions used to represent the data have confidence intervals (as defined by the standard deviation) and the goodness of fit tests, to determine just how well the data used fits the assumed distribution, reflect the uncertainty in the raw data. Additionally much of the uncertainty in the raw data is removed in the initial investigation stages by only considering data which is substantiated and quantified (recall data on tornados was omitted for these reasons). The net effect of performing the detailed statistical analysis is to reduce or at least qualify the uncertainties. The impact of the remaining uncertainties, in the probability of occurrence and damage of a tornado, had on the final results was considered to be less than an order of magnitude and is therefore a 'low' degree of effect.

This part of the risk assessment was considered to contain the dominate degree of uncertainty. The variation in the data concerning the concentrations and total inventory of the radionuclides produced a significant uncertainty. The variation in the total quantity of radium-226 was approximately 36% above and below the best estimate value used in this study. The other radionuclides had similar ranges of uncertainty. This level of uncertainty corresponds to an impact of approximately one order of magnitude in the results (in terms of the exposure).

The impact from these uncertainties, on the risk assessment, is expected to be in the range of a single order of magnitude. The determination of this impact must wait until after the exposure and dose assessment has been made. Uncertainty in a single radionuclide or a group of contaminants does not affect the risk in the same way since the dose received from exposure is dependent on the impact from the contaminant and the pathway considered.

The model and analysis techniques used to evaluate the magnitude of the source term released also resulted in significant uncertainties. The model used postulated a maximum credible release term. The total quantity of residue material released to the environment was assumed to be approximately 8.5% of the total volume of waste mass contained in both silos. This corresponds to approximately 1.65×10^6 pounds of residue material (including the radioactive contaminants).

The model used to determine this magnitude of release assumed that a single silo failed catastrophically with the dispersion of a volume of waste material 1 meter deep (3.28 feet) and 80 feet in diameter. Due to the large source term and the fact that no credit was taken for inhibitors to the ability of the wind to distribute the material the overall effect of these uncertainties is an over prediction of the resulting dose. The effect of the uncertainties was considered to also be approximately one order of magnitude.

Uncertainty In The Dose Assessment

The total dose received by an individual or a population is the sum of dose from each pathway and for each radionuclide. The result of the dose assessment, presented in Section 3.0, clearly indicates that the dominate contributor to the total dose is via the inhalation pathway and from thorium-230. The impact of the uncertainties of the source term as well as the uncertainties in the dose calculations on the overall risk can be summarized by addressing the variation in the dose from thorium-230. Since the uncertainty in the magnitude of the thorium-230 source term was essentially the same as that of radium-226 (approximately 36%) then the impact on the risk is also expected to about one order of magnitude (probably over estimating the dose and therefore the risk).

Uncertainty In The Risk Estimates

The final impact of the error or uncertainty in the basic data, the modeling, and the analytical techniques eventually alters or produces a confidence interval for the risks. The impact from each of the stages of the risk assessment were clearly shown to be non-linear, meaning that the sum of the uncertainties does not directly affect the risk estimates.

6.0 DISCUSSION OF RESULTS

The discussion of results is intended to provide a general perspective of the overall risk assessment and to facilitate the understanding and relationship between the different phases of the study. The overall risk assessment embodied the potential for failure of the silos, the release and transport of contaminated material, the eventual exposure and dose, and finally the risk. The risk aspect of the study covers several different areas: 1) the probability of silo failure coupled the consequences of the failure (such as release), 2) the potential for wide spread contamination, and 3) the consequences of exposure and dose such as the possibility of latent cancer incidence. The following paragraphs present the relationship and the limitations associated with risk calculations covering these three areas. The accepted risk level from exposure to some quantity of radioactive material is not directly comparable to accepted risk levels for structural failure. In order to make a comparison the risks must be based on the same outcome. In other words the consequences being investigated must be the same.

In this study there were essentially three outcomes considered in terms of risk. These were the risk of silo failure, the risk of release of silo contents, and the risk of exposure to radioactive material. The risk factors presented in the evaluation of the tornado as a failure initiator represent the consequences of silo failure due to the occurrence of a tornado. The range of risk factors presented indicate the risk from varying intensities of tornados. In this same manner the risk of a specific release can be calculated using the event trees exhibited in Section 2.5. The event trees describing the release and the transport, of the residue material, illustrate the risk of the specific sequences considered. In the cases presented for the tornado initiator the probability of each phase of the study was propagated through to the end. The risks numbers presented describe the probability of the specific consequences considered, those relating to silo failure, residue release, and the transport of the residue. These risks do not have the same basis as the risks associated with the exposure to radioactive material. The risks associated with exposure and dose estimates relate directly to the possibility of latent cancers in the exposed population (or individual).

Attention to the different basis is recommended when working with the various risk estimates. The USEPA considers as an acceptable risk level the value of 1×10^{-6} representing the chance of an induced cancer incidence as a result of exposure to above background radioactive sources. This risk is based on radioactive material present in the environment. The acceptable risk levels associated with the failure and the resulting dose need to be established. The numbers presented in Section 4.0, incorporating the risk of silo failure with the risk from exposure, are intended to show that the overall probability of the entire scenario is small. In other words since the probability of an F5 tornado event is small as compared to the that of degradation failure then the significance of the tornado as an initiator is reduced.

Further comparison of the probabilities or risk estimates of the initiators with the risk estimates based on the dose is made by examining the overall scenarios considered. There were essentially three exposure scenarios evaluated and they relate directly to the release potential. The three scenarios were further subdivided as to exposure into acute and chronic. There were two acute cases and just one chronic scenario. Certainly other chronic scenarios could have been examined which would relate to the presence of lead, polonium, and bismuth in the soil or as a result of decay of radon released. These additional scenarios were found to either be insignificant contributors to the overall dose or were taken into account in the dose resulting from inhaled radon.

Evaluating the three exposure scenarios as was done in Sections 3 and 4 provides insight to the principal dose contributors. The magnitude of the resulting dose can then be used as a basis for comparing the various risk estimates. This is done with the tornado event and the acute A1 release as compared to the chronic radon release and exposure scenario. The resulting dose from the acute A1 case are on the average an order of magnitude higher than those for the chronic radon case. The magnitude of the dose is used as the first indicator for the comparison of risk. At this level of evaluation the perception of near equal risks can be misleading. The next stage should consider the likelihood of these doses. In the case of the chronic emission of radon the likelihood of receiving some dose is near unity. The likelihood on the other hand of receiving the dose associated with the acute A1 scenario is extremely remote.

The comparison of the risks is then placed on two levels simultaneously one with respect to the magnitude of the dose and the other with the likelihood of exposure. To eliminate one of these scenarios (chronic versus acute A1) based only on one of the two comparison levels equates to eliminating a significant criteria without justification. The commercial nuclear power industry accepts as a reasonable risk level of 1×10^{-7} for a reactor meltdown over the life of the plant. This risk level is comparable to the USEPA level for latent cancer from exposure to radiation. The magnitude of the dose in the case of a reactor meltdown is extremely small, as evidenced from the incident at Three Mile Island. The comparative risk estimate for this scenario would have been on the order of 1×10^{-14} . This risk is comparable to the scenario of high dose resulting from the acute A1 case coincident with the low probability of occurrence.

The results of this study show the complexity and the uncertainty in evaluating the risks associated with failure, release, and dose. In each phase of the study the analysis attempted to illustrate both the maximum or most conservative scenario as well as the wide range of possible outcomes. In the case of the source term the range of values for the radium and thorium content varied significantly but the important facet is that there is an appreciable quantity of radioactive material present. A factor of 2 or even 3 decrease in the source term (1650 or 1100 Ci of radium instead of 3300) will result in a corresponding reduction in the final risk by a factor of

2 or 3. This decrease in the source term would reduce the acute A1 results to 0.75 and 0.5 rem to the nearest resident (500 meter exposure point). The risks would then be within the range of that associated with the chronic radon release. The net effect on the risk comparison, however would not change significantly due the overall risk estimate.

A similar situation exists when considering the transport and exposure of the radon as compared to the potential for release and transport of the residue material in the acute case A1. There is significant uncertainties involved with the calculation of the transport factors. AIRDOS was used to estimate the transport of both the residue and the radon. The choice of the most conservative stability class (Pasquill Category - F) was made in order to conservatively estimate the total impact. The use of A through E stability classes instead of F decreases the total dose by less than an order of magnitude. Recalculation using another stability class does not result in increased certainty or validity. The perspective remains the same in terms of the magnitude and significance of the failure potential, the release of residue material, and the resultant doses.

The results of this risk assessment clearly show that the total risks for the scenarios considered indicate the significance of the threat of release and exposure from the material in the K-65 silos. The chronic radon emission and the potential for the acute release of the radon contained in the head space are probably the more important since the likelihood of these events is either one or close to one. The acute release of residue material has a sufficiently small probability of occurrence that the risk can be considered to be the lesser of the three scenarios but is by no means insignificant. The risks posed by the other radionuclides (radon daughters) were found to result in sufficiently low doses that the scenarios could be eliminated.

555

7.0 References

- ASI, 1990. Analysis of K-65 Residue Material At The Surface, Advanced Sciences Incorporated in conjunction with IT (International Technologies)
- Battelle, 1990. Analysis of K-65 Residue Material As Part Of The Vitrification Study, Battelle at Pacific Northwest Labs.
- Bechtel, 1990. Study and Evaluation of K-65 Silos for the Feed Materials Production Center, Bechtel National, Inc., January 1990 DE-AC05-810R20722.
- Camargo, 1986. K-65 Silos Study & Evaluation Report, Camargo Associates, Limited; Cincinnati, Ohio. February 1986
- Dames, 1975. Meteorological and Engineering Approach to the Regionalization of Tornado Wind Criteria For Nuclear Power Plant Design, Dames and Moore, September 1975.
- Gilbert, T. et al., 1989. A Manual for Implementing Residual Radioactive Material Guidelines, U.S. DOE.
- Grumski, 1987. Feasability Investigation for Control of Radon Emission From The K-65 Silos, Joseph T. Grumski, Westinghouse Materials Company of Ohio; July 30, 1987.
- Kocher, D.C. 1983. Dose Rate Conversion Factors for External Exposure to Photons and Electrons, Health Physics 45(3):665.
- Long, R. R. 1958. Vortex Motion in a Viscous Fluid, J. Meteorol. 15(1) (1958) 108 - 112
- Maiden, D. E. 1976. Numerical Simulation of Tornado Wind Loading on Structures, Calif. Univ. Livermore (USA), June 1976.
- McDonald, J. R. 1975. Development of a Design Basis Tornado and Structural Design Criteria For Lawrence Livermore Laboratory's Site 300, November 1975.
- Muenow, 1985. Nondestructive Evaluation of K-65 Tank Numbers One and Two NLO Facility, Richard A. Muenow; Muenow and Associates, Inc. 1985.
- Rotz, J. V. 1974. Tornado and Extreme Wind Design Criteria for Nuclear Power Plants, Topical Report BC-TOP-3-A, Revision 3, Bechtel Power Corporation, San Francisco, Calif. Aug. (1974).

- Till, John E. and Meyer, Robert H., 1983.** Radiological Assessment: A Textbook on Environmental Dose Analysis. U.S. NRC NUREG/CR-3332.
- U.S. Environmental Protection Agency, 1989.** Risk Assessment Guidance for Superfund: Human Health Evaluation Manual Part A, Interim Final, Office of Emergency and Remedial Response, Washington, D.C. OSWER Directive 9285.7-01a.
- U.S. Environmental Protection Agency, 1972.** "Estimates of Ionizing Radiation Doses in the United States, 1960-2000," Report of Special Studies Group, Division of Criteria and Standards, Office of Radiation Programs. Washington, D.C.
- U.S. Environmental Protection Agency, 1985.** "Remedial Action at Waste Disposal Sites (Revised)," EPA 625/6-806, Hazardous Waste Engineering Research Laboratory, Cincinnati, Ohio.
- U.S. National Oceanic and Atmospheric Administration, 1970 - 1989.** Storm Data, Volumes 12 through 31.
- U.S. Nuclear Regulatory Commission. 1977.** Calculation of Annual Doses to Man from Routine Releases of Reactor Effluents for the Purpose of Evaluating Compliance with 10 CFR Part 50, Appendix I. Regulatory Guide 1.109, Revision 1. Washington, D.C.
- U.S. Nuclear Regulatory Commission. 1981.** "Disposal or Onsite Storage of Thorium or Uranium Wastes from Past Operations," Federal Register, Vol. 46, No. 5, pages 52061-52063.

Appendix A

The following pages contains both input and output from the AIRDOS code obtained as part of the modeling of the chronic radon release from the K-65 silos located at the FMPC. The first page Attachment 1 delineates a typical set of input data used. The remaining pages Attachments 2 and 3 lists the output concentrations for each specified distance and for each of 16 principal directions.

Input data for the AIRDOS modeling of chronic radon release

OPTION
 &OPTI OPTION=1,1,,0,0,,,0,0,LIPO=1,NSTB=2,TSUBB=1.0,GSFAC=0.2 &END
 GRID
 &GRID NRL=2,NRU=16,IDIST=25,50,100,200,250,300,350,
 400,450,500,750,1000,1250,1500,2000,2500 &END
 PLUME RISE
 &PLUM PR=0.0 &END
 METEOROLOGICAL DATA
 &METE LID=5.0,RR=102,TA=285.3 &END
 PHYSICAL STACK DATA
 1
 &PHYS PH=0.0 &END
 WIND FREQUENCY DATA
 STAR
 DEFAULT
 RADIONUCLIDE DATA
 1
 &RADI NUC='RN-222',REL=650.0 &END
 MODIFICATIONS OF NUCLIDE DATA
 1
 &MODI NUC='RN-222',LAMSUR=5.48E-6,SC=1E-9,VD=1.8E-7,VG=0 &END
 AG DATA
 &AGDT FV=7.6,0,92.4,FB=0.8,0,99.2,FM=0,0,100 &END
 AG ARRAYS
 FILE 23FARMA.DAT
 SKIP 5
 USER
 (16I5)
 (8F10.0)
 POPULATION ARRAY
 FILE 24POPA.DAT
 SKIP 3
 USER
 (8(I9,1X))
 COMMENTS
 TEST RUN OF FMPC CASE OF RADON RELEASE FROM SILOS
 *

Case 2: Intermediate results used in the modeling comparison between measured and predicted values

0 OUTPUT OF AIRDOS-EPA COMPUTER CODE
0 OPTIONS SELECTED-
0 PROGRAM TERMINATED AFTER PRINTING RADIONUCLIDE CONCENTRATIONS
0 RADIONUCLIDE CONCENTRATIONS ARE LISTED FOR DIRECTION AND DISTANCE FROM FACILITY
0 RADIONUCLIDE CONCENTRATIONS LISTED ARE SECTOR-AVERAGED VALUES
0 PLUME RISE IS COMPUTED FOR BUOYANT PLUMES BY BRIGGS EQUATIONS

1 METEOROLOGICAL AND PLANT INFORMATION SUPPLIED TO PROGRAM-----

0 AVERAGE AIR TEMPERATURE (DEG K) 285.3
0 AVERAGE VERTICAL TEMPERATURE GRADIENT OF THE AIR (DEG K/METER)
0 IN STABILITY CLASS E 0.0728
0 IN STABILITY CLASS F 0.1090
0 IN STABILITY CLASS G 0.1455
0 RAINFALL RATE (CM/YEAR) 102.00
0 HEIGHT OF LID (METERS) 5
0 NUMBER OF STACKS IN THE PLANT 1

FRACTION OF TIME IN EACH STABILITY CLASS

SECTOR

	A	B	C	D	E	F	G
1	0.1311	0.0654	0.1110	0.4815	0.1169	0.0541	0.0400
2	0.1579	0.0613	0.1403	0.3509	0.1666	0.0177	0.1053
3	0.1767	0.2045	0.1385	0.2649	0.1549	0.0109	0.0495
4	0.3362	0.0426	0.1118	0.1733	0.1834	0.0662	0.0867
5	0.1507	0.0721	0.1085	0.2225	0.2568	0.1200	0.0684
6	0.0841	0.0559	0.1040	0.2719	0.3681	0.0939	0.0220
7	0.1441	0.1059	0.2382	0.3059	0.1146	0.0089	0.0822
8	0.1186	0.1039	0.2701	0.3086	0.0920	0.0178	0.0890
9	0.0005	0.9948	0.0010	0.0021	0.0005	0.0002	0.0009
10	0.1203	0.1143	0.1673	0.2610	0.1935	0.0646	0.0791
11	0.0037	0.0024	0.0045	0.0084	0.9773	0.0012	0.0015
12	0.0951	0.0598	0.1563	0.4796	0.1468	0.0218	0.0408
13	0.1006	0.0605	0.1098	0.3874	0.2537	0.0480	0.0400
14	0.0946	0.0622	0.1191	0.2692	0.3347	0.0812	0.0390
15	0.0941	0.0449	0.1045	0.4043	0.2571	0.0763	0.0188
16	0.1073	0.0552	0.1002	0.5142	0.1709	0.0282	0.0240

FREQUENCIES OF WIND DIRECTIONS AND RECIPROCAL-AVERAGED WIND SPEEDS

WIND TOWARD

	A	B	C	D	E	F	G
1	0.91	1.08	1.49	2.36	1.20	0.80	1.04
2	0.86	1.20	1.28	1.65	1.00	0.93	1.31
3	0.94	2.46	1.02	1.17	0.91	0.77	0.93
4	1.15	1.07	1.00	1.07	0.86	0.77	0.80
5	0.84	1.16	1.09	1.11	1.04	0.82	0.83
6	0.97	1.65	1.66	1.80	1.80	1.63	0.77
7	1.55	1.64	2.28	2.37	1.50	0.77	1.25
8	1.31	2.43	2.64	2.52	1.22	0.77	1.14
9	1.16	6.93	1.74	2.12	1.43	1.00	1.76
10	1.16	1.49	1.41	1.94	1.24	1.19	1.34
11	1.03	1.10	1.09	1.67	2.55	0.88	0.94

WIND SPEEDS FOR EACH STABILITY CLASS

FREQUENCY (METERS/SEC)

	A	B	C	D	E	F	G
1	0.005	0.003	0.003	0.003	0.004	0.007	0.005
2	0.003	0.003	0.003	0.003	0.004	0.007	0.005
3	0.003	0.003	0.003	0.003	0.004	0.007	0.005
4	0.003	0.003	0.003	0.003	0.004	0.007	0.005
5	0.004	0.004	0.004	0.004	0.005	0.006	0.005
6	0.007	0.007	0.007	0.007	0.008	0.009	0.008
7	0.005	0.005	0.005	0.005	0.006	0.007	0.006
8	0.005	0.005	0.005	0.005	0.006	0.007	0.006
9	0.005	0.005	0.005	0.005	0.006	0.007	0.006
10	0.005	0.005	0.005	0.005	0.006	0.007	0.006
11	0.005	0.005	0.005	0.005	0.006	0.007	0.006

12	0.011	0.90	0.92	1.17	1.84	1.02	0.77	1.08
13	0.013	0.92	1.07	1.11	1.69	1.48	1.01	1.32
14	0.013	0.95	1.08	1.23	1.54	1.48	1.18	1.03
15	0.014	0.91	1.15	1.49	2.25	1.36	0.94	0.98
16	0.010	0.94	1.14	1.45	2.40	1.17	0.80	0.81

WIND DIRECTIONS ARE NUMBERED COUNTERCLOCKWISE STARTING AT 1 FOR DUE NORTH
 FREQUENCIES OF WIND DIRECTIONS AND TRUE-AVERAGE WIND SPEEDS

0
1
0
0
0
0

WIND TOWARD FREQUENCY WIND SPEEDS FOR EACH STABILITY CLASS

(METER/SEC)

A B C D E F G

1	0.005	1.16	1.63	2.39	3.79	1.83	0.87	1.54
2	0.003	1.07	1.80	2.12	2.84	1.43	1.21	2.30
3	0.003	1.22	3.74	1.64	1.86	1.16	0.77	1.37
4	0.003	1.68	1.49	1.43	1.62	1.07	0.77	0.88
5	0.004	0.98	1.63	1.84	1.69	1.59	0.93	0.95
6	0.007	1.43	2.51	2.57	2.75	2.76	2.19	0.77
7	0.005	2.42	2.67	3.42	3.31	2.25	0.77	2.19
8	0.005	2.16	3.57	3.88	3.77	2.10	0.77	1.85
9	0.670	1.63	6.94	3.11	3.45	2.70	2.30	2.44
10	0.005	1.74	2.39	2.38	3.33	2.15	1.67	1.97
11	0.228	1.42	1.70	1.96	3.04	2.57	1.08	1.30
12	0.011	1.13	1.26	2.17	3.39	1.50	0.77	1.55
13	0.013	1.20	1.69	1.85	3.15	2.41	1.41	2.01
14	0.013	1.26	1.58	1.95	2.76	2.50	1.66	1.60
15	0.014	1.17	1.69	2.27	3.64	2.13	1.24	1.47
16	0.010	1.25	1.79	2.44	3.87	1.80	0.86	0.98

2	2500	RN-222	1.12E-05	2.02E-10	5.60E-12	2.07E-10	6.77E+04
3	50	RN-222	8.04E-04	1.45E-08	2.35E-10	1.47E-08	5.36E+04
3	100	RN-222	2.22E-04	3.99E-09	1.18E-10	4.11E-09	5.36E+04
3	200	RN-222	6.13E-05	1.10E-09	5.88E-11	1.16E-09	5.36E+04
3	250	RN-222	1.03E-04	1.85E-09	4.70E-11	1.90E-09	5.36E+04
3	300	RN-222	8.40E-05	1.51E-09	3.92E-11	1.55E-09	5.36E+04
3	350	RN-222	7.07E-05	1.27E-09	3.36E-11	1.31E-09	5.35E+04
3	400	RN-222	6.11E-05	1.10E-09	2.94E-11	1.13E-09	5.35E+04
3	450	RN-222	5.40E-05	9.73E-10	2.61E-11	9.99E-10	5.35E+04
3	500	RN-222	4.82E-05	8.68E-10	2.35E-11	8.92E-10	5.35E+04
3	750	RN-222	3.14E-05	5.65E-10	1.56E-11	5.80E-10	5.35E+04
3	1000	RN-222	2.32E-05	4.18E-10	1.17E-11	4.29E-10	5.35E+04
3	1250	RN-222	1.88E-05	3.38E-10	9.38E-12	3.47E-10	5.35E+04
3	1500	RN-222	1.56E-05	2.81E-10	7.81E-12	2.89E-10	5.34E+04
3	2000	RN-222	1.17E-05	2.11E-10	5.85E-12	2.17E-10	5.34E+04
3	2500	RN-222	9.36E-06	1.68E-10	4.68E-12	1.73E-10	5.33E+04
4	50	RN-222	1.40E-03	2.52E-08	3.04E-10	2.55E-08	5.98E+04
4	100	RN-222	3.87E-04	6.97E-09	1.52E-10	7.12E-09	5.98E+04
4	200	RN-222	1.07E-04	1.93E-09	7.60E-11	2.00E-09	5.98E+04
4	250	RN-222	1.42E-04	2.56E-09	6.08E-11	2.62E-09	5.98E+04
4	300	RN-222	1.13E-04	2.04E-09	5.07E-11	2.09E-09	5.97E+04
4	350	RN-222	9.39E-05	1.69E-09	4.34E-11	1.73E-09	5.97E+04
4	400	RN-222	8.00E-05	1.44E-09	3.80E-11	1.48E-09	5.97E+04
4	450	RN-222	7.17E-05	1.29E-09	3.38E-11	1.32E-09	5.97E+04
4	500	RN-222	6.36E-05	1.15E-09	3.04E-11	1.18E-09	5.97E+04
4	750	RN-222	4.06E-05	7.31E-10	2.02E-11	7.51E-10	5.97E+04
4	1000	RN-222	2.97E-05	5.35E-10	1.52E-11	5.51E-10	5.97E+04
4	1250	RN-222	2.43E-05	4.37E-10	1.21E-11	4.49E-10	5.96E+04
4	1500	RN-222	2.02E-05	3.64E-10	1.01E-11	3.74E-10	5.96E+04
4	2000	RN-222	1.51E-05	2.73E-10	7.57E-12	2.80E-10	5.95E+04
4	2500	RN-222	1.21E-05	2.18E-10	6.05E-12	2.24E-10	5.95E+04
5	50	RN-222	2.17E-03	3.90E-08	4.54E-10	3.95E-08	8.86E+04
5	100	RN-222	5.98E-04	1.08E-08	2.27E-10	1.10E-08	8.86E+04
5	200	RN-222	1.65E-04	2.97E-09	1.14E-10	3.08E-09	8.86E+04
5	250	RN-222	2.06E-04	3.71E-09	9.09E-11	3.80E-09	8.86E+04
5	300	RN-222	1.64E-04	2.95E-09	7.57E-11	3.03E-09	8.86E+04

5	RN-222	1.36E-04	2.44E-09	6.49E-11	2.51E-09	8.86E+04
5	RN-222	1.15E-04	2.08E-09	5.68E-11	2.13E-09	8.86E+04
5	RN-222	1.06E-04	1.90E-09	5.05E-11	1.95E-09	8.85E+04
5	RN-222	9.41E-05	1.69E-09	4.54E-11	1.74E-09	8.85E+04
5	RN-222	6.07E-05	1.09E-09	3.03E-11	1.12E-09	8.85E+04
5	RN-222	4.47E-05	8.04E-10	2.27E-11	8.27E-10	8.84E+04
5	RN-222	3.63E-05	6.53E-10	1.81E-11	6.71E-10	8.84E+04
5	RN-222	3.02E-05	5.44E-10	1.51E-11	5.59E-10	8.84E+04
5	RN-222	2.26E-05	4.07E-10	1.13E-11	4.19E-10	8.83E+04
5	RN-222	1.81E-05	3.26E-10	9.04E-12	3.35E-10	8.82E+04
6	RN-222	1.93E-03	3.47E-08	4.73E-10	3.52E-08	1.50E+05
6	RN-222	5.32E-04	9.58E-09	2.36E-10	9.81E-09	1.50E+05
6	RN-222	1.47E-04	2.64E-09	1.18E-10	2.76E-09	1.50E+05
6	RN-222	2.04E-04	3.66E-09	9.45E-11	3.76E-09	1.50E+05
6	RN-222	1.65E-04	2.97E-09	7.88E-11	3.04E-09	1.50E+05
6	RN-222	1.38E-04	2.49E-09	6.75E-11	2.55E-09	1.50E+05
6	RN-222	1.19E-04	2.14E-09	5.91E-11	2.20E-09	1.50E+05
6	RN-222	1.08E-04	1.94E-09	5.25E-11	1.99E-09	1.50E+05
6	RN-222	9.64E-05	1.74E-09	4.72E-11	1.78E-09	1.50E+05
6	RN-222	6.31E-05	1.14E-09	3.15E-11	1.17E-09	1.50E+05
6	RN-222	4.68E-05	8.43E-10	2.36E-11	8.66E-10	1.50E+05
6	RN-222	3.78E-05	6.80E-10	1.89E-11	6.99E-10	1.50E+05
6	RN-222	3.15E-05	5.66E-10	1.57E-11	5.82E-10	1.50E+05
6	RN-222	2.36E-05	4.24E-10	1.18E-11	4.36E-10	1.50E+05
6	RN-222	1.88E-05	3.39E-10	9.42E-12	3.49E-10	1.50E+05
7	RN-222	1.23E-03	2.22E-08	2.82E-10	2.25E-08	1.03E+05
7	RN-222	3.42E-04	6.16E-09	1.41E-10	6.30E-09	1.03E+05
7	RN-222	9.49E-05	1.71E-09	7.05E-11	1.78E-09	1.03E+05
7	RN-222	1.34E-04	2.41E-09	5.64E-11	2.47E-09	1.03E+05
7	RN-222	1.07E-04	1.93E-09	4.70E-11	1.98E-09	1.03E+05
7	RN-222	8.93E-05	1.61E-09	4.03E-11	1.65E-09	1.03E+05
7	RN-222	7.63E-05	1.37E-09	3.52E-11	1.41E-09	1.03E+05
7	RN-222	6.70E-05	1.21E-09	3.13E-11	1.24E-09	1.03E+05
7	RN-222	5.94E-05	1.07E-09	2.82E-11	1.10E-09	1.03E+05
7	RN-222	3.77E-05	6.79E-10	1.88E-11	6.98E-10	1.03E+05
7	RN-222	2.75E-05	4.96E-10	1.41E-11	5.10E-10	1.03E+05

7	1250	RN-222	2.25E-05	4.06E-10	1.13E-11	4.17E-10	1.03E+05
7	1500	RN-222	1.88E-05	3.38E-10	9.38E-12	3.47E-10	1.03E+05
7	2000	RN-222	1.41E-05	2.53E-10	7.03E-12	2.60E-10	1.03E+05
7	2500	RN-222	1.12E-05	2.02E-10	5.62E-12	2.08E-10	1.03E+05
8	50	RN-222	1.35E-03	2.44E-08	2.71E-10	2.47E-08	1.01E+05
8	100	RN-222	3.76E-04	6.77E-09	1.35E-10	6.90E-09	1.01E+05
8	200	RN-222	1.04E-04	1.88E-09	6.77E-11	1.95E-09	1.01E+05
8	250	RN-222	1.33E-04	2.40E-09	5.42E-11	2.45E-09	1.01E+05
8	300	RN-222	1.06E-04	1.90E-09	4.51E-11	1.95E-09	1.01E+05
8	350	RN-222	8.73E-05	1.57E-09	3.87E-11	1.61E-09	1.01E+05
8	400	RN-222	7.41E-05	1.33E-09	3.39E-11	1.37E-09	1.01E+05
8	450	RN-222	6.52E-05	1.17E-09	3.01E-11	1.20E-09	1.01E+05
8	500	RN-222	5.77E-05	1.04E-09	2.71E-11	1.07E-09	1.01E+05
8	750	RN-222	3.63E-05	6.53E-10	1.80E-11	6.71E-10	1.01E+05
8	1000	RN-222	2.63E-05	4.74E-10	1.35E-11	4.87E-10	1.01E+05
8	1250	RN-222	2.16E-05	3.90E-10	1.08E-11	4.00E-10	1.01E+05
8	1500	RN-222	1.80E-05	3.24E-10	9.01E-12	3.34E-10	1.01E+05
8	2000	RN-222	1.35E-05	2.43E-10	6.76E-12	2.50E-10	1.01E+05
8	2500	RN-222	1.08E-05	1.94E-10	5.40E-12	2.00E-10	1.01E+05
9	50	RN-222	1.45E-02	2.60E-07	1.02E-08	2.71E-07	1.38E+07
9	100	RN-222	3.65E-03	6.57E-08	5.09E-09	7.08E-08	1.38E+07
9	200	RN-222	9.23E-04	1.66E-08	2.54E-09	1.92E-08	1.38E+07
9	250	RN-222	4.09E-03	7.37E-08	2.04E-09	7.57E-08	1.38E+07
9	300	RN-222	3.41E-03	6.13E-08	1.70E-09	6.30E-08	1.38E+07
9	350	RN-222	2.92E-03	5.25E-08	1.45E-09	5.40E-08	1.38E+07
9	400	RN-222	2.55E-03	4.59E-08	1.27E-09	4.72E-08	1.38E+07
9	450	RN-222	2.27E-03	4.08E-08	1.13E-09	4.19E-08	1.38E+07
9	500	RN-222	2.04E-03	3.67E-08	1.02E-09	3.77E-08	1.38E+07
9	750	RN-222	1.36E-03	2.44E-08	6.78E-10	2.51E-08	1.38E+07
9	1000	RN-222	1.02E-03	1.83E-08	5.09E-10	1.88E-08	1.38E+07
9	1250	RN-222	8.14E-04	1.47E-08	4.07E-10	1.51E-08	1.38E+07
9	1500	RN-222	6.78E-04	1.22E-08	3.39E-10	1.25E-08	1.38E+07
9	2000	RN-222	5.09E-04	9.16E-09	2.54E-10	9.41E-09	1.38E+07
9	2500	RN-222	4.07E-04	7.32E-09	2.03E-10	7.53E-09	1.38E+07
10	50	RN-222	1.57E-03	2.83E-08	3.63E-10	2.87E-08	1.03E+05
10	100	RN-222	4.34E-04	7.81E-09	1.82E-10	7.99E-09	1.03E+05

10	200	RN-222	1.20E-04	2.16E-09	9.08E-11	2.25E-09	1.03E+05
10	250	RN-222	1.65E-04	2.97E-09	7.26E-11	3.04E-09	1.03E+05
10	300	RN-222	1.32E-04	2.38E-09	6.05E-11	2.44E-09	1.03E+05
10	350	RN-222	1.10E-04	1.98E-09	5.19E-11	2.04E-09	1.03E+05
10	400	RN-222	9.43E-05	1.70E-09	4.54E-11	1.74E-09	1.03E+05
10	450	RN-222	8.46E-05	1.52E-09	4.03E-11	1.56E-09	1.03E+05
10	500	RN-222	7.53E-05	1.36E-09	3.63E-11	1.39E-09	1.03E+05
10	750	RN-222	4.85E-05	8.73E-10	2.42E-11	8.97E-10	1.03E+05
10	1000	RN-222	3.57E-05	6.43E-10	1.81E-11	6.61E-10	1.03E+05
10	1250	RN-222	2.90E-05	5.22E-10	1.45E-11	5.36E-10	1.03E+05
10	1500	RN-222	2.42E-05	4.35E-10	1.21E-11	4.47E-10	1.03E+05
10	2000	RN-222	1.81E-05	3.26E-10	9.05E-12	3.35E-10	1.03E+05
10	2500	RN-222	1.45E-05	2.60E-10	7.24E-12	2.68E-10	1.03E+05
11	50	RN-222	4.05E-02	7.28E-07	9.51E-09	7.38E-07	4.71E+06
11	100	RN-222	1.11E-02	2.01E-07	4.75E-09	2.05E-07	4.71E+06
11	200	RN-222	3.07E-03	5.53E-08	2.38E-09	5.77E-08	4.71E+06
11	250	RN-222	3.83E-03	6.89E-08	1.90E-09	7.08E-08	4.71E+06
11	300	RN-222	3.18E-03	5.73E-08	1.58E-09	5.89E-08	4.71E+06
11	350	RN-222	2.72E-03	4.90E-08	1.36E-09	5.04E-08	4.71E+06
11	400	RN-222	2.38E-03	4.29E-08	1.19E-09	4.40E-08	4.71E+06
11	450	RN-222	2.12E-03	3.81E-08	1.06E-09	3.92E-08	4.71E+06
11	500	RN-222	1.90E-03	3.43E-08	9.50E-10	3.52E-08	4.71E+06
11	750	RN-222	1.27E-03	2.28E-08	6.33E-10	2.34E-08	4.70E+06
11	1000	RN-222	9.49E-04	1.71E-08	4.75E-10	1.76E-08	4.70E+06
11	1250	RN-222	7.60E-04	1.37E-08	3.80E-10	1.41E-08	4.70E+06
11	1500	RN-222	6.33E-04	1.14E-08	3.17E-10	1.17E-08	4.70E+06
11	2000	RN-222	4.75E-04	8.54E-09	2.37E-10	8.78E-09	4.70E+06
11	2500	RN-222	3.79E-04	6.83E-09	1.90E-10	7.02E-09	4.70E+06
12	50	RN-222	3.01E-03	5.41E-08	8.67E-10	5.50E-08	2.23E+05
12	100	RN-222	8.30E-04	1.49E-08	4.33E-10	1.54E-08	2.23E+05
12	200	RN-222	2.30E-04	4.13E-09	2.17E-10	4.35E-09	2.23E+05
12	250	RN-222	3.74E-04	6.73E-09	1.73E-10	6.90E-09	2.23E+05
12	300	RN-222	3.05E-04	5.49E-09	1.44E-10	5.63E-09	2.23E+05
12	350	RN-222	2.57E-04	4.63E-09	1.24E-10	4.75E-09	2.23E+05
12	400	RN-222	2.22E-04	4.00E-09	1.08E-10	4.10E-09	2.23E+05
12	450	RN-222	1.98E-04	3.56E-09	9.63E-11	3.66E-09	2.22E+05

12	500	RN-222	1.77E-04	3.19E-09	8.66E-11	3.27E-09	2.22E+05
12	750	RN-222	1.16E-04	2.08E-09	5.77E-11	2.14E-09	2.22E+05
12	1000	RN-222	8.58E-05	1.54E-09	4.33E-11	1.59E-09	2.22E+05
12	1250	RN-222	6.92E-05	1.25E-09	3.46E-11	1.28E-09	2.22E+05
12	1500	RN-222	5.76E-05	1.04E-09	2.88E-11	1.07E-09	2.22E+05
12	2000	RN-222	4.32E-05	7.78E-10	2.16E-11	7.99E-10	2.22E+05
12	2500	RN-222	3.45E-05	6.21E-10	1.73E-11	6.39E-10	2.22E+05
13	50	RN-222	3.54E-03	6.37E-08	9.85E-10	6.47E-08	2.64E+05
13	100	RN-222	9.77E-04	1.76E-08	4.92E-10	1.81E-08	2.64E+05
13	200	RN-222	2.70E-04	4.85E-09	2.46E-10	5.10E-09	2.64E+05
13	250	RN-222	4.20E-04	7.57E-09	1.97E-10	7.76E-09	2.64E+05
13	300	RN-222	3.42E-04	6.16E-09	1.64E-10	6.32E-09	2.64E+05
13	350	RN-222	2.88E-04	5.19E-09	1.41E-10	5.33E-09	2.64E+05
13	400	RN-222	2.49E-04	4.48E-09	1.23E-10	4.60E-09	2.64E+05
13	450	RN-222	2.24E-04	4.03E-09	1.09E-10	4.14E-09	2.64E+05
13	500	RN-222	2.00E-04	3.61E-09	9.84E-11	3.71E-09	2.64E+05
13	750	RN-222	1.31E-04	2.36E-09	6.56E-11	2.43E-09	2.64E+05
13	1000	RN-222	9.76E-05	1.76E-09	4.92E-11	1.81E-09	2.63E+05
13	1250	RN-222	7.86E-05	1.42E-09	3.93E-11	1.45E-09	2.63E+05
13	1500	RN-222	6.55E-05	1.18E-09	3.27E-11	1.21E-09	2.63E+05
13	2000	RN-222	4.91E-05	8.83E-10	2.45E-11	9.08E-10	2.63E+05
13	2500	RN-222	3.92E-05	7.06E-10	1.96E-11	7.26E-10	2.63E+05
14	50	RN-222	4.19E-03	7.54E-08	1.03E-09	7.64E-08	2.70E+05
14	100	RN-222	1.15E-03	2.08E-08	5.16E-10	2.13E-08	2.70E+05
14	200	RN-222	3.18E-04	5.72E-09	2.58E-10	5.98E-09	2.70E+05
14	250	RN-222	4.47E-04	8.05E-09	2.06E-10	8.25E-09	2.70E+05
14	300	RN-222	3.62E-04	6.51E-09	1.72E-10	6.68E-09	2.70E+05
14	350	RN-222	3.03E-04	5.45E-09	1.47E-10	5.60E-09	2.70E+05
14	400	RN-222	2.60E-04	4.69E-09	1.29E-10	4.82E-09	2.70E+05
14	450	RN-222	2.36E-04	4.25E-09	1.15E-10	4.36E-09	2.70E+05
14	500	RN-222	2.11E-04	3.80E-09	1.03E-10	3.90E-09	2.70E+05
14	750	RN-222	1.38E-04	2.48E-09	6.88E-11	2.55E-09	2.70E+05
14	1000	RN-222	1.02E-04	1.84E-09	5.16E-11	1.89E-09	2.70E+05
14	1250	RN-222	8.25E-05	1.48E-09	4.12E-11	1.53E-09	2.69E+05
14	1500	RN-222	6.87E-05	1.24E-09	3.43E-11	1.27E-09	2.69E+05
14	2000	RN-222	5.15E-05	9.26E-10	2.57E-11	9.52E-10	2.69E+05

14	2500	RN-222	4.11E-05	7.41E-10	2.06E-11	7.61E-10	2.69E+05
15	50	RN-222	3.80E-03	6.84E-08	9.90E-10	6.94E-08	2.89E+05
15	100	RN-222	1.04E-03	1.88E-08	4.95E-10	1.93E-08	2.89E+05
15	200	RN-222	2.88E-04	5.18E-09	2.47E-10	5.42E-09	2.88E+05
15	250	RN-222	4.16E-04	7.49E-09	1.98E-10	7.69E-09	2.88E+05
15	300	RN-222	3.37E-04	6.07E-09	1.65E-10	6.23E-09	2.88E+05
15	350	RN-222	2.83E-04	5.09E-09	1.41E-10	5.24E-09	2.88E+05
15	400	RN-222	2.44E-04	4.39E-09	1.24E-10	4.51E-09	2.88E+05
15	450	RN-222	2.23E-04	4.02E-09	1.10E-10	4.13E-09	2.88E+05
15	500	RN-222	2.00E-04	3.60E-09	9.89E-11	3.70E-09	2.88E+05
15	750	RN-222	1.32E-04	2.37E-09	6.59E-11	2.44E-09	2.88E+05
15	1000	RN-222	9.83E-05	1.77E-09	4.94E-11	1.82E-09	2.88E+05
15	1250	RN-222	7.90E-05	1.42E-09	3.95E-11	1.46E-09	2.88E+05
15	1500	RN-222	6.58E-05	1.18E-09	3.29E-11	1.22E-09	2.88E+05
15	2000	RN-222	4.93E-05	8.88E-10	2.47E-11	9.12E-10	2.88E+05
15	2500	RN-222	3.94E-05	7.10E-10	1.97E-11	7.29E-10	2.88E+05
16	50	RN-222	2.50E-03	4.49E-08	7.01E-10	4.56E-08	2.12E+05
16	100	RN-222	6.90E-04	1.24E-08	3.50E-10	1.28E-08	2.12E+05
16	200	RN-222	1.91E-04	3.43E-09	1.75E-10	3.61E-09	2.12E+05
16	250	RN-222	3.01E-04	5.42E-09	1.40E-10	5.56E-09	2.12E+05
16	300	RN-222	2.45E-04	4.41E-09	1.17E-10	4.53E-09	2.12E+05
16	350	RN-222	2.06E-04	3.71E-09	1.00E-10	3.81E-09	2.12E+05
16	400	RN-222	1.78E-04	3.21E-09	8.76E-11	3.29E-09	2.12E+05
16	450	RN-222	1.60E-04	2.87E-09	7.78E-11	2.95E-09	2.12E+05
16	500	RN-222	1.43E-04	2.57E-09	7.00E-11	2.64E-09	2.12E+05
16	750	RN-222	9.35E-05	1.68E-09	4.67E-11	1.73E-09	2.12E+05
16	1000	RN-222	6.94E-05	1.25E-09	3.50E-11	1.28E-09	2.12E+05
16	1250	RN-222	5.60E-05	1.01E-09	2.80E-11	1.04E-09	2.12E+05
16	1500	RN-222	4.66E-05	8.39E-10	2.33E-11	8.63E-10	2.12E+05
16	2000	RN-222	3.49E-05	6.29E-10	1.75E-11	6.46E-10	2.12E+05
16	2500	RN-222	2.79E-05	5.03E-10	1.40E-11	5.17E-10	2.12E+05

GROUND-LEVEL CHI/Q VALUES FOR RN-222 AT VARIOUS DISTANCES IN EACH COMPASS DIRECTION

DISTANCE (METERS) CHI/Q TOWARD INDICATED DIRECTION (SEC/CUBIC METER)

1 0

0

N NNW NW WNW W WSW SW SSW

50 0.670E-04 0.564E-04 0.390E-04 0.680E-04 0.105E-03 0.937E-04 0.599E-04 0.657E-04
100 0.185E-04 0.156E-04 0.108E-04 0.188E-04 0.290E-04 0.258E-04 0.166E-04 0.182E-04
200 0.510E-05 0.434E-05 0.297E-05 0.519E-05 0.801E-05 0.712E-05 0.460E-05 0.507E-05
250 0.770E-05 0.630E-05 0.500E-05 0.691E-05 0.100E-04 0.988E-05 0.651E-05 0.647E-05
300 0.621E-05 0.507E-05 0.407E-05 0.550E-05 0.796E-05 0.799E-05 0.521E-05 0.513E-05
350 0.519E-05 0.424E-05 0.343E-05 0.456E-05 0.658E-05 0.670E-05 0.433E-05 0.423E-05
400 0.445E-05 0.363E-05 0.296E-05 0.388E-05 0.560E-05 0.577E-05 0.370E-05 0.360E-05
450 0.404E-05 0.320E-05 0.262E-05 0.348E-05 0.512E-05 0.523E-05 0.325E-05 0.316E-05
500 0.361E-05 0.285E-05 0.234E-05 0.309E-05 0.456E-05 0.468E-05 0.288E-05 0.280E-05
750 0.235E-05 0.182E-05 0.152E-05 0.197E-05 0.294E-05 0.306E-05 0.183E-05 0.176E-05
1000 0.174E-05 0.134E-05 0.113E-05 0.144E-05 0.217E-05 0.227E-05 0.134E-05 0.128E-05
1250 0.141E-05 0.109E-05 0.910E-06 0.118E-05 0.176E-05 0.183E-05 0.109E-05 0.105E-05
1500 0.117E-05 0.908E-06 0.758E-06 0.980E-06 0.147E-05 0.153E-05 0.911E-06 0.875E-06
2000 0.878E-06 0.680E-06 0.568E-06 0.735E-06 0.110E-05 0.114E-05 0.683E-06 0.656E-06
2500 0.702E-06 0.544E-06 0.454E-06 0.587E-06 0.877E-06 0.914E-06 0.546E-06 0.524E-06

S SSE SE ESE E ENE NE NNE

50 0.702E-03 0.764E-04 0.196E-02 0.146E-03 0.172E-03 0.203E-03 0.184E-03 0.121E-03
100 0.177E-03 0.211E-04 0.541E-03 0.403E-04 0.474E-04 0.559E-04 0.507E-04 0.335E-04
200 0.448E-04 0.581E-05 0.149E-03 0.111E-04 0.131E-04 0.154E-04 0.139E-04 0.926E-05
250 0.199E-03 0.800E-05 0.186E-03 0.181E-04 0.204E-04 0.217E-04 0.202E-04 0.146E-04
300 0.165E-03 0.642E-05 0.154E-03 0.148E-04 0.166E-04 0.175E-04 0.164E-04 0.119E-04
350 0.142E-03 0.535E-05 0.132E-03 0.125E-04 0.140E-04 0.147E-04 0.137E-04 0.100E-04
400 0.124E-03 0.457E-05 0.116E-03 0.108E-04 0.121E-04 0.126E-04 0.118E-04 0.864E-05
450 0.110E-03 0.410E-05 0.103E-03 0.960E-05 0.109E-04 0.114E-04 0.108E-04 0.775E-05
500 0.989E-04 0.365E-05 0.924E-04 0.859E-05 0.972E-05 0.102E-04 0.972E-05 0.693E-05
750 0.658E-04 0.235E-05 0.615E-04 0.561E-05 0.637E-05 0.668E-05 0.640E-05 0.454E-05
1000 0.493E-04 0.173E-05 0.461E-04 0.416E-05 0.473E-05 0.496E-05 0.477E-05 0.337E-05
1250 0.395E-04 0.141E-05 0.369E-04 0.336E-05 0.381E-05 0.400E-05 0.383E-05 0.272E-05
1500 0.329E-04 0.117E-05 0.307E-04 0.280E-05 0.318E-05 0.333E-05 0.319E-05 0.226E-05
2000 0.247E-04 0.878E-06 0.230E-04 0.210E-05 0.238E-05 0.250E-05 0.239E-05 0.170E-05
2500 0.197E-04 0.702E-06 0.184E-04 0.168E-05 0.190E-05 0.200E-05 0.191E-05 0.136E-05

OUTPUT OF AIRDOS-EPA COMPUTER CODE

OPTIONS SELECTED..

PROGRAM TERMINATED AFTER PRINTING RADIONUCLIDE CONCENTRATIONS
 RADIONUCLIDE CONCENTRATIONS ARE LISTED FOR DIRECTION AND DISTANCE FROM FACILITY
 RADIONUCLIDE CONCENTRATIONS LISTED ARE SECTOR-AVERAGED VALUES
 PLUME RISE IS COMPUTED FOR BUOYANT PLUMES BY BRIGGS EQUATIONS

METEOROLOGICAL AND PLANT INFORMATION SUPPLIED TO PROGRAM----

AVERAGE AIR TEMPERATURE (DEG K) 285.3
 AVERAGE VERTICAL TEMPERATURE GRADIENT OF THE AIR (DEG K/METER)
 IN STABILITY CLASS E 0.0728
 IN STABILITY CLASS F 0.1090
 IN STABILITY CLASS G 0.1455
 RAINFALL RATE (CM/YEAR) 40.00
 HEIGHT OF LID (METERS) 3
 NUMBER OF STACKS IN THE PLANT 1

STACK INFORMATION..

HEIGHT (METERS)	DIAMETER (METERS)	EFFLUENT VELOCITY (METERS/SEC)	RATE OF HEAT EMISSION (CAL/SECOND)	STACK NUMBER
0	0.0000	0.0000	0.00E+00	1
0	0.0000	0.0000	0.00E+00	2
0	0.0000	0.0000	0.00E+00	3
0	0.0000	0.0000	0.00E+00	4
0	0.0000	0.0000	0.00E+00	5
0	0.0000	0.0000	0.00E+00	6

RELEASE RATES FOR RADIONUCLIDES
 STACK NUCLEIDE RELEASE RATE (CURIES/YEAR)

NUCLIDE	PLUME DEPLETION AND DEPOSITION PARAMETERS	GRAVITATIONAL DEPOSITION VELOCITY	SCAVENGING COEFFICIENT	EFFECTIVE DECAY CONSTANT
FALL VELOCITY (METERS/SEC)	(METERS/SEC)	(METERS/SEC)	(METERS/SEC)	(PER DAY)
1	RN-222	0.650E+03		

RN-222 0.000 0.0000 0.131E-05 0.181E+00
 FREQUENCY OF ATMOSPHERIC STABILITY CLASSES FOR EACH DIRECTION

SECTOR	FRACTION OF TIME IN EACH STABILITY CLASS						
	A	B	C	D	E	F	G
1	0.1311	0.0654	0.1110	0.4815	0.1169	0.0541	0.0400
2	0.1579	0.0613	0.1403	0.3509	0.1666	0.0177	0.1053
3	0.1767	0.2045	0.1385	0.2649	0.1549	0.0109	0.0495
4	0.3362	0.0426	0.1118	0.1733	0.1834	0.0662	0.0867
5	0.1507	0.0721	0.1095	0.2225	0.2568	0.1200	0.0684
6	0.0841	0.0559	0.1040	0.2719	0.3681	0.0939	0.0220
7	0.1441	0.1059	0.2382	0.3059	0.1146	0.0089	0.0822
8	0.1186	0.1039	0.2701	0.3086	0.0920	0.0178	0.0890
9	0.0005	0.9948	0.0010	0.0021	0.0005	0.0002	0.0009
10	0.1203	0.1143	0.1673	0.2610	0.1935	0.0646	0.0791
11	0.0037	0.0024	0.0045	0.0094	0.9773	0.0012	0.0015
12	0.0951	0.0598	0.1563	0.4796	0.1468	0.0218	0.0408
13	0.1006	0.0605	0.1098	0.3874	0.2537	0.0480	0.0400
14	0.0946	0.0622	0.1191	0.2692	0.3347	0.0812	0.0390
15	0.0941	0.0449	0.1045	0.4043	0.2571	0.0763	0.0188
16	0.1073	0.0552	0.1002	0.5142	0.1709	0.0282	0.0240

FREQUENCIES OF WIND DIRECTIONS AND RECIPROCAL-AVERAGED WIND SPEEDS

WIND TOWARD	FREQUENCY (METERS/SEC)							WIND SPEEDS FOR EACH STABILITY CLASS						
	A	B	C	D	E	F	G	A	B	C	D	E	F	G
1	0.005	0.91	1.08	1.49	2.36	1.20	0.80	1.04						
2	0.003	0.86	1.20	1.28	1.65	1.00	0.93	1.31						
3	0.003	0.94	2.46	1.02	1.17	0.91	0.77	0.93						
4	0.003	1.15	1.07	1.00	1.07	0.86	0.77	0.80						
5	0.004	0.84	1.16	1.09	1.11	1.04	0.82	0.83						
6	0.007	0.97	1.65	1.66	1.80	1.80	1.63	0.77						
7	0.005	1.55	1.64	2.28	2.37	1.50	0.77	1.25						
8	0.005	1.31	2.43	2.64	2.52	1.22	0.77	1.14						
9	0.670	1.16	6.93	1.74	2.12	1.43	1.00	1.76						
10	0.005	1.16	1.49	1.44	1.94	1.24	1.19	1.34						
11	0.228	1.03	1.10	1.09	1.67	2.55	0.88	0.94						

12 0.011 0.90 0.92 1.17 1.84 1.02 0.77 1.08
 13 0.013 0.92 1.07 1.11 1.69 1.48 1.01 1.32
 14 0.013 0.95 1.08 1.23 1.54 1.48 1.18 1.03
 15 0.014 0.91 1.15 1.49 2.25 1.36 0.94 0.98
 16 0.010 0.94 1.14 1.45 2.40 1.17 0.80 0.81

WIND DIRECTIONS ARE NUMBERED COUNTERCLOCKWISE STARTING AT 1 FOR DUE NORTH
 FREQUENCIES OF WIND DIRECTIONS AND TRUE-AVERAGE WIND SPEEDS

0
 1
 0
 0
 0
 0
 0
 0

WIND TOWARD FREQUENCY WIND SPEEDS FOR EACH STABILITY CLASS
 (METER/SEC)

	A	B	C	D	E	F	G	
1	0.005	1.16	1.63	2.39	3.79	1.83	0.87	1.54
2	0.003	1.07	1.80	2.12	2.84	1.43	1.21	2.30
3	0.003	1.22	3.74	1.64	1.86	1.16	0.77	1.37
4	0.003	1.68	1.49	1.43	1.62	1.07	0.77	0.88
5	0.004	0.98	1.63	1.84	1.69	1.59	0.93	0.95
6	0.007	1.43	2.51	2.57	2.75	2.76	2.19	0.77
7	0.005	2.42	2.67	3.42	3.31	2.25	0.77	2.19
8	0.005	2.16	3.57	3.88	3.77	2.10	0.77	1.85
9	0.670	1.63	6.94	3.11	3.45	2.70	2.30	2.44
10	0.005	1.74	2.39	2.38	3.33	2.15	1.67	1.97
11	0.228	1.42	1.70	1.96	3.04	2.57	1.08	1.30
12	0.011	1.13	1.26	2.17	3.39	1.50	0.77	1.55
13	0.013	1.20	1.69	1.85	3.15	2.41	1.41	2.01
14	0.013	1.26	1.58	1.95	2.76	2.50	1.66	1.60
15	0.014	1.17	1.69	2.27	3.64	2.13	1.24	1.47
16	0.010	1.25	1.79	2.44	3.87	1.80	0.86	0.98

0
 1
 0

WIND DIRECTIONS ARE NUMBERED COUNTERCLOCKWISE STARTING AT 1 FOR DUE NORTH
 ESTIMATED RADIONUCLIDE CONCENTRATIONS

0 AREA NUCLIDE AIR CONCEN DRY DEP RATE WET DEP RATE GND DEP RATE EFF REL RATE
 (PCI/CM**3) (PCI/CM**2/S) (PCI/CM**2/S) (PCI/CM**2/S) (PCI/CM**2/S)

WIND TOWARD DISTANCE
 (METERS)

0							
1	25	RN-222	5.02E-03	0.00E+00	9.72E-07	9.72E-07	1.05E+05
1	50	RN-222	1.38E-03	0.00E+00	4.86E-07	4.86E-07	1.05E+05
1	100	RN-222	3.81E-04	0.00E+00	2.43E-07	2.43E-07	1.05E+05
1	200	RN-222	1.05E-04	0.00E+00	1.21E-07	1.21E-07	1.05E+05

1	250	RN-222	2.49E-04	0.00E+00	9.71E-08	9.71E-08	1.05E+05
1	300	RN-222	2.05E-04	0.00E+00	8.09E-08	8.09E-08	1.05E+05
1	350	RN-222	1.74E-04	0.00E+00	6.94E-08	6.94E-08	1.05E+05
1	400	RN-222	1.52E-04	0.00E+00	6.07E-08	6.07E-08	1.05E+05
1	450	RN-222	1.34E-04	0.00E+00	5.39E-08	5.39E-08	1.05E+05
1	500	RN-222	1.20E-04	0.00E+00	4.85E-08	4.85E-08	1.05E+05
1	750	RN-222	8.06E-05	0.00E+00	3.23E-08	3.23E-08	1.05E+05
1	1000	RN-222	6.04E-05	0.00E+00	2.42E-08	2.42E-08	1.05E+05
1	1250	RN-222	4.83E-05	0.00E+00	1.94E-08	1.94E-08	1.05E+05
1	1500	RN-222	4.02E-05	0.00E+00	1.61E-08	1.61E-08	1.05E+05
1	2000	RN-222	3.01E-05	0.00E+00	1.21E-08	1.21E-08	1.05E+05
1	2500	RN-222	2.41E-05	0.00E+00	9.66E-09	9.66E-09	1.05E+05
2	25	RN-222	4.20E-03	0.00E+00	7.53E-07	7.53E-07	6.80E+04
2	50	RN-222	1.16E-03	0.00E+00	3.77E-07	3.77E-07	6.80E+04
2	100	RN-222	3.22E-04	0.00E+00	1.88E-07	1.88E-07	6.80E+04
2	200	RN-222	8.94E-05	0.00E+00	9.41E-08	9.41E-08	6.80E+04
2	250	RN-222	1.97E-04	0.00E+00	7.53E-08	7.53E-08	6.80E+04
2	300	RN-222	1.61E-04	0.00E+00	6.27E-08	6.27E-08	6.80E+04
2	350	RN-222	1.36E-04	0.00E+00	5.38E-08	5.38E-08	6.80E+04
2	400	RN-222	1.18E-04	0.00E+00	4.70E-08	4.70E-08	6.79E+04
2	450	RN-222	1.04E-04	0.00E+00	4.18E-08	4.18E-08	6.79E+04
2	500	RN-222	9.25E-05	0.00E+00	3.76E-08	3.76E-08	6.79E+04
2	750	RN-222	6.24E-05	0.00E+00	2.51E-08	2.51E-08	6.79E+04
2	1000	RN-222	4.68E-05	0.00E+00	1.88E-08	1.88E-08	6.78E+04
2	1250	RN-222	3.74E-05	0.00E+00	1.50E-08	1.50E-08	6.78E+04
2	1500	RN-222	3.11E-05	0.00E+00	1.25E-08	1.25E-08	6.77E+04
2	2000	RN-222	2.33E-05	0.00E+00	9.36E-09	9.36E-09	6.76E+04
2	2500	RN-222	1.86E-05	0.00E+00	7.48E-09	7.48E-09	6.75E+04
3	25	RN-222	2.92E-03	0.00E+00	6.29E-07	6.29E-07	5.36E+04
3	50	RN-222	8.04E-04	0.00E+00	3.15E-07	3.15E-07	5.36E+04
3	100	RN-222	2.22E-04	0.00E+00	1.57E-07	1.57E-07	5.36E+04
3	200	RN-222	6.13E-05	0.00E+00	7.86E-08	7.86E-08	5.36E+04
3	250	RN-222	1.62E-04	0.00E+00	6.29E-08	6.29E-08	5.35E+04
3	300	RN-222	1.33E-04	0.00E+00	5.24E-08	5.24E-08	5.35E+04
3	350	RN-222	1.13E-04	0.00E+00	4.49E-08	4.49E-08	5.35E+04
3	400	RN-222	9.81E-05	0.00E+00	3.93E-08	3.93E-08	5.35E+04
3	450	RN-222	8.67E-05	0.00E+00	3.49E-08	3.49E-08	5.35E+04
3	500	RN-222	7.76E-05	0.00E+00	3.14E-08	3.14E-08	5.35E+04
3	750	RN-222	5.21E-05	0.00E+00	2.09E-08	2.09E-08	5.35E+04

3	1000	RN-222	3.91E-05	0.00E+00	1.57E-08	1.57E-08	5.34E+04
3	1250	RN-222	3.12E-05	0.00E+00	1.25E-08	1.25E-08	5.34E+04
3	1500	RN-222	2.60E-05	0.00E+00	1.04E-08	1.04E-08	5.33E+04
3	2000	RN-222	1.95E-05	0.00E+00	7.81E-09	7.81E-09	5.33E+04
3	2500	RN-222	1.55E-05	0.00E+00	6.24E-09	6.24E-09	5.32E+04
4	25	RN-222	5.08E-03	0.00E+00	8.14E-07	8.14E-07	5.98E+04
4	50	RN-222	1.40E-03	0.00E+00	4.07E-07	4.07E-07	5.98E+04
4	100	RN-222	3.87E-04	0.00E+00	2.03E-07	2.03E-07	5.98E+04
4	200	RN-222	1.07E-04	0.00E+00	1.02E-07	1.02E-07	5.97E+04
4	250	RN-222	2.14E-04	0.00E+00	8.13E-08	8.13E-08	5.97E+04
4	300	RN-222	1.75E-04	0.00E+00	6.77E-08	6.77E-08	5.97E+04
4	350	RN-222	1.47E-04	0.00E+00	5.81E-08	5.81E-08	5.97E+04
4	400	RN-222	1.27E-04	0.00E+00	5.08E-08	5.08E-08	5.97E+04
4	450	RN-222	1.12E-04	0.00E+00	4.51E-08	4.51E-08	5.97E+04
4	500	RN-222	9.98E-05	0.00E+00	4.06E-08	4.06E-08	5.97E+04
4	750	RN-222	6.74E-05	0.00E+00	2.71E-08	2.71E-08	5.96E+04
4	1000	RN-222	5.05E-05	0.00E+00	2.03E-08	2.03E-08	5.96E+04
4	1250	RN-222	4.04E-05	0.00E+00	1.62E-08	1.62E-08	5.95E+04
4	1500	RN-222	3.36E-05	0.00E+00	1.35E-08	1.35E-08	5.95E+04
4	2000	RN-222	2.52E-05	0.00E+00	1.01E-08	1.01E-08	5.94E+04
4	2500	RN-222	2.01E-05	0.00E+00	8.07E-09	8.07E-09	5.93E+04
5	25	RN-222	7.87E-03	0.00E+00	1.22E-06	1.22E-06	8.86E+04
5	50	RN-222	2.17E-03	0.00E+00	6.08E-07	6.08E-07	8.86E+04
5	100	RN-222	5.98E-04	0.00E+00	3.04E-07	3.04E-07	8.86E+04
5	200	RN-222	1.65E-04	0.00E+00	1.52E-07	1.52E-07	8.86E+04
5	250	RN-222	3.16E-04	0.00E+00	1.22E-07	1.22E-07	8.86E+04
5	300	RN-222	2.59E-04	0.00E+00	1.01E-07	1.01E-07	8.85E+04
5	350	RN-222	2.19E-04	0.00E+00	8.68E-08	8.68E-08	8.85E+04
5	400	RN-222	1.90E-04	0.00E+00	7.59E-08	7.59E-08	8.85E+04
5	450	RN-222	1.67E-04	0.00E+00	6.75E-08	6.75E-08	8.85E+04
5	500	RN-222	1.50E-04	0.00E+00	6.07E-08	6.07E-08	8.85E+04
5	750	RN-222	1.01E-04	0.00E+00	4.04E-08	4.04E-08	8.84E+04
5	1000	RN-222	7.55E-05	0.00E+00	3.03E-08	3.03E-08	8.83E+04
5	1250	RN-222	6.03E-05	0.00E+00	2.42E-08	2.42E-08	8.83E+04
5	1500	RN-222	5.02E-05	0.00E+00	2.02E-08	2.02E-08	8.82E+04
5	2000	RN-222	3.76E-05	0.00E+00	1.51E-08	1.51E-08	8.80E+04
5	2500	RN-222	3.00E-05	0.00E+00	1.21E-08	1.21E-08	8.79E+04
6	25	RN-222	7.01E-03	0.00E+00	1.27E-06	1.27E-06	1.50E+05
6	50	RN-222	1.93E-03	0.00E+00	6.33E-07	6.33E-07	1.50E+05

6	100	RN-222	5.32E-04	0.00E+00	3.16E-07	3.16E-07	1.50E+05
6	200	RN-222	1.47E-04	0.00E+00	1.58E-07	1.58E-07	1.50E+05
6	250	RN-222	3.23E-04	0.00E+00	1.26E-07	1.26E-07	1.50E+05
6	300	RN-222	2.66E-04	0.00E+00	1.05E-07	1.05E-07	1.50E+05
6	350	RN-222	2.27E-04	0.00E+00	9.03E-08	9.03E-08	1.50E+05
6	400	RN-222	1.97E-04	0.00E+00	7.90E-08	7.90E-08	1.50E+05
6	450	RN-222	1.74E-04	0.00E+00	7.02E-08	7.02E-08	1.50E+05
6	500	RN-222	1.56E-04	0.00E+00	6.32E-08	6.32E-08	1.50E+05
6	750	RN-222	1.05E-04	0.00E+00	4.21E-08	4.21E-08	1.50E+05
6	1000	RN-222	7.86E-05	0.00E+00	3.16E-08	3.16E-08	1.50E+05
6	1250	RN-222	6.29E-05	0.00E+00	2.52E-08	2.52E-08	1.50E+05
6	1500	RN-222	5.24E-05	0.00E+00	2.10E-08	2.10E-08	1.50E+05
6	2000	RN-222	3.92E-05	0.00E+00	1.57E-08	1.57E-08	1.50E+05
6	2500	RN-222	3.13E-05	0.00E+00	1.26E-08	1.26E-08	1.50E+05
7	25	RN-222	4.46E-03	0.00E+00	7.55E-07	7.55E-07	1.03E+05
7	50	RN-222	1.23E-03	0.00E+00	3.77E-07	3.77E-07	1.03E+05
7	100	RN-222	3.42E-04	0.00E+00	1.89E-07	1.89E-07	1.03E+05
7	200	RN-222	9.49E-05	0.00E+00	9.43E-08	9.43E-08	1.03E+05
7	250	RN-222	2.00E-04	0.00E+00	7.54E-08	7.54E-08	1.03E+05
7	300	RN-222	1.63E-04	0.00E+00	6.29E-08	6.29E-08	1.03E+05
7	350	RN-222	1.37E-04	0.00E+00	5.39E-08	5.39E-08	1.03E+05
7	400	RN-222	1.18E-04	0.00E+00	4.71E-08	4.71E-08	1.03E+05
7	450	RN-222	1.04E-04	0.00E+00	4.19E-08	4.19E-08	1.03E+05
7	500	RN-222	9.24E-05	0.00E+00	3.77E-08	3.77E-08	1.03E+05
7	750	RN-222	6.26E-05	0.00E+00	2.51E-08	2.51E-08	1.03E+05
7	1000	RN-222	4.69E-05	0.00E+00	1.88E-08	1.88E-08	1.03E+05
7	1250	RN-222	3.75E-05	0.00E+00	1.51E-08	1.51E-08	1.03E+05
7	1500	RN-222	3.12E-05	0.00E+00	1.25E-08	1.25E-08	1.03E+05
7	2000	RN-222	2.34E-05	0.00E+00	9.40E-09	9.40E-09	1.03E+05
7	2500	RN-222	1.87E-05	0.00E+00	7.51E-09	7.51E-09	1.03E+05
8	25	RN-222	4.88E-03	0.00E+00	7.25E-07	7.25E-07	1.01E+05
8	50	RN-222	1.35E-03	0.00E+00	3.62E-07	3.62E-07	1.01E+05
8	100	RN-222	3.76E-04	0.00E+00	1.81E-07	1.81E-07	1.01E+05
8	200	RN-222	1.04E-04	0.00E+00	9.06E-08	9.06E-08	1.01E+05
8	250	RN-222	1.95E-04	0.00E+00	7.25E-08	7.25E-08	1.01E+05
8	300	RN-222	1.57E-04	0.00E+00	6.04E-08	6.04E-08	1.01E+05
8	350	RN-222	1.32E-04	0.00E+00	5.18E-08	5.18E-08	1.01E+05
8	400	RN-222	1.13E-04	0.00E+00	4.53E-08	4.53E-08	1.01E+05
8	450	RN-222	9.94E-05	0.00E+00	4.02E-08	4.02E-08	1.01E+05

8	500	RN-222	8.85E-05	0.00E+00	3.62E-08	3.62E-08	1.01E+05
8	750	RN-222	6.01E-05	0.00E+00	2.41E-08	2.41E-08	1.01E+05
8	1000	RN-222	4.51E-05	0.00E+00	1.81E-08	1.81E-08	1.01E+05
8	1250	RN-222	3.60E-05	0.00E+00	1.45E-08	1.45E-08	1.01E+05
8	1500	RN-222	3.00E-05	0.00E+00	1.20E-08	1.20E-08	1.01E+05
8	2000	RN-222	2.25E-05	0.00E+00	9.02E-09	9.02E-09	1.01E+05
8	2500	RN-222	1.80E-05	0.00E+00	7.21E-09	7.21E-09	1.01E+05
9	25	RN-222	5.74E-02	0.00E+00	2.72E-05	2.72E-05	1.38E+07
9	50	RN-222	1.45E-02	0.00E+00	1.36E-05	1.36E-05	1.38E+07
9	100	RN-222	3.65E-03	0.00E+00	6.81E-06	6.81E-06	1.38E+07
9	200	RN-222	9.22E-04	0.00E+00	3.40E-06	3.40E-06	1.38E+07
9	250	RN-222	6.80E-03	0.00E+00	2.72E-06	2.72E-06	1.38E+07
9	300	RN-222	5.66E-03	0.00E+00	2.27E-06	2.27E-06	1.38E+07
9	350	RN-222	4.85E-03	0.00E+00	1.95E-06	1.95E-06	1.38E+07
9	400	RN-222	4.24E-03	0.00E+00	1.70E-06	1.70E-06	1.38E+07
9	450	RN-222	3.77E-03	0.00E+00	1.51E-06	1.51E-06	1.38E+07
9	500	RN-222	3.39E-03	0.00E+00	1.36E-06	1.36E-06	1.38E+07
9	750	RN-222	2.26E-03	0.00E+00	9.08E-07	9.08E-07	1.38E+07
9	1000	RN-222	1.70E-03	0.00E+00	6.81E-07	6.81E-07	1.38E+07
9	1250	RN-222	1.36E-03	0.00E+00	5.44E-07	5.44E-07	1.38E+07
9	1500	RN-222	1.13E-03	0.00E+00	4.54E-07	4.54E-07	1.38E+07
9	2000	RN-222	8.47E-04	0.00E+00	3.40E-07	3.40E-07	1.38E+07
9	2500	RN-222	6.78E-04	0.00E+00	2.72E-07	2.72E-07	1.38E+07
10	25	RN-222	5.72E-03	0.00E+00	9.72E-07	9.72E-07	1.03E+05
10	50	RN-222	1.57E-03	0.00E+00	4.86E-07	4.86E-07	1.03E+05
10	100	RN-222	4.34E-04	0.00E+00	2.43E-07	2.43E-07	1.03E+05
10	200	RN-222	1.20E-04	0.00E+00	1.21E-07	1.21E-07	1.03E+05
10	250	RN-222	2.53E-04	0.00E+00	9.71E-08	9.71E-08	1.03E+05
10	300	RN-222	2.07E-04	0.00E+00	8.09E-08	8.09E-08	1.03E+05
10	350	RN-222	1.75E-04	0.00E+00	6.94E-08	6.94E-08	1.03E+05
10	400	RN-222	1.52E-04	0.00E+00	6.07E-08	6.07E-08	1.03E+05
10	450	RN-222	1.34E-04	0.00E+00	5.39E-08	5.39E-08	1.03E+05
10	500	RN-222	1.20E-04	0.00E+00	4.85E-08	4.85E-08	1.03E+05
10	750	RN-222	8.06E-05	0.00E+00	3.23E-08	3.23E-08	1.03E+05
10	1000	RN-222	6.04E-05	0.00E+00	2.42E-08	2.42E-08	1.03E+05
10	1250	RN-222	4.83E-05	0.00E+00	1.94E-08	1.94E-08	1.03E+05
10	1500	RN-222	4.02E-05	0.00E+00	1.61E-08	1.61E-08	1.03E+05
10	2000	RN-222	3.01E-05	0.00E+00	1.21E-08	1.21E-08	1.03E+05
10	2500	RN-222	2.41E-05	0.00E+00	9.66E-09	9.66E-09	1.02E+05

11	25	RN-222	1.47E-01	0.00E+00	2.54E-05	2.54E-05	4.71E+06
11	50	RN-222	4.05E-02	0.00E+00	1.27E-05	1.27E-05	4.71E+06
11	100	RN-222	1.11E-02	0.00E+00	6.36E-06	6.36E-06	4.71E+06
11	200	RN-222	3.07E-03	0.00E+00	3.18E-06	3.18E-06	4.71E+06
11	250	RN-222	6.35E-03	0.00E+00	2.54E-06	2.54E-06	4.71E+06
11	300	RN-222	5.29E-03	0.00E+00	2.12E-06	2.12E-06	4.71E+06
11	350	RN-222	4.53E-03	0.00E+00	1.82E-06	1.82E-06	4.71E+06
11	400	RN-222	3.96E-03	0.00E+00	1.59E-06	1.59E-06	4.71E+06
11	450	RN-222	3.52E-03	0.00E+00	1.41E-06	1.41E-06	4.70E+06
11	500	RN-222	3.17E-03	0.00E+00	1.27E-06	1.27E-06	4.70E+06
11	750	RN-222	2.11E-03	0.00E+00	8.47E-07	8.47E-07	4.70E+06
11	1000	RN-222	1.58E-03	0.00E+00	6.35E-07	6.35E-07	4.70E+06
11	1250	RN-222	1.27E-03	0.00E+00	5.08E-07	5.08E-07	4.70E+06
11	1500	RN-222	1.05E-03	0.00E+00	4.23E-07	4.23E-07	4.70E+06
11	2000	RN-222	7.90E-04	0.00E+00	3.17E-07	3.17E-07	4.69E+06
11	2500	RN-222	6.32E-04	0.00E+00	2.54E-07	2.54E-07	4.69E+06
12	25	RN-222	1.09E-02	0.00E+00	2.32E-06	2.32E-06	2.23E+05
12	50	RN-222	3.01E-03	0.00E+00	1.16E-06	1.16E-06	2.23E+05
12	100	RN-222	8.30E-04	0.00E+00	5.80E-07	5.80E-07	2.23E+05
12	200	RN-222	2.29E-04	0.00E+00	2.90E-07	2.90E-07	2.23E+05
12	250	RN-222	5.93E-04	0.00E+00	2.32E-07	2.32E-07	2.22E+05
12	300	RN-222	4.89E-04	0.00E+00	1.93E-07	1.93E-07	2.22E+05
12	350	RN-222	4.16E-04	0.00E+00	1.66E-07	1.66E-07	2.22E+05
12	400	RN-222	3.62E-04	0.00E+00	1.45E-07	1.45E-07	2.22E+05
12	450	RN-222	3.20E-04	0.00E+00	1.29E-07	1.29E-07	2.22E+05
12	500	RN-222	2.87E-04	0.00E+00	1.16E-07	1.16E-07	2.22E+05
12	750	RN-222	1.92E-04	0.00E+00	7.72E-08	7.72E-08	2.22E+05
12	1000	RN-222	1.44E-04	0.00E+00	5.78E-08	5.78E-08	2.22E+05
12	1250	RN-222	1.15E-04	0.00E+00	4.62E-08	4.62E-08	2.22E+05
12	1500	RN-222	9.59E-05	0.00E+00	3.85E-08	3.85E-08	2.22E+05
12	2000	RN-222	7.18E-05	0.00E+00	2.88E-08	2.88E-08	2.21E+05
12	2500	RN-222	5.74E-05	0.00E+00	2.30E-08	2.30E-08	2.21E+05
13	25	RN-222	1.29E-02	0.00E+00	2.64E-06	2.64E-06	2.64E+05
13	50	RN-222	3.54E-03	0.00E+00	1.32E-06	1.32E-06	2.64E+05
13	100	RN-222	9.76E-04	0.00E+00	6.59E-07	6.59E-07	2.64E+05
13	200	RN-222	2.70E-04	0.00E+00	3.29E-07	3.29E-07	2.64E+05
13	250	RN-222	6.70E-04	0.00E+00	2.63E-07	2.63E-07	2.64E+05
13	300	RN-222	5.54E-04	0.00E+00	2.19E-07	2.19E-07	2.64E+05
13	350	RN-222	4.72E-04	0.00E+00	1.88E-07	1.88E-07	2.64E+05

793

13	400	RN-222	4.11E-04	0.00E+00	1.65E-07	1.65E-07	2.64E+05
13	450	RN-222	3.63E-04	0.00E+00	1.46E-07	1.46E-07	2.64E+05
13	500	RN-222	3.26E-04	0.00E+00	1.32E-07	1.32E-07	2.63E+05
13	750	RN-222	2.18E-04	0.00E+00	8.77E-08	8.77E-08	2.63E+05
13	1000	RN-222	1.64E-04	0.00E+00	6.57E-08	6.57E-08	2.63E+05
13	1250	RN-222	1.31E-04	0.00E+00	5.25E-08	5.25E-08	2.63E+05
13	1500	RN-222	1.09E-04	0.00E+00	4.37E-08	4.37E-08	2.63E+05
13	2000	RN-222	8.16E-05	0.00E+00	3.28E-08	3.28E-08	2.62E+05
13	2500	RN-222	6.52E-05	0.00E+00	2.62E-08	2.62E-08	2.62E+05
14	25	RN-222	1.52E-02	0.00E+00	2.76E-06	2.76E-06	2.70E+05
14	50	RN-222	4.19E-03	0.00E+00	1.38E-06	1.38E-06	2.70E+05
14	100	RN-222	1.15E-03	0.00E+00	6.91E-07	6.91E-07	2.70E+05
14	200	RN-222	3.18E-04	0.00E+00	3.45E-07	3.45E-07	2.70E+05
14	250	RN-222	7.06E-04	0.00E+00	2.76E-07	2.76E-07	2.70E+05
14	300	RN-222	5.82E-04	0.00E+00	2.30E-07	2.30E-07	2.70E+05
14	350	RN-222	4.95E-04	0.00E+00	1.97E-07	1.97E-07	2.70E+05
14	400	RN-222	4.31E-04	0.00E+00	1.73E-07	1.73E-07	2.70E+05
14	450	RN-222	3.81E-04	0.00E+00	1.53E-07	1.53E-07	2.70E+05
14	500	RN-222	3.42E-04	0.00E+00	1.38E-07	1.38E-07	2.70E+05
14	750	RN-222	2.29E-04	0.00E+00	9.19E-08	9.19E-08	2.69E+05
14	1000	RN-222	1.72E-04	0.00E+00	6.89E-08	6.89E-08	2.69E+05
14	1250	RN-222	1.37E-04	0.00E+00	5.51E-08	5.51E-08	2.69E+05
14	1500	RN-222	1.14E-04	0.00E+00	4.59E-08	4.59E-08	2.69E+05
14	2000	RN-222	8.56E-05	0.00E+00	3.44E-08	3.44E-08	2.69E+05
14	2500	RN-222	6.84E-05	0.00E+00	2.75E-08	2.75E-08	2.68E+05
15	25	RN-222	1.38E-02	0.00E+00	2.65E-06	2.65E-06	2.89E+05
15	50	RN-222	3.80E-03	0.00E+00	1.32E-06	1.32E-06	2.89E+05
15	100	RN-222	1.04E-03	0.00E+00	6.62E-07	6.62E-07	2.88E+05
15	200	RN-222	2.87E-04	0.00E+00	3.31E-07	3.31E-07	2.88E+05
15	250	RN-222	6.69E-04	0.00E+00	2.65E-07	2.65E-07	2.88E+05
15	300	RN-222	5.54E-04	0.00E+00	2.21E-07	2.21E-07	2.88E+05
15	350	RN-222	4.73E-04	0.00E+00	1.89E-07	1.89E-07	2.88E+05
15	400	RN-222	4.12E-04	0.00E+00	1.65E-07	1.65E-07	2.88E+05
15	450	RN-222	3.66E-04	0.00E+00	1.47E-07	1.47E-07	2.88E+05
15	500	RN-222	3.28E-04	0.00E+00	1.32E-07	1.32E-07	2.88E+05
15	750	RN-222	2.19E-04	0.00E+00	8.81E-08	8.81E-08	2.88E+05
15	1000	RN-222	1.65E-04	0.00E+00	6.60E-08	6.60E-08	2.88E+05
15	1250	RN-222	1.32E-04	0.00E+00	5.28E-08	5.28E-08	2.88E+05
15	1500	RN-222	1.10E-04	0.00E+00	4.40E-08	4.40E-08	2.88E+05

15	2000	RN-222	8.20E-05	0.00E+00	3.29E-08	3.29E-08	2.87E+05
15	1500	RN-222	6.55E-05	0.00E+00	2.63E-08	2.63E-08	2.87E+05
16	1000	RN-222	9.05E-03	0.00E+00	1.88E-06	1.88E-06	2.12E+05
16	500	RN-222	2.50E-03	0.00E+00	9.38E-07	9.38E-07	2.12E+05
16	100	RN-222	6.90E-04	0.00E+00	4.69E-07	4.69E-07	2.12E+05
16	200	RN-222	1.91E-04	0.00E+00	2.34E-07	2.34E-07	2.12E+05
16	250	RN-222	4.78E-04	0.00E+00	1.87E-07	1.87E-07	2.12E+05
16	300	RN-222	3.95E-04	0.00E+00	1.56E-07	1.56E-07	2.12E+05
16	350	RN-222	3.36E-04	0.00E+00	1.34E-07	1.34E-07	2.12E+05
16	400	RN-222	2.92E-04	0.00E+00	1.17E-07	1.17E-07	2.12E+05
16	450	RN-222	2.59E-04	0.00E+00	1.04E-07	1.04E-07	2.12E+05
16	500	RN-222	2.32E-04	0.00E+00	9.37E-08	9.37E-08	2.12E+05
16	750	RN-222	1.55E-04	0.00E+00	6.24E-08	6.24E-08	2.12E+05
16	1000	RN-222	1.17E-04	0.00E+00	4.68E-08	4.68E-08	2.12E+05
16	1250	RN-222	9.32E-05	0.00E+00	3.74E-08	3.74E-08	2.12E+05
16	1500	RN-222	7.76E-05	0.00E+00	3.11E-08	3.11E-08	2.12E+05
16	2000	RN-222	5.81E-05	0.00E+00	2.33E-08	2.33E-08	2.11E+05
16	2500	RN-222	4.64E-05	0.00E+00	1.86E-08	1.86E-08	2.11E+05

GROUND-LEVEL CHI/Q VALUES FOR RN-222 AT VARIOUS DISTANCES IN EACH COMPASS DIRECTION

DISTANCE (METERS) CHI/Q TOWARD INDICATED DIRECTION (SEC/CUBIC METER)

	N	NNW	NW	WNW	W	WSW	SW	SSW
25	0.243E-03	0.204E-03	0.142E-03	0.246E-03	0.382E-03	0.340E-03	0.216E-03	0.237E-03
50	0.670E-04	0.564E-04	0.390E-04	0.680E-04	0.105E-03	0.937E-04	0.599E-04	0.657E-04
100	0.185E-04	0.156E-04	0.108E-04	0.188E-04	0.290E-04	0.258E-04	0.166E-04	0.182E-04
200	0.509E-05	0.434E-05	0.297E-05	0.519E-05	0.800E-05	0.712E-05	0.460E-05	0.507E-05
250	0.121E-04	0.957E-05	0.785E-05	0.104E-04	0.153E-04	0.157E-04	0.971E-05	0.944E-05
300	0.996E-05	0.782E-05	0.645E-05	0.847E-05	0.126E-04	0.129E-04	0.789E-05	0.764E-05
350	0.846E-05	0.660E-05	0.548E-05	0.714E-05	0.106E-04	0.110E-04	0.664E-05	0.640E-05
400	0.735E-05	0.571E-05	0.476E-05	0.617E-05	0.921E-05	0.957E-05	0.573E-05	0.551E-05
450	0.650E-05	0.502E-05	0.420E-05	0.542E-05	0.812E-05	0.847E-05	0.503E-05	0.482E-05
500	0.582E-05	0.449E-05	0.376E-05	0.484E-05	0.726E-05	0.759E-05	0.448E-05	0.429E-05
750	0.391E-05	0.303E-05	0.253E-05	0.327E-05	0.489E-05	0.509E-05	0.304E-05	0.292E-05
1000	0.293E-05	0.227E-05	0.189E-05	0.245E-05	0.366E-05	0.381E-05	0.228E-05	0.219E-05
1250	0.234E-05	0.181E-05	0.151E-05	0.196E-05	0.293E-05	0.305E-05	0.182E-05	0.175E-05
1500	0.195E-05	0.151E-05	0.126E-05	0.163E-05	0.244E-05	0.254E-05	0.152E-05	0.146E-05